Annexin A6 involvement in the organization of cholesterol-rich membrane microdomains : evidence from cells of the Niemann-Pick type C disease patients and biomimetic lipid monolayers

Magdalena Hamczyk Domoń

N° d'ordre: Année 2011

THESE DE L'UNIVERSITE DE LYON

délivrée par

L'UNIVERSITE CLAUDE BERNARD LYON 1
et préparée en cotutelle avec

NENCKI INSTITUTE OF EXPERIMENTAL BIOLOGY
POLISH ACADEMY OF SCIENCES

ECOLE DOCTORALE INTERDISCIPLINAIRE SCIENCES SANTE

Pour l'obtention
Du DIPLOME DE DOCTORAT
(Arrêté du 7 août 2006 / arrêté du 6 janvier 2005)

Soutenue publiquement le 13 décembre 2011

par

HAMCZYK DOMOŃ Magdalena Małgorzata

Annexin A6 involvement in the organization of cholesterol-rich membrane microdomains. Evidence from cells of the Niemann-Pick type C disease patients and biomimetic lipid monolayers

Directeurs de thèse:

Dr BESSON Françoise / Pr PIKUŁA Sławomir

JURY:
Mme BANDOROWICZ-PIKUŁA Joanna
Mme BESSON Françoise
M BUCHET René
Mme CASTANO Sabine - rapporteur
M PIKUŁA Sławomir
M SIKORSKI Aleksander F. - rapporteur

UNIVERSITE CLAUDE BERNARD - LYON 1

Président de l'Université	**M. A. Bonmartin**
Vice-président du Conseil d'Administration	M. le Professeur G. Annat
Vice-président du Conseil des Etudes et de la Vie Universitaire	M. le Professeur D. Simon
Vice-président du Conseil Scientifique	M. le Professeur J-F. Mornex
Secrétaire Général	M. G. Gay

COMPOSANTES SANTE

Faculté de Médecine Lyon Est – Claude Bernard	Directeur : M. le Professeur J. Etienne
Faculté de Médecine et de Maïeutique Lyon Sud – Charles Mérieux	Directeur : M. le Professeur F-N. Gilly
UFR d'Odontologie	Directeur : M. le Professeur D. Bourgeois
Institut des Sciences Pharmaceutiques et Biologiques	Directeur : M. le Professeur F. Locher
Institut des Sciences et Techniques de la Réadaptation	Directeur : M. le Professeur Y. Matillon
Département de formation et Centre de Recherche en Biologie Humaine	Directeur : M. le Professeur P. Farge

COMPOSANTES ET DEPARTEMENTS DE SCIENCES ET TECHNOLOGIE

Faculté des Sciences et Technologies	Directeur : M. le Professeur F. Gieres
Département Biologie	Directeur : M. le Professeur F. Fleury
Département Chimie Biochimie	Directeur : Mme le Professeur H. Parrot
Département GEP	Directeur : M. N. Siauve
Département Informatique	Directeur : M. le Professeur S. Akkouche
Département Mathématiques	Directeur : M. le Professeur A. Goldman
Département Mécanique	Directeur : M. le Professeur H. Ben Hadid
Département Physique	Directeur : Mme S. Fleck
Département Sciences de la Terre	Directeur : Mme le Professeur I. Daniel
UFR Sciences et Techniques des Activités Physiques et Sportives	Directeur : M. C. Collignon
Observatoire de Lyon	Directeur : M. B. Guiderdoni
Ecole Polytechnique Universitaire de Lyon 1	Directeur : M. P. Fournier
Ecole Supérieure de Chimie Physique Electronique	Directeur : M. G. Pignault
Institut Universitaire de Technologie de Lyon 1	Directeur : M. le Professeur C. Coulet
Institut de Science Financière et d'Assurances	Directeur : M. le Professeur J-C. Augros
Institut Universitaire de Formation des Maîtres	Directeur : M. R. Bernard

NENCKI INSTITUTE OF EXPERIMENTAL BIOLOGY

Polish Academy of Sciences

Board of Directors

Director	Adam Szewczyk
Deputy Director for Scientific Research	Urszula Sławińska
Deputy Director for Scientific Research	Hanna Fabczak
Administrative Director	Anna Jachner-Miśkiewicz

Scientific Departments and Laboratories

Department of Cell Biology	Katarzyna Kwiatkowska
Laboratory of Cell Membrane Physiology	Elżbieta Wyroba
Laboratory of Transcription Regulation	Bożena Kamińska-Kaczmarek
Laboratory of Physiology of Cell Movements	Stanisław Fabczak
Laboratory of Plasma Membrane Receptors	Andrzej Sobota
Laboratory of Signal Transduction	Tomasz Wilanowski
Department of Biochemistry	Maria Jolanta Rędowicz
Laboratory of Biochemistry of Lipids	Sławomir Pikuła
Laboratory of Bioenergetics and Biomembranes	Jerzy Duszyński
Laboratory of Cell Signaling and Metabolic Disorders	Agnieszka Dobrzyń
Laboratory of Cellular Metabolism	Krzysztof Zabłocki
Laboratory of Comparative Enzymology	Wojciech Rode
Laboratory of Intracellular Ion Channels	Adam Szewczyk
Laboratory of Molecular Bases of Aging	Ewa Sikora
Laboratory of Molecular Basis of Cell Motilty	Maria Jolanta Rędowicz
Laboratory of Motor Proteins	Andrzej A. Kasprzak
Department of Molecular and Cellular Neurobiology	Magorzata Kossut
Laboratory of Bioinformatics and Systems Biology	Krzysztof Pawłowski
Laboratory of Calcium Binding Proteins	Anna Filipek
Laboratory of Epileptogenesis	Katarzyna Łukasiuk
Laboratory for Mechanisms of Transport Through Biomembranes	Katarzyna A. Nałęcz
Laboratory of Molecular Basis of Brain Plasticity	Jolanta Skangiel-Kramska
Laboratory of Molecular Neurobiology	Leszek Kaczmarek
Laboratory of Neurobiology of Development and Evolution	Krzysztof Turlejski
Laboratory of Neuroplasticity	Magorzata Kossut
Department of Neurophysiology	Andrzej Wróbel
Laboratory of Defensive Conditioned Reflexes	Tomasz Werka
Laboratory of Ethology	Ewa Joanna Godzińska
Laboratory of Limbic System	Stefan Kasicki
Laboratory of Molecular and Systemic Neuromorphology	Grzegorz Wilczyński
Interinstitute Laboratory of Neuromuscular Plasticity	Urszula Sławińska
Laboratory of Neuropsychology	Elżbieta Szeląg
Laboratory of Psychophysiology	Anna Grabowska
Laboratory of Reinnervation Processes	Julita Czarkowska-Bauch
Laboratory of Visual System	Andrzej Wróbel
Supporting Units	
Lasboratory of Cell Engeneering	Agata Klejman
Laboratory of Cytometry	Katarzyna Piwocka
The Animal House	Anna Passini
Laboratory of Confocal Microscopy	Wanda Kłopocka
Laboratory of Electron Microscopy	Elżbieta Wyroba
Information Technology Unit	Mirosław Sikora

Acknowledgements

This PhD thesis was prepared in the University Lyon 1 in Villeurbanne (France) and in the Nencki Institute of Experimental Biology in Warsaw (Poland) under the co-supervision of Professor Françoise BESSON and Professor Sławomir PIKUŁA. I would like to thank them for their guidance, encouragement, and enthusiasm.

I wish to thank following people for their suggestions, discussions, teaching and technical help

Nencki Institute of Experimental Biology:
Professor Joanna BANDOROWICZ-PIKUŁA
Agnieszka STRZELECKA-KILISZEK, PhD
Michalina KOSIOREK, Msc
Anna ĆMOCH, Msc
Paulina PODSZYWAŁOW-BARTNICKA, PhD
Karolina GÓRECKA, PhD
Anna BELNIAK, PhD
Małgorzata Eliza SZTOLSZTENER, PhD
Le Duy DO, Msc
Marcin WOŚ, Msc

University Claude Bernard Lyon 1:
Professor René BUCHET
Mehmed Nail NASIR, PhD
Gladys MATAR, PhD
Laurence BESSUEILLE, PhD
Anne BRIOLAY, PhD
Geraldine BECHKOFF, PhD
Michèle BOSCH,
Saida MEBAREK-ASSAM, PhD
Véronique ROCHE
Cyril THOUVEREY, PhD

Laboratory of Confocal Microscopy (Warsaw):
Wanda KŁOPOCKA
Joanna KUCHARSKA
Artur WOLNY
Jarosław KORCZYNSKI

I would like to thank Professor Wiesława LEŚNIAK for proofreading the text and providing helpful suggestions resulting in substantial improvements in the use of English.

I would like to thank the following organizations for supporting and sponsoring my scientific development:

French Embassy in Warsaw,
Ministry of Science and Higher Education

This work was partially supported by the National Science Center, grant No. N N401 642740 by the Polish Ministry of Science and Higher Education, grant No. N N401 139839, by POLONIUM, CNRS and PICS

Finally, I want to thank my family, my parents, my husband and my daughter for their love, support and encouragement throughout the years of this project

Contents

Abbreviations **7**
CHAPTER 1: INTRODUCTION **10**
1.1 Lipid microdomains 11
1.1.1 Lipid microdomains in membranes 11
1.1.2. Identification of DRMs in intracellular membranes 13
1.2 Cholesterol in the cell 15
1.2.1 Cholesterol distribution in the cell 15
1.2.2 Cholesterol homeostasis 16
1.2.3 Cholesterol transport by receptor mediated endocytosis 17
1.3 Niemann-Pick type C disease 21
1.3.1 Clinical diagnosis of NPC disease 21
1.3.2 Genetic and biochemical identification of NPC disease 21
1.3.3 Therapeutic strategies for NPC disease 22
1.4 Annexins 23
1.4.1 Annexins as proteins implicated in cholesterol transport and interactions with membranes 23
1.4.2 Annexins associated with cholesterol in membrane microdomains. 25
1.4.3 Annexin-related pathologies 30
CHAPTER 2: AIMS **32**
CHAPTER 3: MATERIALS AND METHODS **34**
3.1 Fibroblast cell lines 35
3.1.1 Clinical diagnosis of Niemann-Pick type C disease 35
3.1.2 Cell culture 35
3.1.3 FACScan analysis 36
3.2 Techniques related to the preparation of membrane fractions 36
3.2.1 Cell fractionation 36
3.2.2 Isolation of detergent resistant membranes (DRMs) 37
3.2.3 Titrations of proteins and cholesterol 38
3.2.3.1 Determination of protein concentration 38
3.2.3.2 Determination of cholesterol concentration 38
3.2.4 Immunodetections 39
3.2.4.1 Immunocytochemistry 39
3.2.4.2 Dot blot analysis 40
3.2.4.3 Sodium dodecyl sulfate polyacrylamide gel electrophoresis and Western blotting 41
3.2.5 Lipid analysis 41
3.2.5.1 Lipid extraction 41
3.2.5.2 Thin-layer chromatography (TLC) 42
3.3 Techniques related to interfacial monolayer analysis 42
3.3.1 Expression and purification of different human recombinant annexin A6 42
3.3.2 Stability of AnxA6-1, its W343F mutant and AnxA6-2 45
3.3.3 Surface pressure measurements 46
3.3.4 Brewster angle microscopy imaging (BAM) 46
3.3.5 Polarization modulation infrared reflection absorption spectroscopy (PM-IRRAS) 47
3.4. Other techniques 49
3.4.1 Statistical analysis 49
3.5. Reagents 49

CHAPTER 4: RESULTS **51**
4.1. Detergent resistant membranes of Niemann-Pick type C fibroblasts 52
4.1.1. Characteristics of NPC fibroblasts 52
4.1.2 Distribution of cholesterol-enriched microdomains in NPC L1 and control fibroblasts 54
4.1.3. Biochemical characterization of detergent resistant membranes (DRMs) 56
4.1.4 Distribution of AnxA6 and cholesterol-enriched microdomains in NPC L1 and control fibroblasts 57
4.1.5. Analysis of AnxA6 interactions with DRMs in the absence and presence of Ca^{2+} 58
4.1.6 Characterization of the lipid content of DRMs 60
4.1.7 Identification of lipid microdomains in the membranes of cellular organelles involved in endocytosis 62
4.2. Interaction of AnxA6 with cholesterol in vitro 63
4.2.1 Interfacial properties of human recombinant annexin A6 isoform 1 63
4.2.2. Analysis of the interactions of AnxA6 with lipid monolayers 66
4.2.3. Interactions of AnxA6-1 with lipid monolayers mimicking membrane microdomains 72
4.2.4. Factors affecting the interactions between AnxA6 and cholesterol *in vitro* 74
4.2.4.1. Role of the hydroxyl group of cholesterol 74
4.2.4.2. Importance of the VAAEIL sequence of AnxA6-1 75
4.2.4.3. Importance of the linker region of AnxA6-1 76
CHAPTER 5: DISCUSSION **79**
5.1 Comparisom between lipid microdomains of NPC and control fibroblasts 80
5.2 Annexin A6 – the protein implicated in endocytosis is also implicated in lipid raft formation in NPC disease 82
5.3 Interaction between AnxA6 and lipid microdomain-mimicking monolayers depends on the presence of cholesterol and Ca^{2+} 84
5.4 AnnexinA6 interactions with lipid rafts are based on its interactions with cholesterol . 85
5.4.1 AnxA6 interactions with cholesterol depend on pH and the presence of Ca^{2+} 86
5.4.3 The –OH group of cholesterol is implicated in the AnxA6-cholesterol interaction 88
5.4.4 The linker region and the VAAEIL sequence of AnxA6 are implicated in the AnxA6-cholesterol interaction 89
5.5 Concluding remarks 91
References **92**
Summary **110**
List of publications **112**

Abbreviations

ACAT	- acyl Co-A:cholesterol acyl transferase
ANXA1-A11	- annexin gene
AnxA6	- annexin A6
ASM	- acid sphingomyelinase
BAM	- Brewster Angle Microscopy
BHK	- baby hamster kidney cells
BMP	- bis(monoacylglycerol)phosphate
BSA	- bovine serum albumin
BV-2	- microglia cells
CCP	- clathrin coated pit
CCV	- clathrin coated vesicle
CD	- circular dichroism
CD55	- decay accelerating factor
cDNA	- complementary deoxyribonucleic acid
CDs	- cyclodextrins
CERT	- ceramide transport protein
CHO	- Chinese chamster ovary
Chol	- cholesterol
Chol-Ac	- cholesteryl acetate
COPs	- endosomal coat proteins
COS7	- African green monkey kidney cells
CRP	- C-reactive protein
CTB	- cholera toxin B subunit
DABCO	- 1,4-diazabicyclo[2.2.2]octane
DHCR7	- 7-dehydrochoesterol reductase
DMEM	- Dulbecco's Modified Eagle Medium
DMPE	- dimyristoylphosphatidylethanolamine
DMPS	- 1,2-dimyristoyl-L- glycero-3-phospho-L-serine
DMSO	- dimethyl sulfoxide
DNaseI	- deoxyribonuclease
DPPC	- 1,2-dipalmitoyl-*sn*-glycero-3-phosphocholine
DRMs	- detergent resistant membranes
EDTA	- ethylenediaminetetraacetinc acid
EE	- early endosomes
EGF	- epidermal growth factor
EGTA	- ethylene glycol-bis(2-amino-ethylether)-N,N,N’,N’-tetra acetic acid
ER	- endoplasmic reticulum
ERC	- endocytic recycling compartment
ET	- exposure time
FACScan	- Fluorescence activated cell sorter
FBS	- fetal bovine serum
FITC	- fluorescein isothiocyanate

G0/G1	- resting cells phase
G2/M	- cell division phase
GA	- Golgi apparatus
GL	- gray level
GM1	- monosialotetrahexosylganglioside
GPI	- glycosylphosphatidylinositol
GSLs	- glcosphingolipids
GTP	- guanozyno-5'-trifosforan
HAM F-10	- Ham's nutrient mixture
Hek293	- human embryonic kidney cells
HepG2	- hepatocellular liver carcinoma cells
HIV	- human immunodeficiency virus
HM	- heavy membranes
HMGR	- 3-hydroxy-3-methylglutaryl coenzyme A reductase HMG CoA reductase
HRP	- horseradish peroxidase conjugate
HT29 cells	- human colon adenocarcinoma cells
IPTG	- isopropyl β-D-1-thiogalactopyranoside
LAL	- lysosomal acid lipase
LB	- Luria-Bertani medium
LBPA	- lyso-bis-phosphatidic acid
L_d	- liquid-disordered
LDL	- low-density lipoprotein
LDLR	- low-density lipoprotein receptor
LE	- late endosomes
LE/LY	- late endosome/lysosome compartment
L_o	- liquid-ordered
LSO	- lysosome-like storage organelles
LY	- lysosomes
MAM	- mitochondria-associated ER membrane
MDCK	- Madin-Darby Canine Kidney Cells
MLN64	- late endosomal protein participating in the transport of cholesterol
MVB	- multivesicular bodies
MβCD	- methyl-β-cyclodextrin
NPC	- Niemann-Pick type C disease
NPC1	- gene encoding NPC1 protein
NPC1	- Niemann-Pick type C1 protein
NPC2	- Niemann-Pick type C2 protein
NPD	- Niemann-Pick disease
NRK	- normal rat kidney
OD	- optical density
ORP1L	- late endosomal protein participating in the transport of cholesterol
OSBP	- oxysterol binding protein
Osh4	- homolog of oxysterol binding proteins

PA	- phosphatidic acid
PBS	- phosphate buffered saline
PC	- phosphatidylcholine
PCSK9	- proprotein convertase subtilisin/kexin-type 9
PE	- phosphatidylethanolamine
PI	- phosphatidylinositol
PIC	- protease inhibitors cocktail
PLs	- phospholipids
PM	- plasma membrane
PM-IRRAS	- Polarisation Modulation InfraRed Reflection Absorption Spectroscopy
PMSF	- phenylmethylsulfonyl fluoride
PNS	- post-nuclear supernatant
POPC	- 2-Oleoyl-1-palmitoyl-*sn*-glycero-3-phosphocholine
POPS	- 2-Oleoyl-1-palmitoyl-sn-glycero-3-phospho-L-serine
PS	- phosphatidylserine
QCM	- quartz crystal microbalance technique
QCM-D	- quartz crystal microbalance with dissipation monitoring
REC	- recirculating endosome compartment
Rev/min	- revolutions per minute
RGB	- red, green and blue filters
RNase	- ribonuclease
S phase	- DNA synthesis phase
SCAP	- SREBP cleavage activating protein
SDS-PAGE	- sodium dodecyl sulfate polyacrylamide gel electrophoresis
SEC	- sorting endosome compartment
SLB	- supported lipid bilayers
SM	- sphingomyelin
SMPD1	- gene encoding acid sphingomylinase
SREBP	- sterol regulatory element binding protein
SSD	- sterol-sensing domain
TBS	- tris buffered saline
TBST	- tris buffered saline containing 0.05% Tween 20
TGN	- trans-Golgi network
TLC	- thin-layer chromatography
v/v	- volume/volume
w/v	- weight/volume
WIF-B	- hepatoma-derived hybrid cell line

CHAPTER 1
INTRODUCTION

1.1 Lipid microdomains

1.1.1 Lipid microdomains in membranes

Biological membranes are now assumed to encompass a plethora of protein-lipid and protein-protein interactions that compartmentalize the bilayer into temporarily formed ordered structures called membrane microdomains. Lipid-based membrane domains or lipid rafts constitute an important group of structures of the plasma membrane (Simons and Ikonen, 1997; Mukherjee and Maxfield 2004; Lindner and Naim 2009). These are normally believed to be very small (10-200 nm), and under normal conditions, cannot be resolved by light microscopy (Pralle *et al* 2000; Pike, 2009). Also mounting evidence indicates that there is a variety of "rafts" with varying properties, and not just a binary system of "rafts" and "non-rafts" (Hao *et al.,* 2001; Lindner and Naim, 2009). Cholesterol appears to play a major role in the generation of membrane domains, and current evidence indicates that these domains exist in the liquid-ordered (L_o) phase, which is more rigid and have a higher local order relative to the liquid-disordered (L_d) parts of the membrane (Brown and London, 1998). These rafts are most often functionally identified by their resistance to solubilization by cold nonionic detergents like Triton X-100; hence, their alternate name is detergent-resistant membranes (DRMs). Domain separation can be visualized microscopically when the cellular cholesterol concentrations are experimentally lowered, leading to a coalescence of previously dispersed rafts (Hao *et al*., 2001). Domains or rafts have also been reported to exist in membranes of intracellular organelles.

Some of these domains are enriched in specific lipid and protein components and are involved in the regulation of a number of various cellular processes. Some investigators suggest that proteins, both peripheral and transmembrane ones, postranslationally modified with saturated lipids, are recruited to DRMs while those with short, unsaturated and/or branched hydrocarbon chains are not (Bonnin *et al.,* 2003). Indeeed, a relatively large number of observations support the association of glycosylphosphatidylinositol (GPI)-anchored proteins, the most widely studied group of saturated lipid-modified extracellular peripheral proteins, with DRMs (Fig. 1). Such preferential interactions between specialized membrane domains and GPI-anchored proteins were also shown using biomimetic membranes such as supported bilayers (Giocondi *et al.,* 2007). In the case of transmembrane and intracellular peripheral proteins the DRM partitioning is mediated via S-acylation with saturated fatty acids. On the other hand, the other common lipid modifications, such as prenylation and geranylation are considered to play a likely role in targeting proteins to non-microdomain

regions of the membrane (Levental *et al.*, 2010). Recently, by annotating the lipid raft localization of proteins in human protein-protein interaction networks, a systematic analysis of the function of proteins related to lipid rafts was performed. The obtained results demonstrated that lipid raft proteins and their interactions were critical for the structure and stability of the whole network, and that the interactions between them were significantly enriched. This type of analysis revealed that lipid raft proteins have multiple functions and are probably implicated in many biological processes in disease development (Zhang and Li, 2010; Zhang *et al*., 2010).

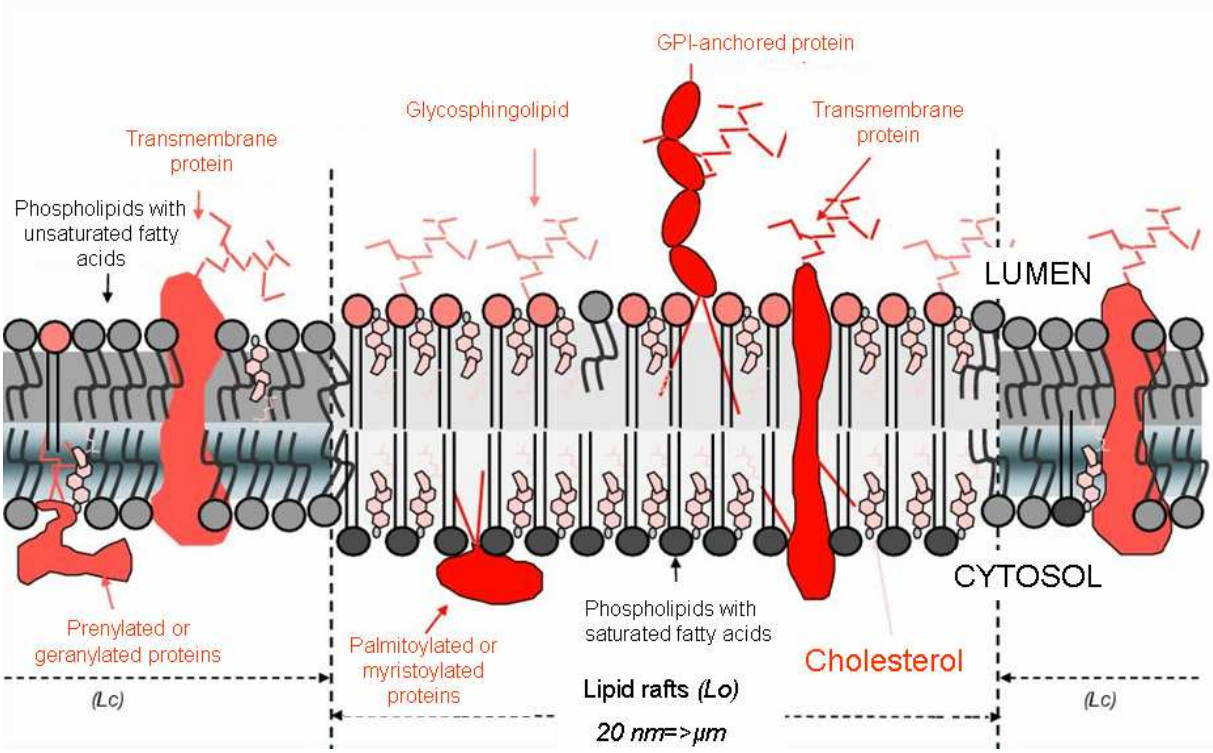

Figure 1. Schematic representation of plasma membrane showing the organization of microdomains characterized by enrichment in (glyco)sphingolipids and cholesterol with associated cell surface proteins. The thickest part of the membrane at the level of rafts reflects higher rigidity of saturated aliphatic chains of lipids forming microdomains. The inner and outer leaflet of the lipid rafts differ in lipid composition. The lipids are represented only by their polar head group and associated sugars. The border between "raft" and "non-raft" region is fluent and subjected to continuous changing. Adopted from Gerlier *et al.*, 2004.

The concept of membrane sub-compartmentalization into heterogeneous microdomains has evolved to a general principle of membrane organization. The existence of dynamic DRMs has been confirmed by different methods. These microdomains are composed of assemblies of glycosphingolipids, cholesterol, sphingomyelin and proteins and serve as functional platforms in membrane signalling and trafficking (Coskun and Simons, 2010; Klose *et al*., 2010; Neumann *et al*., 2010). Cholesterol and sphingomyelin associate in DRM domains and are metabolically co-regulated. Such coordinate regulation occurs in the Golgi

apparatus where the oxysterol binding protein (OSBP) mediates sterol-dependent activation of ceramide transport protein (CERT) activity and sphingomyelin synthesis. CERT activity is dependent on its phosphatidylinositol 4 phosphate-specific pleckstrin homology domain (Banerji *et al*., 2010).

Caveolae are caveolin-1-enriched smooth invaginations of the plasma membrane that form a subpopulation of DRMs. Endocytosis of rafts, including caveolar but also noncaveolar dynamin-dependent and dynamin-independent pathways, is characterized by its cholesterol sensitivity and clathrin-independence (Lajoie and Nabi, 2010).

The mechanism of DRM formation is not well understood. Protein sorting and assembly during membrane biogenesis are accompanied by the appearance of ordered domains of lipids, also called rafts. The rafts are composed of phospholipids, glycosphingolipids and cholesterol. It has been evidenced that cholesterol interacts with sphingomyelin to form a liquid-ordered bilayer phase, but how other lipid molecules are participating in the formation of rafts is not well characterized. The observations accumulated recently suggest that the order created by the quasicrystalline phase may provide an appropriate scaffold for the organization and assembly of raft proteins on both sides of the membrane (Quinn and Wolf, 2010).

Atomic-scale molecular dynamics simulations revealed that cholesterol molecules prefer to be located in the second coordination shell, avoiding direct cholesterol-cholesterol contacts, and form a three-fold symmetric arrangement with the proximal cholesterol molecules. At larger distances, the lateral three-fold organization is broken by thermal fluctuations. For other sterols, with less structural asymmetry, the three-fold arrangement is considerably lost. In conclusion, cholesterol molecules act collectively in lipid membranes. This is the main reason why the liquid-ordered phase only emerges at cholesterol concentrations well above 10 mol% when the collective self-organization of cholesterol molecules arises spontaneously (Martinez-Seara *et al*., 2010).

1.1.2. Identification of DRMs in intracellular membranes

Although DRMs predominantly reside in the plasma membrane, they can be also identified in the intracellular compartments of the cellular secretory pathway. In mammalian cells, it is generally accepted that the endoplasmic reticulum (ER) is poor in lipid rafts (Bonnon *et al*., 2010), and that they are present in the biosynthetic pathway in the Golgi (Simons and Ikonen, 2000). The reason for that is that although cholesterol and ceramide (the precursor of sphingolipids) are both synthesized in the ER, most of the head groups of the

sphingolipids are added only upon reaching the Golgi, and then rafts begin to form. The intracellular membrane microdomains are related to detergent-resistant membranes because, similarly to the latter ones, they are poorly solubilized by cold non-ionic detergents and float in density gradient centrifugation. Such microdomains were found in HT29 cells and were characterized by the presence of the Golgi-resident SPCA1 Ca^{2+}/Mn^{2+} pump and the raft-resident flotillin-2, while SERCA2b was detergent-soluble. Furthermore, cholesterol depletion of these cells resulted in redistribution of flotillin-2 and SPCA1d to the detergent-soluble fractions and inhibited the activity of SPCA1d, while SERCA2b activity was not altered (Baron *et al*., 2010). Moreover, several ER proteins including the erlin-1, erlin-2 or sigma-1 receptor chaperone were identified at lipid raft-like microdomains of the ER membrane. The sigma-1 receptor chaperone, which is highly expressed at a subdomain of ER membrane directly apposing mitochondria, known as the mitochondria-associated ER membrane or MAM, has been shown to associate with steroids as well as cholesterol. The sigma-1 receptor has been implicated in ER lipid metabolism/transport, lipid raft reconstitution at the plasma membrane, trophic factor signalling, cellular differentiation, and cellular protection against beta-amyloid-induced neurotoxicity. Recent studies on the sigma-1 receptor chaperone and other ER proteins clearly suggest that cholesterol may regulate several important functions of the ER including folding, degradation, compartmentalization, segregation of ER proteins, and the biosynthesis of sphingolipids (Hayashi and Su, 2010).

The presence of lipid microdomains in other cellular compartments was also tested. Studies using a new technique employing monoclonal antibody against a homogeneous, mixed, ordered monolayer phase comprised of 60:40 mol% cholesterol:C16-ceramide demonstrated that C16-ceramide/cholesterol structural domains were found at high levels in late endosomes and in the trans-Golgi network, but were not found at statistically significant levels in early endosomes, lysosomes or the endoplasmic reticulum in human embryonic kidney (Hek) 293, hepatocellular liver carcinoma (HepG2), COS7 and BV-2 microglia cells (Goldschmidt-Arzi *et al*., 2011).

Sphingolipid- and cholesterol-rich microdomains at the plasma membrane that coordinate and regulate a variety of signalling processes were implicated in various pathologies including cardiac dysfunctions (Das and Das., 2009; Schwarzer *et al*., 2010), invasion of pathogenic *Escherichia coli* (Tobe, 2010), cell-to-cell HIV-1 transmission (Ono, 2010), Alzheimer's disease (Vetrivel and Thinakaran, 2010) and other neurodegenerative diseases (Parkinson's, amyotrophic lateral sclerosis, Huntington's, those caused by prions) (Schengrund, 2010), obesity and diabetes mellitus (Boini *et al.*, 2010), tumorigenesis and

malignant tumors (Murai *et al*., 2011; Park *et al*., 2010), as well as physiological processes such as brain plasticity (Assaife-Lopes *et al*., 2010; Chichili *et al*., 2010), neuroprotection (Ponce *et al*., 2010), cholesterol homeostasis (Carrasco *et al*., 2010), cell survival and apoptosis (Pommier *et al*., 2010).

Recently accumulated experimental evidence suggests that lipid rafts may be implicated in the etiology of various non-related diseases including lipid storage diseases, such as the Niemann-Pick type C (NPC) disease. There were several attempts to isolate DRMs from NPC cells. Studies using CHO cells (Kosicek *et al*., 2010) demonstrated that cholesterol accumulation upon NPC1 loss may lead to increased lipid raft formation in $NPC1^{-/-}$ cells. Similarly, Lusa *et al*., (2001) have previously reported enhanced association of cholesterol with lipid rafts in Niemann-Pick C1 (NPC1) protein-deficient lipidosis cells. Both of those groups also reported that upon NPC1 loss the accumulated cholesterol in late endosomal/lysosomal compartments is mainly associated with lipid rafts.

1.2 Cholesterol in the cell

1.2.1 Cholesterol distribution in the cell

Cholesterol is an essential structural component of the plasma membrane (especially of the cholesterol-enriched microdomains) and intracellular membranes such as those of endosomes, lysosomes, and the trans-Golgi network, that are in vesicular communication with the plasma membrane,. Other cellular membranes typically have very low levels of cholesterol (Lange *et al*., 1999; Liscum, 2000). In some cases the cholesterol content in the membranes may reach 50% of total lipids (Troup and Wrenn, 2004). In the biosynthetic secretory pathway, cholesterol is low in the endoplasmic reticulum, but its level increases through the Golgi apparatus, with the highest levels in the plasma membrane (Liscum and Munn, 1999). In the endocytic pathway, the endocytic recycling compartment (ERC), which contains recycling membrane proteins and lipids (Mukherjee *et al.*, 1997), also contains high levels of cholesterol (Hao *et al.*, 2002). The cholesterol content of late endosomes and lysosomes is not well documented, but under normal conditions it appears to be lower than in the ERC (Liscum and Munn, 1999; Hao *et al.*, 2002). In polarized epithelial cells, the apical membrane is enriched in cholesterol and sphingolipids relative to the basolateral membrane (Harder and Simons, 1997).

Several years ago, cholesterol was simply thought to rigidify the fluid membrane, thus reducing passive permeability and increasing the mechanical durability of the lipid bilayer.

Cholesterol was also postulated to facilitate post-Golgi protein sorting by regulating the thickness of the lipid bilayer (Bretscher and Munro, 1993). These functions have now been expanded by the key role that cholesterol plays in lipid raft assembly and function (Simons and Ikonen, 2000). Also, its role in signal transduction, immune response, cell infection and cell surface polarity has been investigated (Batetta and Sanna, 2006; Ramjiawan *et al.,* 1996; Reineri *et al*., 2007).

The distribution of cholesterol in intracellular membranes strongly depends on the metabolic activity of a given cell type or tissue and it can be dysregulated in certain pathologies. The correct intracellular distribution of cholesterol among cellular membranes is essential for many biological functions of mammalian cells, including signal transduction and membrane traffic. Intracellular trafficking plays a major role in the proper disposition of internalized cholesterol and in the regulation of cholesterol efflux (Maxfield and Wüstner, 2002). Despite the importance of the transport and distribution of cholesterol within cells for normal physiology and in pathological conditions, many fundamental aspects of intracellular cholesterol traffic are not well understood.

1.2.2 Cholesterol homeostasis

Cholesterol is an essential component of mammalian cell membranes but its excess contributes to several diseases (Soccio and Bresolw, 2004). Mammalian cells tightly regulate their cholesterol content and its intracellular distribution (Simons and Ikonen, 2000). The ER is the primary site of cholesterol synthesis and esterification and the crucial regulatory compartment in cholesterol homeostasis, despite being a cholesterol-poor organelle (65%-80% of total cellular cholesterol is in plasma membrane (PM), whereas only 0.1% to 2% is in ER) (Liscum and Munn, 1999; Maxfield and Wüstner, 2002).

Sterol regulatory element-binding protein (SREBP) transcription factors are part of a homeostatic mechanism whereby cellular cholesterol levels exert negative feedback on cholesterol synthesis (Horton *et al*., 2002). SREBPs are synthesized as transcriptionally inactive ER transmembrane proteins. When cholesterol is abundant, SREBPs remain in ER associated with the escort protein SCAP (SREBP cleavage activating protein) and the ER retention protein Insig (Yang *et al*., 2002). Low cholesterol level induces a conformational change in the sterol-sensing domain of SCAP, (Brown *et al.*, 2002), dissociating Insig and allowing SREBP-SCAP to reach the Golgi.

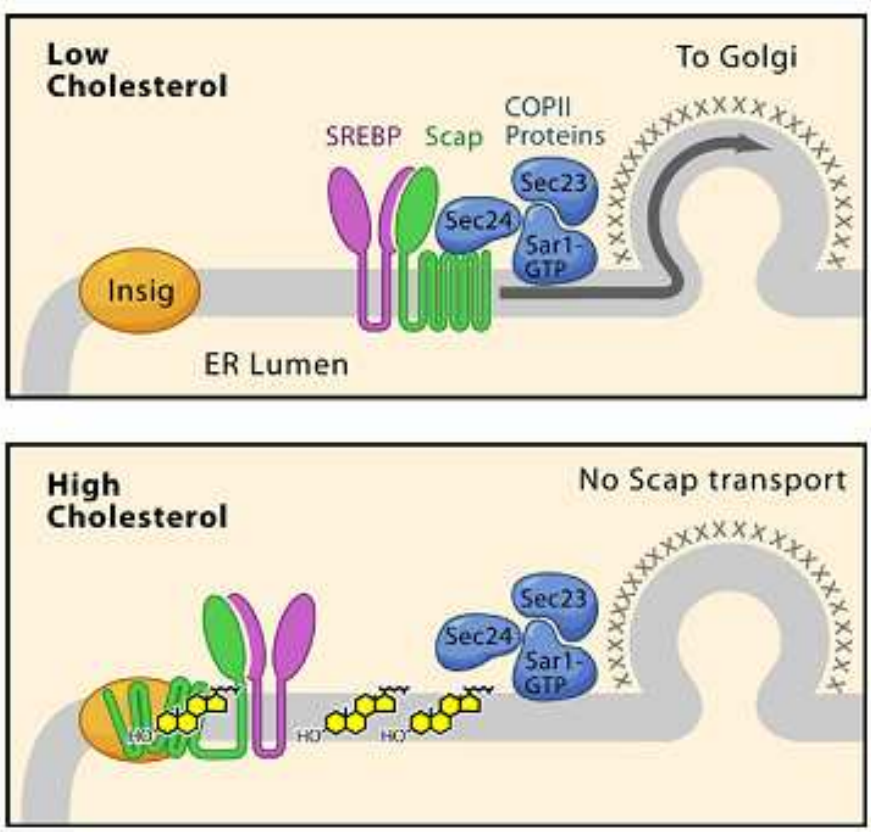

Figure 2. Schematic illustration of the transcriptional regulation of cholesterol homeostasis. (Top panel) When animal cells are deprived of sterols, Scap escorts SREBPs from the ER to Golgi by binding to Sec24, a component of the Sar1/Sec23/Sec24 complex of the COPII protein coat. Once in the Golgi, the SREBPs are proteolytically processed to generate their nuclear forms that activate genes for cholesterol synthesis and uptake. (Bottom panel) Cholesterol negatively regulates the ER-to-Golgi transport by binding to Scap, thereby changing its conformation and triggering the binding of Scap to Insig, an ER anchor protein. Insig prevents the binding of Scap to COPII proteins, thereby halting the transport of SREBPs to the Golgi. Figure from Goldstein *et al*., 2006.

Two proteases in the Golgi release the active form of SREBP, which translocates to the nucleus to activate the transcription of target genes (Fig. 2). Cholesterol synthesis is also regulated posttranscriptionally: high cholesterol accelerates degradation of HMG CoA reductase (HMGR), the rate limiting enzyme in cholesterol synthesis, by promoting association of its sterol-sensing domain with Insig (Sever *et al.*, 2003). The final enzyme of cholesterol synthesis, 7-dehydrocholesterol reductase (DHCR7), also has a sterol-sensing domain and may be similarly regulated.

1.2.3 Cholesterol transport by receptor mediated endocytosis

Cholesterol present in mammalian cells is either (i) synthesized in ER or (ii) internalized from peripheral blood by receptor-mediated endocytosis (Soccio and Breslow, 2004; Ioannou, 2001). LDL particles, ~20 nm in diameter and molecular weight 2500 kDa,

are the main cholesterol transporters. The core of LDL particles consists of about 170 triglyceride and 1600 cholesteryl ester molecules and the surface monolayer comprises about 700 phospholipid molecules and a single copy of apoB-100. In addition, the particles contain about 600 molecules of unesterified cholesterol, of which about one-third is located in the core and two-thirds in the surface (Hevonoja *et al*., 2000).

Cholesterol transport via receptor-mediated endocytosis starts at the cell surface by binding of the LDL particles to cell surface LDL receptors. Then, these receptors are internalized via clathrin-coated pits, and the resulting vesicles shed their coats and fuse with early endosomes (EE) (Fig. 3). Low pH in the early endosomes promotes dissociation of LDL from LDL receptors. The LDL receptors and other recycling proteins then localize to early endosomal tubular extensions, which bud off and fuse with the ERC. A certain amount of early endosomal membrane free cholesterol, from both LDL and endocytosed plasma membrane, may also sort to the ERC in this manner. Vesicles from the ERC return LDL receptors and other recycling proteins and lipids, including cholesterol, to the PM. The LDL particles are further transported inside the cell in multivesicular bodies (MVB) which are also called multivesicular endosomes or endosomal carrier vesicles. MVB are the intermediate vesicles between early and late endosomes (LE). Their particular feature is the presence of membranes implicated in degradation and reverse transport of proteins and lipids to the plasma membrane (Maxfield and Tabas, 2005; Ikonen and Jansen, 2008; Sugii *et al*., 2003). MVB translocate along microtubules and fuse with LE or lysosomes (LY). In comparison to EE, the pH in LE or LY is very low (5.0-6.0). There are also hydrolytic enzymes which degrade LDL to amino acids, cholesterol and fatty acids (Katzmann *et al.*, 2002). Next, cholesterol is exported from LE and LY and delivered to other organelles, including the plasma membrane, the ERC and the ER (Mesmin and Maxfield, 2009). How LDL-derived sterols are trafficked out of LE/LY to reach other organelles is not completely understood, except that the mechanism involves at least two key proteins which reside in LE/LY: the Niemann-Pick type C1 protein and the Niemann-Pick type C2 protein (NPC2). The dysfunction of either of those proteins leads to retention of cholesterol and other lipids in these organelles and delayed movement of lipids from the endocytic pathway to other cellular destinations. Such defects constitute the molecular basis of the inherited autosomal recessive Niemann-Pick type C disease, characterized by abnormal lipid storage in the terminal endocytic compartment (Fig. 3) (Liscum and Sturley, 2004; Maxfield and Tabas, 2005; Vance, 2006; Mukherjee and Maxfield, 2004b).

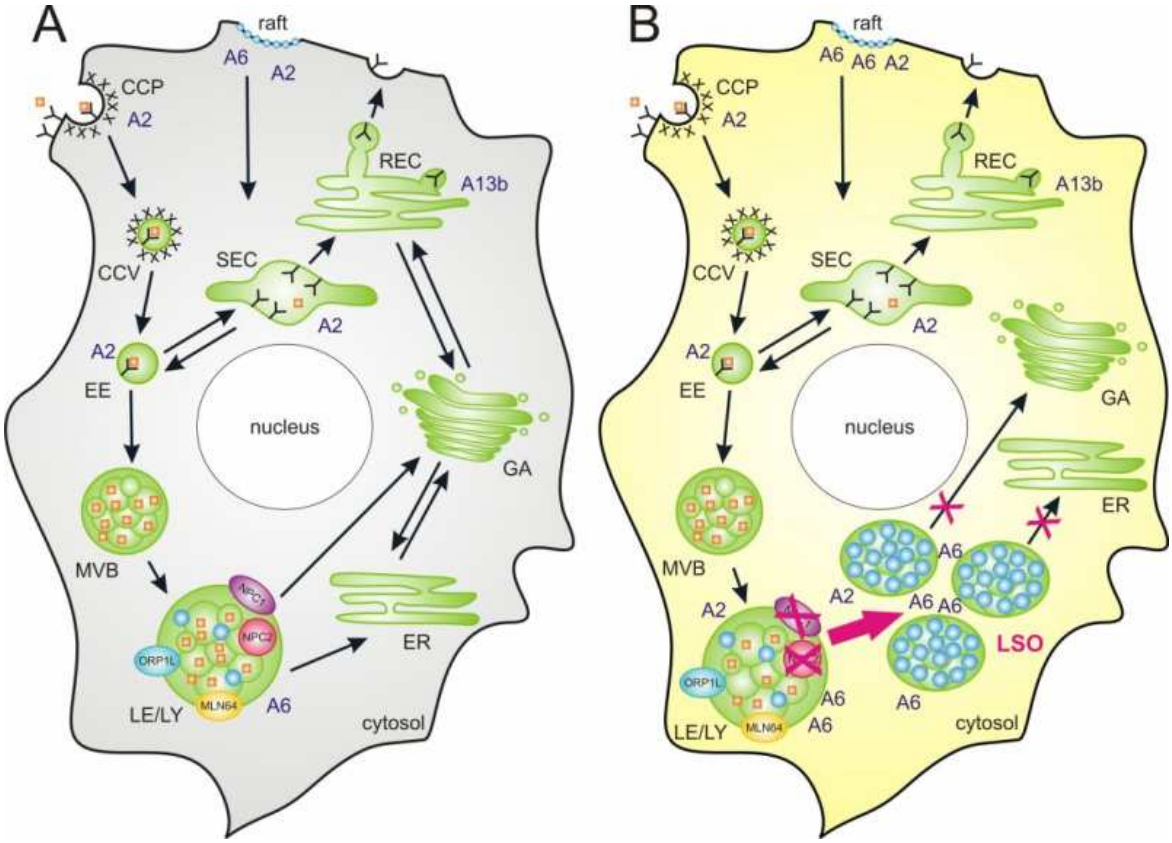

Figure 3. Schematic representation of vesicular transport of low density lipoproteins (LDL) via receptor endocytosis in normal (A) and NPC cells characterized by mutation in the *NPC1* gene encoding the NPC1 protein or in the *HE1/NPC2* gene encoding the NPC2 protein (B). Low level or malfunction of mutated NPC1 or NPC2 proteins lead to disturbances of intracellular cholesterol transport (depicted in panel B by crossed darts) and an overnormative storage of cholesterol in lysosome–like storage organelles (LSO) corresponding to the late endosome/lysosome compartment (LE/LY, pH_{in} 5.0-6.0). Intracellular localization of various annexins (A2, A6, A13b) is also shown. Rafts, cholesterol-enriched membrane microdomains, are also depicted. Other explanations are in the text.

Abbreviations and symbols: CCP – clathrin coated pit; CCV – clathrin coated vesicle (pH_{in} 7.2–7.4); EE – early endosome; SEC – sorting endosome compartment (pH_{in} 5.9–6.0); REC – recirculating endosome compartment; MVB – multivesicular body; GA – Golgi apparatus; ER – endoplasmic reticulum (pH_{in} 7.2–7.4); LE – late endosome (pH_{in} 5.0–6.0); LY – lysosome (pH_{in} 5.0–5.5); NPC1/NPC2 –Niemann–Pick type C1 or C2 proteins; ORP1L and MLN64 – LE proteins participating in the transport of cholesterol; orange squares – LDL particles; black crosses – clathrin network; blue dots – cholesterol. Published in Domon *et al*., 2012, DOI 10.1007/s00018-011-0894-0

It has been proposed that misregulated cholesterol trafficking and intracellular distribution accompany the development and/or sustenance of various unrelated pathologies including Alzheimer's disease, Parkinson's disease and lysosome-storage diseases such as the Niemann-Pick type A/B and type C diseases, Gaucher type I disease, Krabbe disease and perhaps other lipidoses (Liu *et al*., 2010a).

The sphingolipid storage diseases (lysosomal storage disorders) are a collection of ~40 genetically distinct disorders caused by inherited deficiencies of lysosomal hydrolytic activities or lipid transport which result in intracellular accumulation of cholesterol and lipids

in the endosomal/lysosomal network. These disorders have an aggregate prevalence of approximately 1 in 8,000 births worldwide (Meikle *et al*., 1999).

In 1920s based on the pioneering work of Albert Niemann and Ludwig Pick, the eponym "Niemann-Pick disease" (NPD) has since been used to designate a heterogenous group of autosomal recessive lysosomal lipid storage disorders, with common features of hepatosplenomegaly and sphingomyelin storage in reticuloendothelial and parenchymal tissues with or without neurological involvement (Vanier, 2010). Depending on the clinical and biochemical features Niemann-Pick diseases are classified into four groups (A-D).

NPD type A and B occur when the cells lack an enzyme called acid sphingomyelinase (ASM) due to mutations in acid sphingomyelinase *SMPD1* gene. In normal conditions, ASM helps metabolize sphingomyelin, the content of which is particularly high in the brain, where it forms the myelin sheet. If ASM is missing or does not work properly, sphingomyelin builds up inside cells. This leads to abnormal accumulation of sphingomyelin in the cells of many organs in the body, such as liver, spleen and brain (Strzelecka-Kiliszek *et al.,* 2004). Cells of patients with NPD type A usually synthesize only 1% of normal ASM quantity. In cells derived from patients with type B disease, around 10% of normal ASM level was detected (Poulos *et al*., 1984). Type A disease causes death within 2-3 years (McGovern *et al*., 2006), whereas patients with type B can live to adulthood (McGovern *et al*., 2004). Niemann-Pick disease type C (MIM 257220) designates disorders characterized by unique abnormalities in the intracellular transport of endocytosed cholesterol with sequestration of unesterified cholesterol and glycosphingolipids in the late endosome/lysosome compartment, also known as lysosome-like storage organelles (LSO) (Pentchev *et al.,* 1995; Patterson *et al*., 2001; Schiffmann, 2010; Chang *et al*., 2005). NPC disease is due to the mutation in either *NPC1* (Carstea *et al*., 1997) or *NPC2* gene (Naureckiene *et al.,* 2000). There may be a reduced ASM activity in some cells as well.

Patients with type D disease share a common Acadian ancestry (the French Canadian population of Yarmouth County, Nova Scotia), but are otherwise indistinguishable from those with type C. After cloning of the *NPC1* gene, type D was found to be allelic with type C and the designation NPD type C is now used for both entities.

An adult-onset form of the Niemann-Pick disease has been suggested. It is sometimes referred to as type E disease.

1.3 Niemann-Pick type C disease

1.3.1 Clinical diagnosis of NPC disease

Niemann-Pick type C disease is panethnic. The prevalence in Western European countries (France, UK, Germany) has been estimated to be approximately 1 in 150,000 living births (Vanier and Millat, 2003). In Poland, 1-5 babies with NPC are born each year. However, this is probably an underestimate, due to the fact that atypical phenotypes may not be recognized.

Diagnosis of the NPC disease is relatively easy in patients with the most typical symptoms, such as combined hepatosplenomegaly, ataxia and supranuclear vertical gaze palsy. However strikingly different clinical presentations exist, especially in infants and neonates. The genetic defects that cause NPC fall into two complementation groups. The majority (~95%) of the NPC disease cases is associated with mutations in the *NPC1* gene located on chromosome 18q11-q12 (Carstea *et al*., 1993; Carstea *et al*., 1997; Liscum, 2000). The protein product of the *NPC1* gene is a large (1278 amino acids), transmembrane, heavily glycosylated late endosome NPC1 protein (Ioannou, 2000; Ioannou, 2001; Scott and Ioannou, 2004). Only ~5% of NPC cases are associated with mutation in the *HE1/NPC2* gene located on chromosome 14q24.3. NPC2 is a small (151 amino acids) soluble protein that resides in the lumen of late endosomes/lysosomes and the trans-Golgi network (TGN) in normal cells and localizes almost exclusively to the LE/LY in NPC mutants (Naureckiene *et al*., 2000; Blom *et al.,* 2003). Both NPC1 and NPC2 proteins, as cholesterol binding proteins, are implicated in transport of lipids from the late endosome/lysosome compartment to other cellular compartments such as plasma membrane, endoplasmic reticulum and Golgi (Ory, 2000; Ko *et al*., 2003; Infante *et al.*, 2008).

1.3.2 Genetic and biochemical identification of NPC disease

In NPC cells, cholesterol uptake, its delivery to LE/LY, and hydrolysis of cholesterol ester proceed in a regular way. However, cholesterol does not leave the LE/LY compartment and accumulates in large amounts as free unesterified cholesterol, which can be detected by filipin staining. As a result of this block in cholesterol traffic, the rising cholesterol level in the cell cannot be sensed by the ER, and none of the homeostatic mechanisms is initiated. The LE/LY compartment thus continues to accumulate cholesterol, and the LE/LY change morphologically to become highly enlarged LSOs, which contain whorls of membranes inside (Pentchev *et al*., 1995; Liscum and Klansek, 1998; Mukherjee and Maxfield, 2004b) (Fig. 3).

It is important to note that in NPC cells, the storage material in the LSO is not restricted to cholesterol and, in fact, contains a large variety of lipids especially sphingomyelin, lyso-bis-phosphatidic acid (LBPA), neutral and acidic glcosphingolipids (GSLs), phospholipids but also sphingosine and proteins (Liscum, 2000; Vanier, 1999; Pentchev *et al*., 1995).

1.3.3 Therapeutic strategies for NPC disease

Several strategies have been attempted for treatment of NPC disease, however a satisfying method has not been found yet. Some of them employ substrate reduction strategies including statins, low-cholesterol diet, ezetimibe treatments or inhibition of free cholesterol production via hydrolysis of cholesteryl esters by inhibiting lysosomal acid lipase (LAL) (Patterson and Platt, 2004; Liu *et al*., 2009; Rosenbaum *et al.*, 2009; Rosenbaum and Maxfield, 2011).

Other strategies include the use of Miglustat (N-butyl-deoxynojirimycin; Zavesca®) and acid sphingomyelinase treatments (Wraith *et al*., 2010; Patterson *et al*,. 2007; Pineda *et al*., 2009). Recent investigation of the interplay between sphingolipids and cholesterol in the NPC disease has focused on ASM deficiency (Devlin *et al*., 2010). The study demonstrated that despite a normal ASM gene, NPC-deficient cells have much lower levels of ASM activity. Restoration of ASM activity levels reverted cholesterol and bis(monoacylglycerol)phosphate (BMP) accumulation in both NPC1 and NPC2 mutant cells, and restored normal protein trafficking.

Subsequent studies by (Davidson *et al.*, 2009) and (Liu *et al.*, 2009; 2010b) have shown that treatment of *NPC*$^{-/-}$ mice with hydroxypropyl-beta-cyclodextrin (membrane-impermeant cyclic oligosaccharides, which have been used extensively to modulate cholesterol and other lipids' composition of model and biological membranes (Zidovetzki and Levitan, 2007)) demonstrated significant improvements in murine viability and neurological features. Despite their inability to cross membranes, cyclodextrins (CDs) have been shown to be retained by cells (Kilsdonk *et al*., 1995). CDs can be delivered via pinocytosis to LE/LY, where they can replace the function of NPC1 and NPC2 proteins (Rosenbaum *et al*., 2010) and promote cholesterol esterification by acyl Co-A:cholesterol acyl transferase (ACAT) (Abi-Mosleh *et al.*, 2009). The exact nature of CD action to replace NPC1 and NPC2 function in LE/LY is yet to be determined. From the clinical treatment perspective, further optimization of the pharmacological properties of CD-based NPC therapeutics would be

necessary to enhance CD delivery to the lysosomal compartment, enhance its transcytosis across the blood–brain barrier, and decrease CD elimination through urine.

Also, proteostasis modulation with chemical chaperones has been proposed as a therapy for lysosomal storage disorders (Balch *et al*., 2008). Enhancement of the NPC1 I1061T mutant folding by non-specific chemical chaperones that caused better trafficking of NPC1 to LE/LY and reduced NPC phenotype has been recently demonstrated in cultured cells (Gelsthorpe *et al.*, 2008). Further work is needed to identify the specific mutations that are susceptible to such treatment as well as other chemical chaperones that might be more specific for the NPC disease.

Although questions still remain about the precise molecular mechanism of NPC1- and NPC2-mediated cholesterol efflux from LE/LY, we are gathering more information about this critical step in cellular cholesterol homeostasis.

In the Niemann-Pick type C disease, the absence, low level and/or presence of dysfunctional NPC1 and NPC2 proteins may not be the only cause of the disease. A growing number of evidence suggests that malfunction and dysregulated content or intracellular distribution of other proteins should be considered as an important factor contributing to NPC disease etiology. In this regard, annexins (Fig. 3), proteins involved in the regulation of cell membrane dynamics (Fig. 3), are gaining attention of many investigators.

1.4 Annexins

1.4.1 Annexins as proteins implicated in cholesterol transport and interactions with membranes

Many protein families were described as affecting cholesterol transport or as being affected by cholesterol. Annexins were found to co-localize with cholesterol at the plasma membrane, undergo similar trafficking throughout the endocytic pathway and provide a link between calcium signalling and cholesterol transport (Grewal *et al*., 2010; Enrich *et al*., 2011).

One of the most powerful factors regulating membrane-protein interactions are changes in intracellular Ca^{2+} concentration. Eukaryotic cells contain a wide variety of Ca^{2+}-sensing proteins that participate, as effectors, in mediating responses to changes in cytosolic Ca^{2+} concentration. Annexins are a family of calcium-dependent phospholipid binding proteins which are present in all eukaryotes. There are currently 12 identified human annexins all of which contain unique calcium binding sites, embedded in the highly conserved annexin

repeat motifs within the C-terminal core. In addition to the C terminal core annexins contain a significantly more variable N- terminal tail. Annexins are expressed in different tissues and are able to associate with different intracellular membranes. They are found both in the cytoplasm and bound to membranes, thus they can play a role in membrane related processes (Gerke and Moss, 2002; Mayran *et al.*, 2003).

Annexins, due to their ability to bind biological membranes in a calcium-dependent manner, provide a link between calcium signalling and membrane-related cellular functions, including various signalling pathways, cell differentiation and migration. Members of the annexin protein family are ubiquitously expressed and function as intracellular Ca^{2+} sensors. Most cells contain multiple annexins. It is strongly believed that annexins exert their biological function through influencing membrane dynamics, promoting membrane segregation and membrane fusion (Gerke *et al.*, 2005). Moreover, annexins were found to participate in plasma membrane repair mechanisms by reacting to the influx of extracellular Ca^{2+} evoked by mechanical stress, toxins, pathogens, etc. The combination of the presence of various annexins in a given cell type together with their individual Ca^{2+}-sensitivity allow for spatially confined, graded responses to membrane injury (Draeger *et al.*, 2011).

Annexins are well suited to perform their specific biological activity due to the presence of a unique N-terminal domain which enables each annexin to perform unique functions in a diverse range of cellular processes including cytoskeleton regulation, membrane conductance and organization as well as exo- and endocytosis (Futter and White, 2007). Given their involvement in such a variety of processes it is not surprising that the annexins have also been implicated in a range of pathologies, such as the progression of cancer, diabetes, the autoimmune disorder anti-phospholipid syndrome and others frequently related to dysregulated vesicular traffic (Hayes *et al.*, 2007; Lim and Pervaiz, 2007; Fatimathas and Moss, 2010; Grewal *et al.*, 2010; Grewal and Enrich, 2009).

One of the intriguing features of annexins is their ability to participate in the lateral organization of biological and artificial lipid membranes. It was found for example that artificial membranes formed from POPC/POPS exhibit phase separation into POPC- or POPS-enriched domains in a Ca^{2+} concentration-dependent manner. Annexin A1 (AnxA1) was found to interact with these membranes in the presence of calcium and to form irreversible complexes with POPS-enriched microdomains; the attachment of AnxA1 to POPC enriched regions of membrane was fully reversible (Faiss *et al.*, 2008). The appearance of microdomains has also been observed when AnxA6 was interacting with PC/PS interfacial monolayers deposited onto a calcium containing subphase (Golczak *et al.*, 2004). The

question arises whether annexins might act in a similar manner also *in vivo*, affecting lateral organization of lipids, especially cholesterol, and of other membrane components and to contribute, in this way, to biogenesis, function and disappearance of cholesterol-enriched microdomains.

1.4.2 Annexins associated with cholesterol in membrane microdomains.

According to the equilibrium model, lipid rafts are membrane regions enriched in cholesterol, sphingolipids and many membrane proteins. Proteins can associate with lipid rafts via at least three different modes (i) partitioning into the outer leaflet of the lipid bilayer via GPI anchors (Simons and Ikonen, 1997; Brown and London, 2000), (ii) partitioning into lipid rafts due to the intrinisic properties of transmembrane domains, such as a stretch of hydrophobic residues in contact with the outer leaflet of the plasma membrane, as in the case of transmembrane proteins such as the hemagglutinin of the influenza virus (Scheifele *et al*., 1997) or (iii) by association with the inner leaflet via acylation, palmitoylation (Yang *et al*., 2010) or by direct interaction with cholesterol.

Many members of the annexin family were found in membrane microdomains in plasma and intracellular membranes of different cell types. Proteomic and immunochemical studies revealed the presence of annexins at DRMs (Feuk-Lagerstedt *et al*., 2007; Godoy and Riquelme, 2008; Staubach *et al.*, 2009), suggesting that annexins may participate in biogenesis, stabilization and dynamics of membrane microdomains (lipid rafts). Different annexins seem to participate to different extents in the organization of lipid rafts; their association and thus their role being regulated by changes in cytosol conditions (Ca^{2+} or pH) and membrane lipid content (cholesterol, acidic phospholipids) (Gerke and Moss, 2002).

Experimental evidence favors the idea that some annexins may resemble other cholesterol-interacting proteins, and that their intracellular localization and membrane binding is determined by cholesterol (Fig. 3) (Lambert *et al*., 2004). Some experimental data suggest that certain functions of annexins may be regulated by cholesterol and, last but not least, that annexins may participate in cholesterol traffic and storage. Factors were identified that play a role in regulation of annexin-membrane interactions, including calcium, pH and membrane lipid composition. Annexins may contribute to the organization, stabilization and dynamics of lipid rafts by affecting their lateral membrane distribution. Furthermore, by attracting other proteins and signalling molecules onto lipid rafts and by influencing soluble versus membrane protein interactions, they may serve as regulatory molecules in various signalling pathways.

As it was already mentioned, annexins belong to a multigene family of ubiquitous mammalian proteins, represented by 12 subfamilies encoded by *ANXA1-A11*, and *ANXA13* genes and many more isoforms, genre- and tissue-specific. They are Ca^{2+}-dependent phospholipid-binding proteins composed of two domains: a condensed core responsible for Ca^{2+} and phospholipid binding and a variable N-terminal tail. Annexins are expressed in different tissues and are able to associate with plasma membrane and intracellular membranes of various organelles. They are found both in the cytoplasm and bound to membranes, thus they can play a role in membrane related processes (Gerke and Moss, 2002; Mayran *et al*., 2003).

AnxA1: The quartz crystal microbalance (QCM) technique, in combination with solid-supported lipid bilayers, were used to monitor the interaction of annexin A1 (AnxA1) with lipid membranes. The affinity constants determined for the binding of AnxA1 to lipid membranes of different compositions reveal that at low calcium ion concentration, the presence of cholesterol increases the binding affinity of AnxA1 to lipid membranes, reinforcing the idea that cholesterol might be important for forming a high affinity interface for the attachment of the protein (Kastl *et al.*, 2002).

AnxA2: It is proposed that AnxA2 forms cholesterol-rich platforms that organize the membranes of early endosomes at the onset of the degradation pathway (Harder *et al*., 1997; Oliferenko *et al.*, 1999). It was suggested that in the presence of Ca^{2+} AnxA2 binds to and possibly promotes the lateral association of glycosphingolipid- and cholesterol-rich membrane microdomains (Babiychuk and Draeger, 2000; Babiychuk and Draeger, 2006).

AnxA2 has been localized at membrane lipid rafts (Heyraud *et al*., 2008). Moreover, it has been demonstrated that catecholamine-evoked formation of lipid rafts in the plasma membrane, essential for exocytosis, can be attributed to the AnxA2 tetramer. On the basis of this finding it was proposed that AnxA2 may act as a calcium-dependent promoter of lipid microdomains required for structural and spatial organization of the exocytotic machinery (Ayala–Sanmartin, 2001). Furthermore, there is a growing number of evidence suggesting that cholesterol is a very important factor influencing AnxA2 and other annexins interactions with membranes of cellular organelles (Chasserot-Golaz *et al*., 2005; de Diego *et al*., 2002). AnxA2 was shown to be associated with chromaffin granules in the presence of EGTA (Ayala–Sanmartin *et al*., 2001). This bound AnxA2 was released from the membranes by methyl-β-cyclodextrin (MβCD), which depleted cholesterol from the membranes. Restoration of the cholesterol content of chromaffin granule membranes with cholesterol/MβCD complexes restored the Ca^{2+}-independent binding of AnxA2 (Ayala–Sanmartin *et al*., 2001).

The core domain of AnxA2 was found to be responsible for the cholesterol-mediated effects (Chasserot-Golaz *et al*., 2005). A similar phenomenon was previously described (Harder *et al.*, 1997). Even a low concentration of cholesterol sequestering agents such as filipin or digitonin quantitatively released AnxA2 from the membranes of early endosomes of baby hamster kidney (BHK) cells. In the absence of Ca^{2+}, AnxA2, especially in its tetrameric form, bound to liposomes containing phosphatidylserine, and addition of cholesterol to these liposomes increased the binding. Also liposomes containing phosphatidylserine and cholesterol were aggregated by the tetrameric form of AnxA2 at submicromolar Ca^{2+} concentrations (Ayala-Sanmartin *et al*., 2001). In the case of liposomes containing phosphatidic acid (PA), the supplementation with cholesterol in the absence of Ca^{2+} increased AnxA2 binding and this binding was only marginally affected by MβCD (Mayran *et al*., 2003). These results are in contrast with other studies (Ross *et al*., 2003) in which, using quartz crystal microbalance with dissipation monitoring (QCM-D) and liposome techniques, it has been demonstrated that the AnxA2 heterotetramer does not bind in a Ca^{2+}-independent manner to cholesterol-containing membranes. These contraries may be due to the fact that the tests (Ross *et al*., 2003) were performed using AnxA2 heterotetramer purified from porcine intestine while the other researchers used recombinant AnxA2. It is possible that the specific membrane structure (Zeuschner *et al*., 2001) allows localization of AnxA2 at cholesterol-rich membranes *in vivo*. The results obtained for AnxA2, initiated the analysis of AnxA6 – another important member of the annexin family.

AnxA5: Analysis performed in (Ayala-Sanmartin *et al*., 2001) revealed that in the absence of Ca^{2+}, AnxA5 was unable to bind to PC/PS (75/25 by weight) or PC/PS/cholesterol (50/25/25, by weight) liposomes, however in the presence of calcium the amount of bound AnxA5 was significantly higher for the PC/PS/cholesterol than for PC/PS liposomes at pH 7.4. Other *in vitro* tests (including surface plasmon resonance analysis) with AnxA5 suggest that phosphatidylserine plays a dominant role in AnxA5 binding to liposomal membranes (Jeon *et al*., 2010). However, the binding level of AnxA5 to liposomes increased with an increase in the cholesterol content. This may suggest that cholesterol in liposomes may act as a “phospholipid arrangement factor”. It is worth noticing that in the absence of PS cholesterol did not exert the binding enhancement effect. Stability of AnxA5 binding was significantly improved by the increase in cholesterol content. *In vitro* experiments using reconstituted systems confirmed that annexins may affect lipid phase behavior and protein partitioning into giant liposomes, as in the case of AnxA5 (Johnson *et al.*, 2010). The interaction of AnxA5

with artificial membranes was strongly affected by the presence of cholesterol (Jeon *et al*., 2010).

AnxA6: AnxA6 (Fig. 4) is the largest member of the family of annexins. Due to alternative mRNA splicing of the 21st exon, in mammalian cells, AnxA6 is expressed in two isoforms: AnxA6-1 and AnxA6-2, the latter lacking the 524-VAAEIL-529 sequence at the start of repeat 7 (Smith *et al*., 1994). AnxA6-1 prevails in normal tissues and cells, such as mouse Balb/3T3 fibroblasts (Kaetzel *et al*., 1994), while AnxA6-2 is more abundant in neoplastic cells (Edwards and Moss, 1995). Concerning the functional differences between isoforms, the available data suggest that the EGF-dependent Ca^{2+} influx in A431 cells transfected with AnxA6 isoforms is specifically inhibited by AnxA6-1 and that the smaller splice variant has no discernible effect on cellular phenotype and growth rate (Fleet *et al*., 1999). On the other hand, AnxA6-2 is characterized by a higher affinity for Ca^{2+}, lower hydrophobicity and lower negative surface charge, as compared to AnxA6-1 (Kaetzel *et al*., 1994).

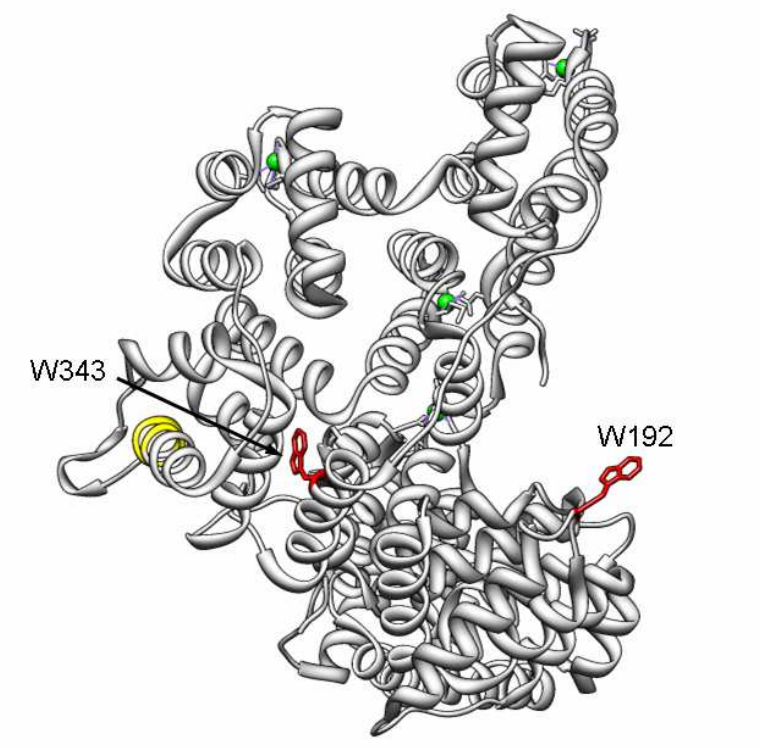

Figure 4. Crystal structure of AnxA6 (Freye-Minks *et al*., 2003). Localization of tryptophan residues W192 and W343 (in red) and the VAEILL sequence (in yellow). The Ca^{2+} ions are marked in green. The figure was prepared using Chimera, version 1.5.3 software from PDB coordinates (PDB accession number 1M9I).

Although the physiological role of AnxA6 is still unknown, it has been demonstrated that this protein is implicated in processes related to vesicular transport such as endo- and exocytosis, membrane aggregation, and membrane fusion (de Diego *et al*., 2002; Jackle *et al*.,

1994; Pol *et al*., 1997; Grewal *et al*., 2000). It has been shown to be predominantly associated with membranes of late endosome and prelysosomal compartments of NRK fibroblasts, WIF-B hepatoma, and rat kidney cells (de Diego *et al*., 2002; Pons *et al*., 2000; Pons *et al*., 2001). Although the majority of AnxA6 is most likely targeted to membranes via Ca^{2+}-dependent binding to negatively charged phospholipids (Golczak *et al*., 2004) it was also demonstrated that its binding to the membranes depends on the cholesterol content. In addition, it has been shown that AnxA6 is a molecule linking calcium signalling with cholesterol transport, working as a scaffold/targeting protein for several signalling proteins (Enrich *et al*., 2011).

Many researchers observed Ca^{2+}-dependent translocation of AnxA6 to Triton-X100 insoluble caveolin- and cholesterol-enriched membrane fractions (caveolae/membrane rafts). AnxA6 is implicated in the organization of membrane domains, in particular in their association with cytoskeleton in smooth muscle cells (Babiychuk and Draeger, 2000; Babiychuk *et al.*, 1999). Since AnxA6 can bind phospholipids, actin (Hayes *et al*., 2004; Monastyrskaya *et al.*, 2009) and signalling proteins it is also presumed that it could stabilize and regulate the assembly of lipids and proteins during caveolae/membrane raft formation (Grewal *et al*., 2010; Grewal and Enrich, 2009; Grewal and Enrich, 2006).

Previous observations (Ayala-Sanmartin, 2001) suggest that in the absence of Ca^{2+}, AnxA6 was unable to associate with liposomes made of PC/PS (75/25 by weight) or PC/PS/cholesterol (50/25/25 by weight). However, in the presence of Ca^{2+} the amount of bound annexin was significantly higher for the cholesterol-containing liposomes. This demonstrates that cholesterol stimulates binding of AnxA6 to liposomes *in vitro* (Ayala-Sanmartin, 2001).

Other annexins: Other annexins, such as AnxA4, AnxA7, AnxA13, and AnxA8, due to their cellular localization along the endocytic pathway or in the membrane microdomains, or because of their sensibility to cholesterol sequestering agents, are supposed to interact with cholesterol. The impact of different annexins on the organization of membrane domains (lipid rafts) depends on how their membrane association is determined by changes in the cytosol conditions (Ca^{2+} or pH) and on the membrane lipid content (cholesterol, acidic phospholipids) (Gerke and Moss, 2002). Other annexins, in particular AnxA13, much like AnxA2, may define specific platforms on other cellular membranes (Lafont *et al*., 1998). AnxA13b has been assigned to raft-dependent and -independent apical traffic in MDCK cells (Astanina *et al*., 2010). The interaction of annexins with membranes, including lipid rafts, is regulated by phosphorylation (Das and Das, 2009).

1.4.3 Annexin-related pathologies

Several lines of evidence suggest that annexins may also participate in some pathologies including obesity and type II diabetes mellitus (Stögbauer *et al*., 2009) by exerting their biological function through interaction with membrane constituents of the rafts. Studies carried on cell lines from patients suffering from the NPC disease have shown that intracellular distribution of annexins, including their association with late endosome/lysosome compartment in NPC cells, matches cholesterol distribution in these cells (Sztolsztener *et al*., 2010). On the basis of these findings we formulated a hypothesis that some annexins may play a role in intracellular cholesterol storage, including the aberrant storage occurring in NPC disease.

Upon cell activation, AnxA6 is recruited to the plasma membrane, endosomes and caveolae/membrane rafts to interact with signalling proteins, and to the endocytic machinery and actin cytoskeleton to inhibit epidermal growth factor receptor and Ras signalling. In addition, AnxA6 associates with late endosomes to regulate cholesterol export which in turn leads to reduced cytoplasmic phospholipase A_2 activity and caveolae formation. Investigators suggested that AnxA6 may function as an organizer of membrane domains by creating a scaffold for the formation of multifactorial signalling complexes which regulate transient membrane-actin interactions during endocytic transport, and modulate intracellular cholesterol homeostasis (Grewal *et al*., 2010).

Cells expressing high levels of AnxA6 were characterized by accumulation of caveolin-1 in the Golgi complex. This was associated with sequestration of cholesterol in the late endosomal compartment and lower levels of cholesterol in the Golgi and the plasma membrane, both factors likely contributing to the retention of caveolin in the Golgi apparatus and to a reduced number of caveolae at the cell surface. Furthermore, knock down of the *AnxA6* gene and the ectopic expression of the Niemann-Pick C1 protein in AnxA6-overexpressing cells restored the cellular distribution of cav-1 and cholesterol, respectively. The authors also demonstrate that elevated expression of AnxA6 perturb the intracellular distribution of cholesterol and indirectly inhibits the exit of caveolin from the Golgi complex (Cubells *et al*., 2007; Cubells *et al*., 2008).

AnxA2 was found to bind a proprotein convertase subtilisin/kexin-type 9 (PCSK9), which is responsible for degradation of the hepatic low density lipoprotein receptor (LDLR). This AnxA2-PCSK9 complex was found to prevent PCSK9-directed LDLR degradation and this way regulates endogenous low density lipoprotein receptor levels (Mayer *et al.*, 2008; Davignon *et al*., 2010). Therefore AnxA2 started to be considered as a target for the treatment

of hypercholesterolemia. AnxA2 was also implicated in the Niemann-Pick type C disease (Valasek *et al*., 2005). Both AnxA2 and AnxA6, proteins that are important in endocytic trafficking, showed distorted distributions in NPC cells related to the mislocalization of membrane microdomains (te Vruchte *et al*., 2004).

CHAPTER 2

AIMS

The Niemann-Pick type C disease is a lipid storage disorder characterized by abnormal accumulation of cholesterol in the late endosome/lysosome compartment. Even though it was demonstrated that the NPC disease is associated with dysfunction of NPC1 and/or NPC2 proteins, the mechanism of cholesterol accumulation in NPC cells is still not well understood.

Taking into account that cholesterol is the most abundant constituent of lipid microdomains we hypothesize that the abnormal accumulation of cholesterol in NPC cells could lead to disturbed formation of lipid microdomains.

There are some suggestions that (in addition to NPC1 and NPC2) other cellular proteins, especially those implicated in cholesterol transport and present in the lipid microdomains (e.g., AnxA6) could be implicated in the etiology of the disease.

Thus, the aim of the work described in this thesis was to detect and isolate lipid microdomains from NPC and control fibroblasts and to identify AnxA6 in these microdomains. Furthermore, using biophysical methods, we intended to establish the interactions between AnxA6 and cholesterol-enriched microdomains and elucidate the molecular nature of these interactions.

To fulfill the main objectives of my PhD thesis, I focused my research effort on the following specific topics:

1. Characterization of AnxA6-lipid microdomain interactions in NPC and control cells
   - Visualization of lipid rafts markers and isolation of DRMs from NPC and control cells
   - identification of AnxA6 in DRMs of NPC and control cells
   - analysis of the effect of Ca^{2+} on AnxA6 distribution in DRMs from NPC and control cells

2. Analysis of the mechanism of AnxA6 – cholesterol interactions using biomimetic systems
   - characterization of the interfacial properties of the AnxA6-1 isoform, its W343F mutant and of the AnxA6-2 isoform
   - analysis of AnxA6-cholesterol interactions (effects of pH, Ca^{2+}, identification of structural elements involved in these interactions)
   - analysis of Ca^{2+} effect on AnxA6 interactions with other constituents of lipid microdomains

CHAPTER 3

MATERIALS AND METHODS

3.1 Fibroblast cell lines

3.1.1 Clinical diagnosis of Niemann-Pick type C disease

Biopsies of skin were provided by the Department of Metabolic Diseases, Children's Memorial Health Institute in Warsaw (Poland). Due to the wide variability of early symptoms of NPC disease, clinical diagnosis of the condition may be difficult. The diagnostic testing was conducted in the Department of Metabolic Diseases, Children's Memorial Health Institute in Warsaw. Skin fibroblasts taken from the forearm of suspected patients were grown in the laboratory and the cholesterol transport in those cells was tested based on the accumulation of free cholesterol assessed by filipin staining (Rodriguez-Agudo *et al*., 2008) and on the level of LDL-induced cholesteryl ester formation as described in (Ribeiro *et al*., 2001).

Further genotyping analysis ordered by the Laboratory of Biochemistry of Lipids revealed that fibroblasts taken from the forearm of a 3-year old patient (L1) were characterized by two mutations of the *NPC1* gene. Mutation R348X is a defect localized in exon 8 and leads to the creation of a premature termination codon (Sztolsztener *et al*., 2010). Mutation R1186H in exon 23 was previously described by (Vanier and Millat, 2003). The classical lethal female patient L1 presented enlarged liver and spleen (hepatosplenomegaly) at birth and showed the first symptoms of neurodegeneration at the age of 3. Control fibroblasts were taken form the forearm of a healthy individual.

3.1.2 Cell culture

Tissue samples were treated with collagenase (2.5 mg/ml) in HAM F-10 for 24 h at 37 °C in 5% CO_2 humidified atmosphere. After incubation, pieces of skin were disrupted mechanically by passing through the needle and put into fresh medium for 7 days.

The obtained skin fibroblasts were cultured in Dulbecco's Modified Eagle Medium (DMEM, Sigma-Aldrich, Germany) of high glucose content (4.5 g/l), containing 4 mM L-glutamine and supplemented with 10% fetal bovine serum (FBS, Gibco BRL, Great Britain), 100 U/ml penicillin and 100 μg/ml streptomycin at 37 °C in a humidified atmosphere containing 5% CO_2. Fibroblasts were cultured on 100 mm cell culture dishes (Becton Dickinson Labware, USA) until they covered 80-90% of the bottom. To dissociate the fibroblasts, the bottom of the dish was rinsed with phosphate buffered saline (PBS) (125 mM NaCl, 5 mM KCl, 10 mM Na_2HPO_4, 1 mM KH_2PO_4) and next incubated with 10% trypsin (Sigma-Aldrich, Germany) for 3 min at 37 °C. Trypsin was inactivated with DMEM. Next,

cells were either directly used in experiments or frozen. To freeze, cultured cells were centrifuged (500 x g, 3 min), the medium above the pellet was removed and the cells were resuspended in DMEM supplemented with 10% FBS and 5% DMSO (Sigma-Aldrich, Germany). After the cells were aliquoted into appropriate cryogenic vials, they were placed at -80 °C for at least 5 hours and next placed in liquid nitrogen for a long term storage.

To thaw the fibroblasts stored in liquid nitrogen, the vials were thawed quickly in water bath at 40-50 °C, next placed on ice. Then, the thawed material was diluted in cold medium and centrifuged (500 x g, 3 min). The pellet was resuspended in DMEM supplemented with 10% FBS and transferred into a culture dish. After 24 hours, after rinsing the cells with PBS, the medium was changed. Both cell lines used in experiments were at the same passage (7-13). The growth and distribution of NPC and control fibroblasts was observed under an Axiovert 40C inverted microscope (Zeiss, Sweden).

3.1.3 FACScan analysis

For cell cycle analysis (Dressler *et al*., 1988) normal and NPC fibroblasts (10^6) were centrifuged at 1,000 x g for 5 min and the pellet was suspended in 1 ml PBS. Cell suspension was added into absolute ethanol, 70% final concentration and fixed overnight at -20 °C. Then, cells were centrifuged, suspended in 50 μg/ml propidium iodide in PBS containing 0.1 mg/ml RNase and 0.05% Triton X-100, incubated for 40 min at 37 °C, centrifuged, suspended in 2 ml PBS. Then, the cells were counted using a FACScan flow cytometer (Becton-Dickinson, USA) and the cell size, granularity and cell cycle distribution were analyzed using the Cell Quest software (Becton-Dickinson, USA).

3.2 Techniques related to the preparation of membrane fractions

3.2.1 Cell fractionation

To isolate early endosomes, late endosomes and heavy membranes, a step sucrose floatation gradient was used according to the protocol of (Grewal *et al*., 2000). Briefly, control and NPC fibroblasts (2.5 x 10^7 cells) were washed in PBS, scratched in ice cold homogenization buffer (250 mM sucrose, 3 mM imidazole, pH 7.4, 10 μg/ml protease inhibitors cocktail (PIC, Sigma-Aldrich, Germany)) and homogenized by passing through a 22-gauge syringe needle. The homogenates were centrifuged at 1,200 x g for 15 min at 4 °C in a Sigma 2K15 centrifuge. Post-nuclear supernatant (PNS) was brought to a final 40.2% sucrose (w/v) concentration by adding 62% sucrose (in 3 mM imidazole, pH 7.4) and loaded

at the bottom of a 5 ml centrifugation tube (Kendro Laboratory Products, Germany). Sucrose density gradient was formed by pouring stepwise 35%, 25% sucrose and finally the homogenization buffer on top of the PNS. The gradient was centrifuged at 220,000 x g for 120 min at 4 °C in a swing out Sorvall AH-650 rotor (Fig. 5). After centrifugation, the material located at the interphases between homogenization buffer/25%, 25/35%, and 35/40.2% was collected starting from the top.

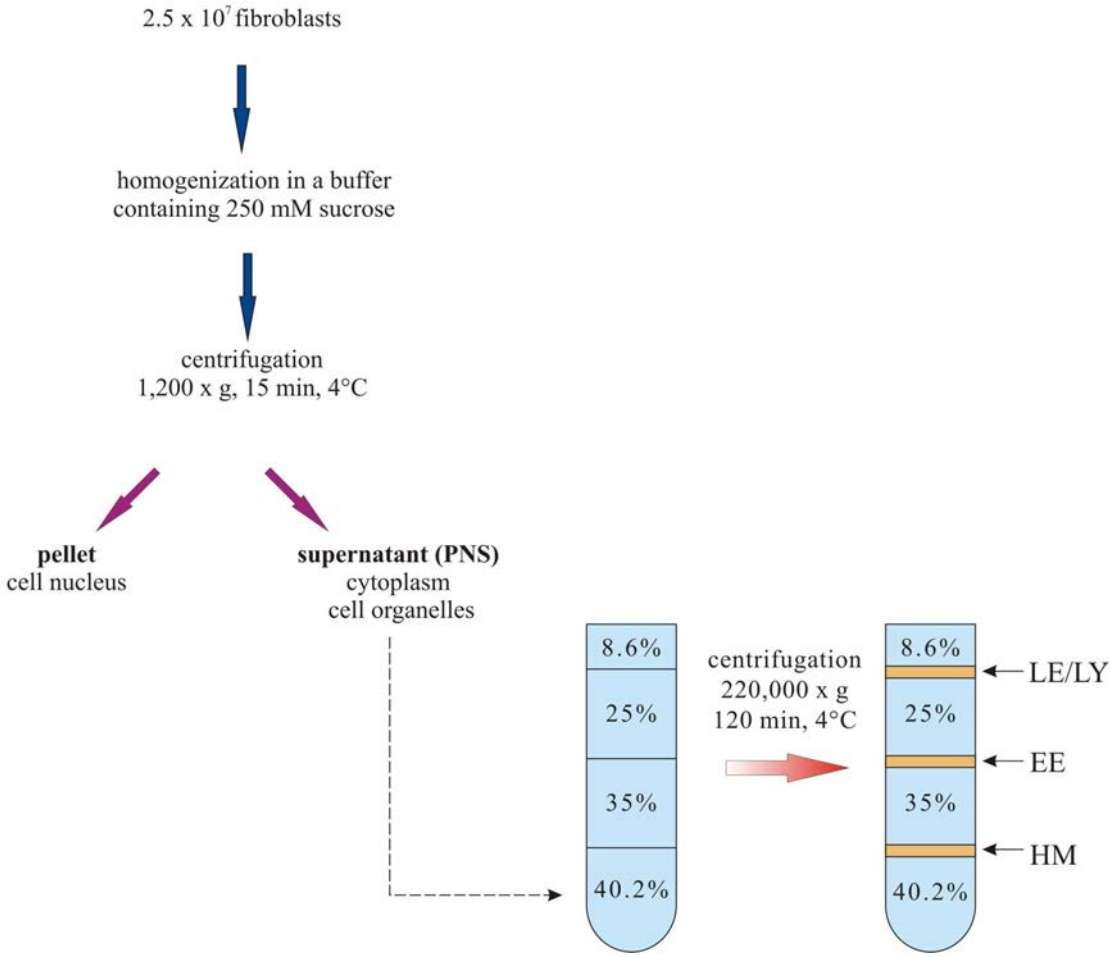

Figure 5. Schematic representation of cell fractionation in sucrose density gradient. Abbreviations used are as follows: PNS – post-nuclear supernatant containing cytoplasm and membranes of all cell organelles except nucleus; LE – late endosomes; EE-early endosomes; HM – heavy membranes

3.2.2 Isolation of detergent resistant membranes (DRMs)

DRMs were isolated according to (Diaz *et al*., 2002), with slight modifications. Briefly, 2.5 x 10^7 NPC or control fibroblasts were homogenized in 1 ml of ice-cold homogenization buffer containing 25 mM Tris-HCl, pH 7.5, 150 mM NaCl, 5 mM ethylenediaminetetraacetinc acid (EDTA) or in ice-cold homogenization buffer composed of 250 mM sucrose, 3 mM imidazole, pH 7.4, containing 40 μM Ca^{2+}. Both buffers were

supplemented with 10 µg/ml PIC, 1 mM Na_2VO_3, 10 mM NaF and 2 mM phenylmethylsulfonyl fluoride (PMSF). The homogenate was then centrifuged at 1,000 x g for 10 min at 4 °C to obtain the PNS. To isolate all cellular membranes, the PNS was centrifuged at 200,000 x g for 1 h at 4 °C.

The PNS, membrane fractions, or early endosomes, late endosomes and heavy membranes (isolated as previously described in Materials and Methods, Section 3.2.1) were incubated with Triton X-100 at a final concentration of 1% for 1 h at 4 °C. The lysate was then supplemented with 2.6 M sucrose to a final concentration of 1.3 M, placed at the bottom of an ultracentrifuge tube, and a discontinuous sucrose gradient (0.2–0.9 M with 0.1 M steps, 0.5 ml each) was placed on top. After centrifugation at 200,000 x g for 16 h at 4 °C, 0.5 ml fractions were collected starting from the top of the gradient. Fractions were stored at −20 °C until use.

Sucrose concentration in each fraction was determined with a refractometer (Polish Optical Works, Poland).

3.2.3 Titrations of proteins and cholesterol

3.2.3.1 Determination of protein concentration

Protein concentration was determined by the method of Bradford (Bradford, 1979). Briefly, 800 µl of standards (containing 2 µg, 4 µg, 6 µg, 8 µg, 10 µg of bovine serum albumin (BSA, Sigma-Aldrich, Germany)) and appropriately diluted samples were placed in plastic cuvettes (optical path length 10 mm). Next, 200 µl of Dye Reagent Concentrate (Bio-Rad, USA) were added and samples were incubated for 5 min. The absorbance was measured at 595 nm. Protein concentration in each sample was calculated using the calibration curve with BSA as a standard.

3.2.3.2 Determination of cholesterol concentration

The total cholesterol content in isolated fractions was determined by means of the Amplex Red Cholesterol Assay (Amplex®Red, Molecular Probes, USA) according to the manufacturer's instruction. Briefly, in this method cholesterol oxidase converts cholesterol to betaine with the formation of 1 mol H_2O_2/1 mol cholesterol. The Amplex®Red reagent reacts with H_2O_2 with 1:1 stoichiometry leading to the reduction of 10-acetyl-3,7-dihydroxyphenoxazine to a red fluorescent oxidation product, resorufin. Samples and cholesterol standards (0–8 µg/ml), were incubated for 1 h at 37 °C and their fluorescence intensities were measured at 25 °C in a quartz cuvette of 10 mm optical path length using

a Fluorolog 3 Spectrofluorimeter (Jobin Yvon Spex, USA) with excitation/emission wavelengths set at 550/584. Emission and excitation slits were set at 1 nm and 2 nm, respectively. Cholesterol content was normalized and presented in micrograms of total cholesterol per 1 μl of the sample.

3.2.4 Immunodetections

3.2.4.1 Immunocytochemistry

In order to analyze cell morphology, control and NPC fibroblasts grown on culture dishes were washed with PBS and fixed with ice cold 95% methanol. Then, cells were stained with 0.5% Gill's hematoxylin (10 min, room temperature), washed in running tap water followed by counterstaining with 0.25% eosin (15 min, room temperature), washing with PBS and examination in phase contrast under an AxioObserver Z.1 inverted microscope (Zeiss, Germany) equipped with RGB filters.

For immunocytochemistry, 5 x 10^4 cells/ml were seeded onto acid-washed glass coverslips, placed in culture dishes and allowed to adhere at 37 °C in a humidified atmosphere containing 5% CO_2 for 24 h. Next, cells were washed with PBS and fixed with 3% paraformaldehyde (20 min, room temperature) (Podszywalow-Bartnicka *et al*., 2007). The fixed cells were washed with PBS, incubated in 50 mM NH_4Cl in PBS (10 min, room temperature) and after washing, permeabilized with 0.08% Triton X-100 in PBS (5 min, 4 °C). After additional washing in buffer composed of 100 mM NaCl, 10 mM Tris-HCl, pH 7.5, the cells were incubated in blocking solution (5% FBS in 100 mM NaCl, 10 mM Tris-HCl, pH 7.5) for 45 min at room temperature.

To detect lipid microdomains, samples were incubated with polyclonal antibody against CD55 (1:100) (Sigma-Aldrich, Germany) prepared in washing buffer (0.5% FBS in 100 mM NaCl, 10 mM Tris-HCl, pH 7.5, 0.05% Tween 20). After 1.5 h incubation at room temperature the cells were washed six times with washing buffer and incubated for 1 h with antirabbit-Alexa Fluor 546 antibody (Invitrogen, Molecular Probes, USA), (1:1,000 dilution). Next, cells were washed with buffer containing 100 mM NaCl, 10 mM Tris-HCl, pH 7.5 and incubated with the cholera toxin B subunit from *Vibrio cholera* (CTB)-FITC conjugate 1:10,000 (Sigma-Aldrich, Germany). To detect AnxA6 and cholesterol, samples were incubated with mouse monoclonal antibody against AnxA6 (1:200 dilution) from BD Transduction Laboratories (BD Biosciences, EU), prepared in washing buffer. After 1.5 h incubation at room temperature the cells were washed six times with washing buffer and incubated for 1 h at room temperature with antimouse-Alexa Fluor 633 antibody (1:1,000),

(Invitrogen, Molecular Probes, USA). Cell cholesterol was stained with 25 μg/ml filipin (a non-esterified cholesterol-specific probe) (te Vruchte *et al.*, 2004) added separately or together with the secondary antibody. The antibodies used for fluorescent microscopy are described in Table 1.

After extensive washing (four times in washing buffer, two times in buffer containing 100 mM NaCl, 10 mM Tris-HCl, pH 7.5 and once in H_2O) samples were mounted with Mowiol® 4-88 (Calbiochem, Germany)/ 1,4-diazabicyclo[2.2.2]octane (DABCO, Sigma, USA). AnxA6 and CD55 images were acquired with a Leica DMI6000 Fluorescence Microscope (Leica, Germany) under specific filters. Filipin fluorescence was visualized directly under the UV light of a fluorescence microscope.

Table 1. Antibodies used in fluorescent microscopy

Antigen	Reactivity	Host	Dilution	Company
Primary antibodies:				
Anti-annexin A6	Human, Rat	Mouse	1:200	Transduction Laboratories, USA
Anti-CD55	Human	Rabbit	1:100	Sigma-Aldrich, Germany
Secondary antibodies:				
Anti-Mouse IgG -Alexa Fluor 633 labeled		Goat	1:1,000	Invitrogen, Molecular Probes, USA
Anti-Rabbit IgG -AlexaFluor 546 labeled		Donkey	1:1,000	Invitrogen, Molecular Probes, USA

3.2.4.2 Dot blot analysis

For dot blot analysis, 6 μl of each fraction was spotted on a nitrocellulose membrane. The membrane was blocked with 5% nonfat milk in 100 mM NaCl, 10 mM Tris-HCl, pH 7.5 for 1 h at room temperature. After washing, the membrane was incubated with the cholera toxin subunit B-horseradish peroxidase conjugate (CTB-HRP) (Sigma-Aldrich, Germany), diluted 1:10,000 in 100 mM NaCl, 10 mM Tris-HCl, pH 7.5 containing 0.05% Tween 20 for 1 h at room temperature and, after washing, HRP activity was detected by a chemiluminescent substrate kit, ECL reagents (Amersham Bioscience, Sweden).

3.2.4.3 Sodium dodecyl sulfate polyacrylamide gel electrophoresis and Western blotting

Isolated fractions were prepared for immunological and SDS-PAGE analysis by addition of the Laemmli sample buffer (Laemmli, 1970) (5 x concentrated, containing 60 mM Tris-HCl, pH 6.8, 25% glycerol, 2% SDS, 0.1% bromophenol blue, 14.4 mM β-mercaptoethanol) and boiling at 100 °C for 5 min. Proteins were separated by SDS-PAGE on 12% acrylamide gels of 1.5 mm thickness, in a buffer containing 25 mM Tris–HCl, pH 8.3, 192 mM glycine, 0.1% SDS, transferred onto nitrocellulose membrane (BioRad, USA) for 1 h at 100 V in buffer containing 25 mM Tris–HCl, pH 8.3, 192 mM glycine, 0.05% SDS, 20% methanol. Immunoblots were washed with Tris buffered saline (TBS) containing 20 mM Tris-HCl, pH 7.5 and 500 mM NaCl and then incubated in blocking solution (5% nonfat milk solution in TBS) for 1 h at room temperature. After washing with TBS containing 0.05% Tween 20 (TBST), immunoblots were probed overnight at 4 °C with primary antibodies against: AnxA6 (1:5,000 dilution) or CD55 (1:500 dilution) prepared in 5% nonfat milk/TBST. After washing (several changes of TBST) the blots were treated for 1.5 h at room temperature with appropriate secondary antibodies: sheep anti-mouse (1:5,000 dilution) or donkey anti-rabbit (1:2,500 dilution) IgG–horseradish peroxidase conjugates (GE Healthcare, Germany) prepared in 3% nonfat milk/TBST. After washing (several changes of TBST and then once with TBS) immunoreactive bands were visualized using ECL reagents (Amersham Biosciences, Austria). Molecular masses of peptides were determined based on their relative electrophoretic mobility using prestained molecular mass standards (Fermentas International, Inc., Canada). The SDS-PAGE was performed with Mini-PROTEAN III system (BioRad, USA).

3.2.5 Lipid analysis

3.2.5.1 Lipid extraction

Lipids from PNS fractions obtained in the presence of Ca^{2+} were extracted with a chloroform/methanol mixture as described previously (Folch *et al*., 1957). Briefly, samples containing 24 µl of each gradient fraction and 476 µl of H_2O were incubated overnight with 2 ml of chloroform:methanol (2:1, v/v) at room temperature. Next, the homogenates were centrifuged (1,500 x g, 10 min, room temperature) to separate the two phases. The upper phase was removed and the lower chloroform phase was rinsed three times with chloroform:methanol:water (3:48:47, v/v) and centrifuged. After the last centrifugation and

removal of the upper phase, the lower chloroform phase containing lipids was evaporated to dryness under a nitrogen stream and stored at -20 °C until use.

3.2.5.2 Thin-layer chromatography (TLC)

Dry lipid extracts were solubilized in 50 µl of chloroform and dotted on the origin line of Silica gel 60 F254 plates (Merck, Germany). A two step separation was performed, the first to separate phospholipids and the next to separate neutral lipids. Plates were developed up to 8 cm from the origin in ethyl acetate:1-propanol:chloroform:methanol:0.25% KCl (25:25:25:10:9, v/v). The solvent was allowed to evaporate for 20 min and plates were developed in the same direction up to 13 cm from the origin in heptane:isopropyl ether:acetic acid (60:40:3, v/v). Lipid bands were visualized by spraying the plate with 10% $CuSO_4$ in 8% H_3PO_4 and heating at 180 °C for 20 min (Banerjee *et al*., 1990). Obtained chromatograms were scanned with an InGenius system (Syngene, Great Britain). Following standards were used: PE – phosphatidylethanolamine (Sigma-Aldrich, Germany), PC – phosphatidylcholine (Sigma-Aldrich, Germany), SM – sphingomyelin (Sigma-Aldrich, Germany), cholesterol (Sigma-Aldrich, Germany), PI – phosphatidylinositol (Sigma-Aldrich, Germany), PS – phosphatidylserine (Sigma-Aldrich, Germany), cholesterol (Sigma-Aldrich, Germany). Each experiment was repeated three times. Due to low resolution between the PS and PI spots, the obtained results were expressed as PS + PI content. Not all the lipids react in the same manner in the presence of the cupric-phosphoric reagent, thus the density of the spots can be considered as approximation only.

3.3 Techniques related to interfacial monolayer analysis

3.3.1 Expression and purification of different human recombinant annexin A6

Human recombinant AnxA6-1, its W343F mutant and AnxA6-2 were expressed in *Escherichia coli* strain B121-(DE3) and purified as described for AnxA5 (Buger *et al*., 1993) with slight modifications (Bandorowicz-Pikula *et al*., 2003). Briefly, an overnight culture of *E.coli* transformed with pRSET5D containing human AnxA6-1, its W343F mutant or AnxA6-2 cDNA inserted between the NcoI and HindIII restriction sites was grown at 37 °C in 400 ml of Luria-Bertani (LB) medium containing 100 µg/ml ampicillin. When the optical density (OD) at 600 nm reached a value of 1.0, isopropyl-ß-D-thiogalactopyranoside (IPTG) was added to a final concentration of 1 mM. After 4 h of growth, the bacterial cells were harvested by centrifugation (5,000 x g, 15 min, 4 °C).

The cells were resuspended in 30 ml of the spheroblast buffer (0.5 mM ethylene glycol-bis(β-aminoethyl ether)-N,N,N0,N0-tetraacetic acid (EGTA), 750 mM sucrose, 200 mM Tris-HCl, pH 8.0) and 30 mg of lysozyme in 40 ml of solution containing 0.25 mM EGTA, 375 mM sucrose, 100 mM Tris-HCl, pH 8.0, were added in order to digest the cell wall. The suspension was incubated for 30 min at 4 °C. The spheroblasts were collected by centrifugation (14,000 x g, 30 min, 4 °C) and resuspended in 40 ml of buffer containing 20 mM Tris-HCl, pH 8.0, 2 mM EDTA, 5 mM $MgCl_2$, 100 mM NaCl, 0.1 mg/ml RNase, 0.1 mg/ml DNaseI, 2 mM PMSF, 1000 K.I.U/ml traskolan, 0.5 μg/ml pepstatin A, 0.1% (w/v) Triton X-100. The bacterial cells were disrupted by osmotic shock. To remove the cell debris the suspension was centrifuged at 120,000 x g for 4 h at 4 ºC.

During the centrifugation step, liposomes were freshly prepared as follows. Asolectin from soya bean (Sigma-Aldrich, Germany) was dissolved in 50 μl of chloroform and dried under a stream of nitrogen. The phospholipid mixture was resuspended by vortexing in the liposome buffer (100 mM NaCl, 3 mM $MgCl_2$ 20 mM Tris-HCl, pH 8.0) and sonicated 3 x 30 sec (Branson, USA). The supernatant after the ultracentrifugation was combined with the liposomes, $CaCl_2$ was added to the final concentration of 10 mM, and the mixture was incubated for 30 min at 4 °C. The mixture was then centrifuged at 120,000 x g for 45 min at 4 °C. The pellet was resuspended in a buffer containing 100 mM NaCl, 3 mM $MgCl_2$, 10 mM EDTA, 20 mM EGTA, 20 mM Tris-HCl, pH 8.0 in order to detach the protein from liposomes. The liposomes were removed by centrifugation (120,000 x g, 45 min, 4 °C) and the supernatant containing AnxA6 was dialyzed overnight against a buffer containing 20 mM Tris-HCl, pH 8.3, 0.1 mM EGTA and 10 mM NaCl (Fig. 6).

The protein solution was loaded on a Q-Sepharose column (diameter 1 cm, bed height 30 cm, flow rate 0.5 ml/min) and washed with 30 ml of solution containing 20 mM Tris-HCl, pH 8.3, 0.1 mM EGTA (flow rate 1 ml/min). The protein was eluted with a linear NaCl gradient (0-500 mM) at a flow rate of about 0.7 ml/min. Fractions were collected for 2 min and their protein content was analyzed by SDS-PAGE on 12% gels followed by staining with Coomassie Brilliant Blue R-250.

Proteins eluted as a single peak in about 350 mM NaCl. Fractions containing AnxA6, its W343F mutant or AnxA6-2 were dialyzed overnight in 10 mM phosphate buffer pH 7.4. Final purification of proteins was achieved by hydroxyapatite column chromatography. Fractions containing the respective peptides were dialyzed against 10 mM phosphate buffer, pH 7.4, 0.1 mM EGTA, loaded on a hydroxyapatite column (diameter 1 cm, bed height 50 cm, flow rate 0.5 ml/min) and eluted at pH 7.4 using a linear gradient of phosphate buffer

concentrations (20-250 mM) at a flow rate of 0.5 ml/min. AnxA6 was recovered in 0.7 ml fractions eluted with 230–250 mM phosphate buffer.

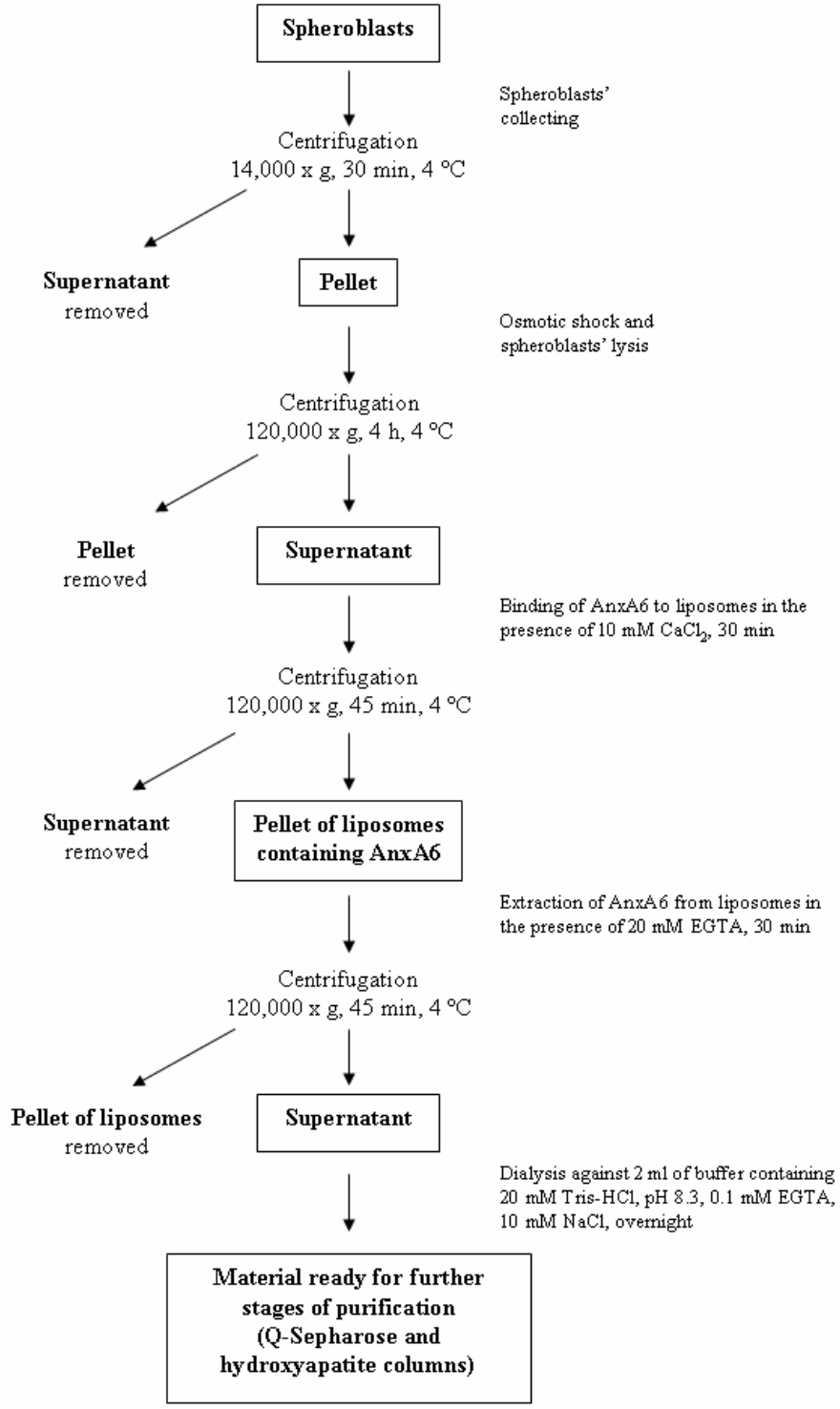

Figure 6. Stages of AnxA6 isoforms and AnxA6-1 W343F mutant purification.

Protein content was analyzed by SDS-PAGE on 12% gels followed by staining with 25% solution of Coomassie Brilliant Blue R-250 prepared in 50% methanol, 10% acetic acid and destaining with H_2O/methanol/acetic acid 72.5:20:7.5 v/v. Next, fractions containing the protein were combined, dialyzed against 10 mM Tris-HCl, pH 7.5 (2 h, 4 ºC), against 5 mM Tris-HCl, pH 7.5 (2 h, 4 ºC), and against 1 mM Tris-HCl, pH 7.5 (2 h, 4 ºC), lyophilized and stored at -80 °C. Chromatography was performed at 4 °C using the Biologic LP System (BioRad, USA) and lyophilization using an Alpha 1-2 laboratory freeze dryer (Martin Christ Gefriertrocknungsanlagen GmbH, Germany).

3.3.2 Stability of AnxA6-1, its W343F mutant and AnxA6-2

The stability of AnxA6-1, its W343F mutant and AnxA6-2 in different buffers used in Langmuir experiments was tested using electrophoresis. Briefly, the proteins were incubated at 21 °C for 15', 30', 45' or 60' in (i) 20 mM citrate buffer, pH 5.0, containing 100 mM NaCl, and 0.1 mM EGTA or in (ii) 20 mM Tris–HCl buffer, pH 7.4, supplemented with 0.1 mM EGTA and 100 mM NaCl. The final concentration of proteins in each buffer was 16 nM. Next, the degradation of proteins was analyzed by SDS-PAGE on 12% gels stained using the Silver staining procedure as described by (Shevchenko *et al*., 1996) with small modifications. Briefly, after electrophoresis, the gel slab was fixed in 50% ethanol, 12% acetic acid in water for 30 min. It was then washed for 10 min with 50% ethanol in water and, additionally, for 10 min with water to remove the remaining acid. The gel was sensitized by a 5 min incubation in 0.02% sodium thiosulfate, and it was then rinsed with two changes of distilled water for 1 min each. After rinsing, the gel was submerged in chilled 0.1% silver nitrate solution and incubated for 20 min at 4 °C. After incubation, the silver nitrate was discarded, and the gel slab was rinsed twice with water for 1 min and then developed in 0.04% formaldehyde in water containing 2% sodium carbonate, with intensive shaking. After the developer turned yellow, it was discarded and replaced with a fresh portion. It is essential that the developing is carried out in an absolutely transparent solution. After the desired intensity of staining was achieved, the developing was terminated by discarding the reagent, followed by washing the gel slab with 5% acetic acid. Silver-stained gels were stored in 1% acetic acid solution at 4 °C until analyzed.

The proteins did not show any evidence of degradation.

3.3.3 Surface pressure measurements

Kinetics of AnxA6-1, its W343F mutant or AnxA6-2 isoform adsorption at the air/water interface or the kinetics of their binding to lipid monolayers was measured as previously described (El Kirat *et al*., 2004). The experiments were performed in a Teflon trough (7 cm^2) at 21.0 ± 0.1 °C equipped with a Wilhelmy-type surface pressure measuring system (Riegler & Kirstein GmbH, Wiesbaden, Germany). The subphase (7 ml) was (i) 20 mM citrate buffer, pH 5.0 containing 0.1 mM EGTA and 100 mM NaCl or (ii) 20 mM citrate buffer, pH 5.0, 100 mM NaCl and 1 mM $CaCl_2$, or (iii) 20 mM Tris–HCl buffer, pH 7.4, 0.1 mM EGTA and 100 mM NaCl or (iiii) 20 mM Tris–HCl buffer, pH 7.4, 100 mM NaCl and 1 mM $CaCl_2$. The subphase was continuously stirred using a magnetic bar spinning at 100 rev/min.

In order to measure AnxA6 adsorption, the protein was injected into the subphase at a final concentration of 16 nM and its adsorption at the air/water interface, measured by tensiometry, was followed as an increase in the surface pressure. In order to investigate the AnxA6-induced changes of the lipid monolayer surface pressure, the monolayers were preformed by spreading 0.545 mM lipid solutions in hexane/ethanol (9:1 v/v) on the subphase until a desired pressure was reached. Several lipids were used: cholesterol (Chol, Sigma-Aldrich, Germany), 1,2-dipalmitoyl-*sn*-glycero-3-phosphocholine (DPPC, Sigma-Aldrich, Germany), DPPC:Chol (70:30 molar ratio), DPPC:Chol (50:50 molar ratio), sphingomyelin (SM, Sigma-Aldrich, Germany), SM:Chol (50:50 molar ratio), SM:DPPC:Chol (30:30:30 molar ratio). Thirty minutes were usually necessary for solvent evaporation and pressure stabilization and AnxA6 was injected into the subphase to a final concentration of 16 nM. The surface pressure was continuously recorded.

3.3.4 Brewster angle microscopy imaging (BAM)

The BAM imaging is based on the principle that for a beam of p-polarized light (p-parallel to the plane of incidence) there is an angle of incidence *alpha* at which no reflection occurs. This angle is called "Brewster angle" and is satisfying the relationship **tangent(***alpha***) = $n_{subphase}$ / n_{air}** , where **n** is the corresponding refractive index. A monolayer at the air-water interface yields a certain amount of reflected light, which is sufficient to produce an image (Fig. 7).

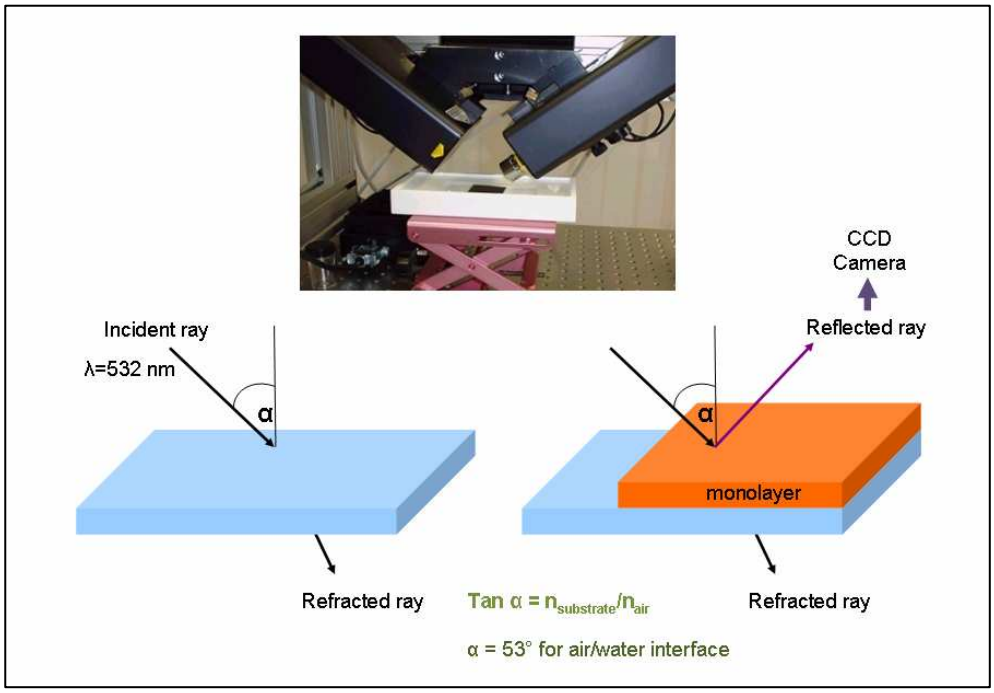

Figure 7. Schematic representation of the principle of Brewster Angle Microscopy. All explanations are in the text. Based on the lecture of Agnes Girard-Egrot.

The morphology of lipid monolayers before and after AnxA6 injection (16 nM final concentration) was investigated using a Brewster angle microscope (NFT iElli-2000, Göttingen, Germany) mounted on a Langmuir trough (R&K, Wiesbaden, Germany) as described in (Nasir *et al*, 2010). The microscope was equipped with a frequency doubled Nd:Yag laser (532 nm, i.e., 50 mW primary output), a polarizer, an analyzer, and a CCD camera. The spatial resolution of the Brewster angle microscope was ~2 μm and the image size was 430 x 320 μm. All experiments were performed at 21.0 ± 0.1 °C. The reference images of the lipids alone were recorded during the compression of monolayers constituted by DPPC or DPPC:Chol (70:30, molar ratio) as previously described (Abi-Rizk *et al*., 2008).

3.3.5 Polarization modulation infrared reflection absorption spectroscopy (PM-IRRAS)

PM-IRRAS is an IR spectroscopic method adapted to the air–water interface (Fig. 8). It combines Fourier transform mid-IR reflection spectroscopy with rapid polarization modulation of the incident beam between parallel (p) and perpendicular (s) polarizations (Blaudez *et al*., 1994). The spectra were recorded on a Nicolet 850 spectrometer equipped

with an HgCdTe detector which was cooled down to −196 °C with liquid nitrogen (Thermo Electron, Nicolet Instrument, Madison, WI) (Nasir *et al*., 2010).

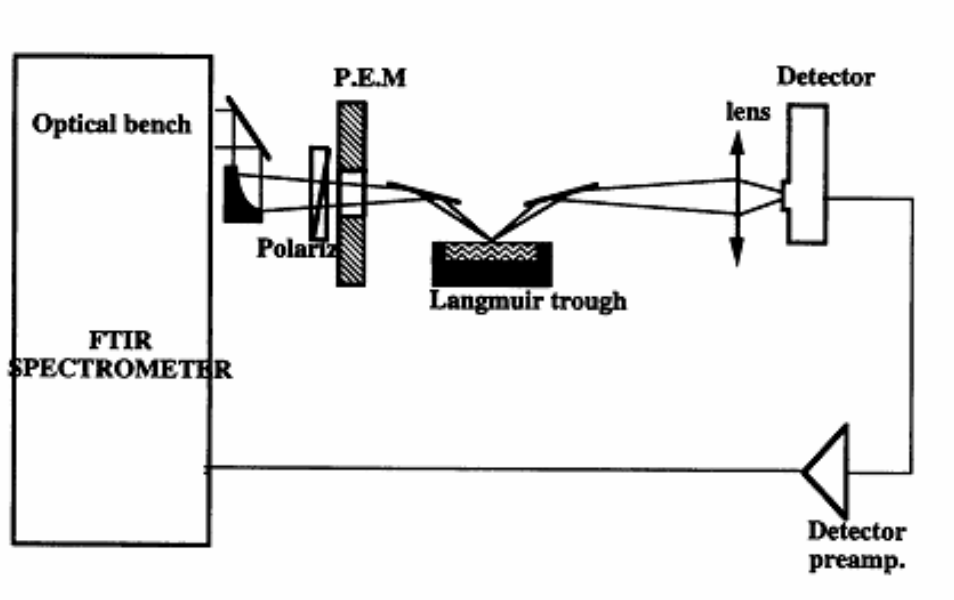

Figure 8. Experimental setup of Polarization Modulation IR Reflection Absorption Spectroscopy (PM IRRAS) at the air/water surface (Cornut *et al*., 1996).

In short, the infrared beam was reflected toward the optical bench by a mirror. The reflected beam was then polarized by a ZnSe polarizer and modulated between parallel (p) and perpendicular (s) polarizations by a photoelastic modulator. The polarized beam was then directed toward the air/water interface onto a small Langmuir trough having a subphase area of 50 ml and a maximum monolayer containment area of 90 cm^2. This trough was equipped with two symmetrical movable barriers and a Nima surface pressure detector system (Nima Technology, UK). The subphase was thermostatted at 21 °C. The optimal angle of incidence was 75° to the interface normal. Afterwards, the beam was reflected on the HgCdTe detector. The detected signal allowed us to obtain the differential reflectivity spectrum after processing as follows:

$$\Delta R/R = (R_p-R_s)J_2(\Phi_0)/[\ (R_p+R_s)+\ (R_p+R_s)\ J_0(\Phi_0)]$$

where J_2 and J_0 are the zero- and second-order Bessel functions, while Φ_0 is the phase of the Bessel functions related to variations of the modulation of polarization according to the wavelength and Rp and Rs are the parallel and perpendicular reflectivity, respectively. In order to remove the liquid water absorption and the contribution of the Bessel function, the

monolayer spectrum was divided by that of the pure subphase. PM-IRRAS spectra were measured after injection of annexinA6 at a final concentration of 16 nM. After stabilization of the surface pressure, the interfacial film was compressed to reach the desired surface pressures and the PM-IRRAS spectra were recorded. For all measurements, the resolution was 8 cm^{-1}. Each spectrum was collected at 1024 scans and is the average of at least three spectra measured in an independent manner.

3.4. Other techniques

3.4.1 Statistical analysis

All data were analyzed using OrginPro 8.0 sotware. Statistical significance of results was tested using the paired t-test and is described in figure legends.

3.5. Reagents

Acetic acid (POCH, Poland)
Acrylamide (Fluka Chemie AG, Switzerland)
Ammonium chloride (Sigma-Aldrich, Germany)
Ampicillin (Sigma-Aldrich, Germany)
Amplex®Red (Molecular Probes, USA)

β-mercaptoethanol (Sigma-Aldrich, Germany)
Bisacrylamide (Fluka Chemie AG, Switzerland)
Bradford Dye Reagent Concentrate (BioRad, USA)
Bromophenol blue (Sigma-Aldrich, Germany)
BSA (Sigma, Germany)

Calcium chloride (Sigma-Aldrich, Germany)
cell culture dishes (Becton Dickinson Labware, USA)
Chloroform (Merck, Germany)
Cholesterol (Sigma-Aldrich, Germany)
Citric acid (Sigma-Aldrich, Germany)
Coomasie Brilliant Blue R-250 (Fluka Chemie AG, Switzerland)
Copper sulfate (POCH, Poland)

DABCO (Sigma, USA)
Disodium hydrogen orthophosphate (POCH, Poland)
DMEM (Sigma-Aldrich, Germany)
DMSO (Sigma-Aldrich, Germany)
DNaseI (Boehringer Mannheim, Germany)
DPPC (Sigma-Aldrich, Germany)

ECL reagents (Amersham Bioscience, USA)
EDTA (Sigma-Aldrich, Germany)
EGTA (Sigma-Aldrich, Germany)
Eosin (Sigma-Aldrich, Germany)
Ethanol (Chimie Plus Laboratories, France)
Ethyl acetate (POCH, Poland)

FBS (Gibco BRL, Great Britain)
Filipin (Sigma-Aldrich, Germany)
Formaldehyde (Sigma-Aldrich, Germany)

Glycerol (Calbiochem, USA)
Glycine (POCH, Poland)
Hematoxylin (Sigma-Aldrich, Germany)

Heptane (POCH, Poland)
Hexane (Prolabo, France)
Hydrochloric acid (POCH, Polska)
Hydroxyapatite (BIO 101, USA)

Imidazole (Merck, Germany)
IPTG (Fermentas, Lithuania)
Isopropyl ether (POCH, Poland)
LB (Bio 101, USA)

Lysozyme (Sigma-Aldrich, Germany)

Magnesium chloride (Sigma-Aldrich, Germany)
Methanol (POCH, Poland)
Mowiol4-88 (Calbiochem, Germany)

Nitrocellulose membrane (BioRad, USA)

Paraformaldehyde (Sigma-Aldrich, Germany)
PC (Sigma-Aldrich, Germany)
PE (Sigma-Aldrich, Germany)
Penicillin (Sigma-Aldrich, Germany)
Pepstatin A (Sigma-Aldrich, Germany)
Phosphatidylinositol (Sigma-Aldrich, Germany)
Phosphoric acid (Sigma-Aldrich, Germany)

PMSF (Sigma-Aldrich, Germany)
Potassium chloride (Sigma-Aldrich, Germany)
Potassium dihydrogen phosphate (POCH, Poland)
prestained molecular mass standards (Fermentas, Canada)
1-propanol (POCH, Poland)
Propidium iodide (Sigma-Aldrich, Germany)
protease inhibitors cocktail PIC (Sigma-Aldrich, Germany)
PS (Sigma-Aldrich, Germany)

Q-Sepharose (Amersham Pharmacia, Sweden)

RNase (Boehringer Mannheim, Germany)

SDS (Sigma-Aldrich, Germany)
Silica gel 60 F254 plates (Merck, Germany)
Silver nitrate (Sigma-Aldrich, Germany)
SM (Sigma-Aldrich, Germany)
Sodium carbonate (Sigma-Aldrich,)
Sodium chloride (Sigma-Aldrich, Germany)
Sodium fluoride (Sigma-Aldrich, Germany)
Sodium thiosulfate (Sigma-Aldrich, Germany)
Sodium vanadate (Sigma-Aldrich, Germany)
Streptomycin (Sigma-Aldrich, Germany)
Sucrose (POCH, Poland)

Trascolan (Jelfa, Poland)
Tris (Sigma-Aldrich, Germany)
Trisodium citrate (Sigma-Aldrich, Germany)
Triton X-100 (Sigma-Aldrich, Germany)
Trypsin (Sigma-Aldrich, Germany)
Tween 20 (Sigma-Aldrich, Germany)

CHAPTER 4

RESULTS

4.1. Detergent resistant membranes of Niemann-Pick type C fibroblasts

4.1.1. Characteristics of NPC fibroblasts

The Niemann-Pick type C disease is a lipid storage disorder characterized by an excessive accumulation of cholesterol in the late endosome/lysosome compartment. Previous reports from our laboratory described 4 NPC patients of different age from the Polish population, 3 of them revealing mutations in the *NPC1* gene (Sztolsztener *et al*., 2010). One of the examined patients represented the rarest case, a lethal variant of NPC. Fibroblasts taken from this patient were characterized by two mutations (R348X and R1186H) in the *NPC1* gene. Therefore, in this report we focused on the NPC L1 fibroblast cell line derived from this patient.

As an initial attempt we decided to examine morphology of NPC L1 fibroblasts to verify the presumption that the mistargeted intracellular transport of cholesterol could influence cell morphology and/or cell cycle.

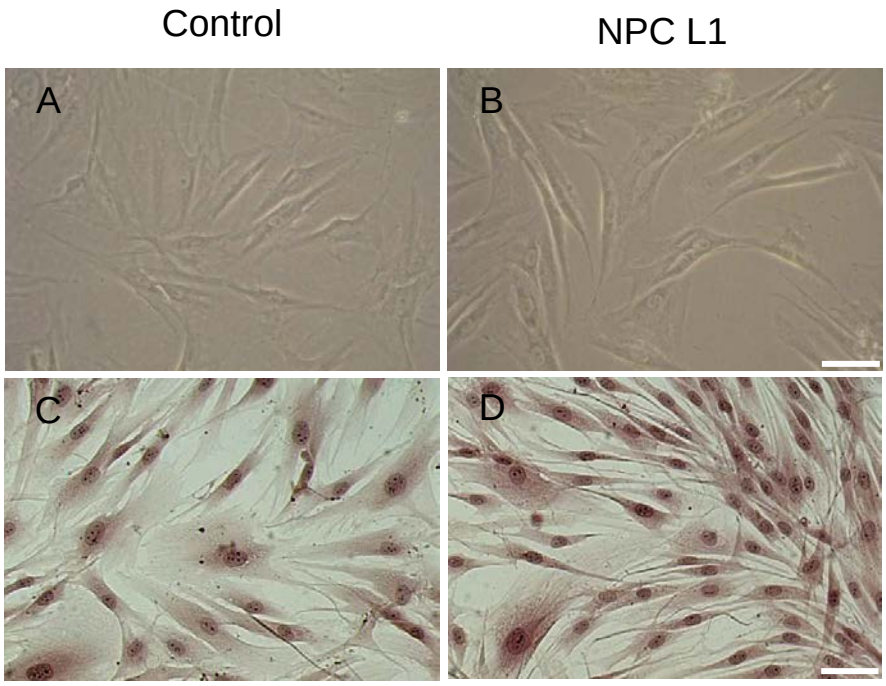

Figure 9. Morphology of NPC L1 and control cell lines. NPC L1 and control fibroblasts were observed under the inverted Axiovert 40C microscope (Zeiss, Sweden) 20 x magnification (A, B). Next, control and NPC fibroblasts were stained with 0.5% Gill's hematoxylin and 0.25% eosin (for further details see Materials and Methods, paragraph 3.2.4.1) and observed under phase contrast and RGB filters under the inverted AxioObserver Z.1 microscope (Zeiss, Germany) 20 x magnification (C, D). Scale bars, 100 μm

NPC L1 and control fibroblasts were observed under an inverted microscope with 20 x magnification (Fig. 9A and B). Next, the cells were stained with Gill's hematoxylin and eosin

(Fig. 9C and D). No differences in morphology were detected. Both cell lines grew adherent to the dish, they contained single nucleus and they were characterized by a spindle or stellate shape with long slender cytoplasmic processes.

In order to determine various cell parameters, propidium iodide staining was performed on NPC L1 and control fibroblasts. Obtained results revealed that there were no significant differences in cell size (Fig. 10A) or cell granularity (Fig. 10B) between NPC L1 and control cells. In addition, there was no discernible difference in cell viability and cell cycle (Fig. 10C). The majority of NPC L1 cells as well as control cells were at the G0/G1 phase.

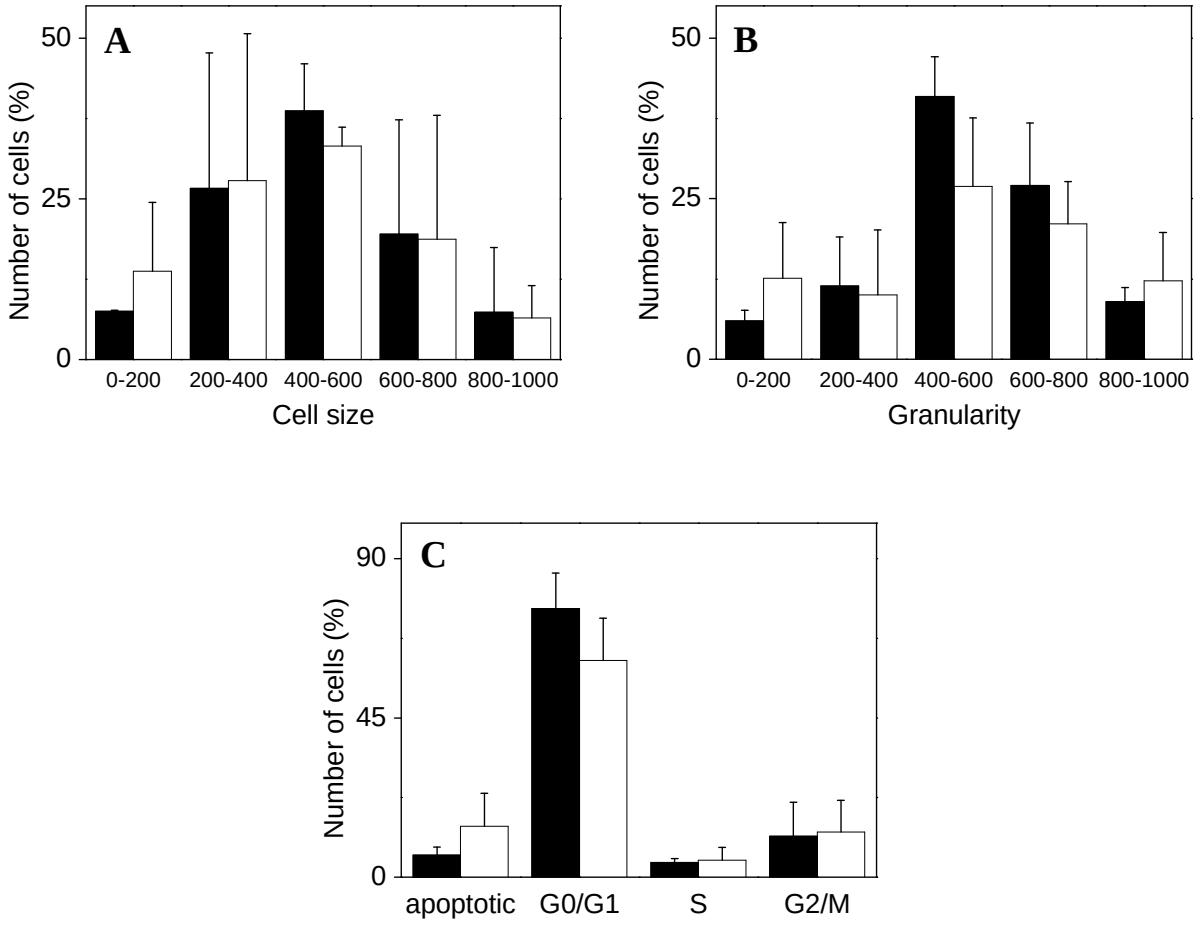

Figure 10. The cell size, granularity and cell cycle phase, and of NPC L1 (white bars) and control cells (black bars) were compared. Apoptotic cells, resting cells (G0/G1), DNA synthesizing (S) and dividing cells (G2/M) were counted on a FACScan flow cytometer (Becton-Dickinson, USA) and the cell size, granularity and cell cycle phase distribution were analyzed using the Cell Quest software (Becton-Dickinson, USA). Data are the mean of three independent experiments ± standard error. Published in Domon *et al.*, BBRC, 2011

The protein and cholesterol contents in the post-nuclear supernatant from NPC L1 and control fibroblasts were also compared (Fig. 11). In order to isolate the PNS fractions, cells

were incubated in the homogenization buffer and centrifuged as previously described in Materials and Methods, paragraph 3.2.2. The cholesterol content in both PNS samples was determined using the Amplex Red Cholesterol Assay (Materials and Methods, paragraph 3.2.3.2).

This analysis revealed that the PNS derived from NPC L1 cells contained more proteins and more cholesterol than that from control fibroblasts obtained from a healthy individual (Fig. 11). In view of the results presented in Fig. 10, the observed differences in the cholesterol and protein cell contents are not the result of differences in the cell cycle phase.

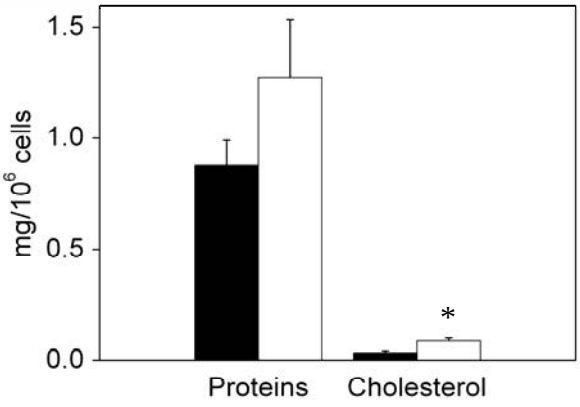

Figure 11. Protein and cholesterol content in NPC L1 (white bars) and control (black bars) fibroblasts. The amount of protein and cholesterol are expressed in mg/10^6 cells. The data are mean of three independent experiments ± standard error. Significant differences are marked (Student's t test): * $p<0.05$
Published in Domon *et al*., BBRC, 2011

4.1.2 Distribution of cholesterol-enriched microdomains in NPC L1 and control fibroblasts

Due to the characteristics of NPC L1 fibroblasts described in the former paragraph, especially a high content of cholesterol, we hypothesized that membranes of NPC L1 fibroblasts may contain more cholesterol-enriched regions, i.e., lipid microdomains similar to lipid rafts or DRMs. In order to analyze the cellular distribution of lipid microdomains, we decided to use fluorescence microscopy to examine the distribution of membrane markers characteristic for the cholesterol-enriched membrane microdomains, as well as the localization of membrane cholesterol.

The distribution of lipid microdomains in NPC L1 and control cells was examined using two markers (i.e., the GPI-anchored protein CD55 and ganglioside GM1, Legembre *et al.*, 2006; Hofman *et al*., 2008; Sandvig and van Deurs, 2002) under Leica DMI6000 Fluorescence Microscope (Leica, Germany) (Fig. 12A). The merge images of CD55 and GM1 staining suggested co-localization of these two markers at the plasma membrane in the control fibroblasts, while in NPC L1 cells a co-localization of CD55 and GM1 was also observed in

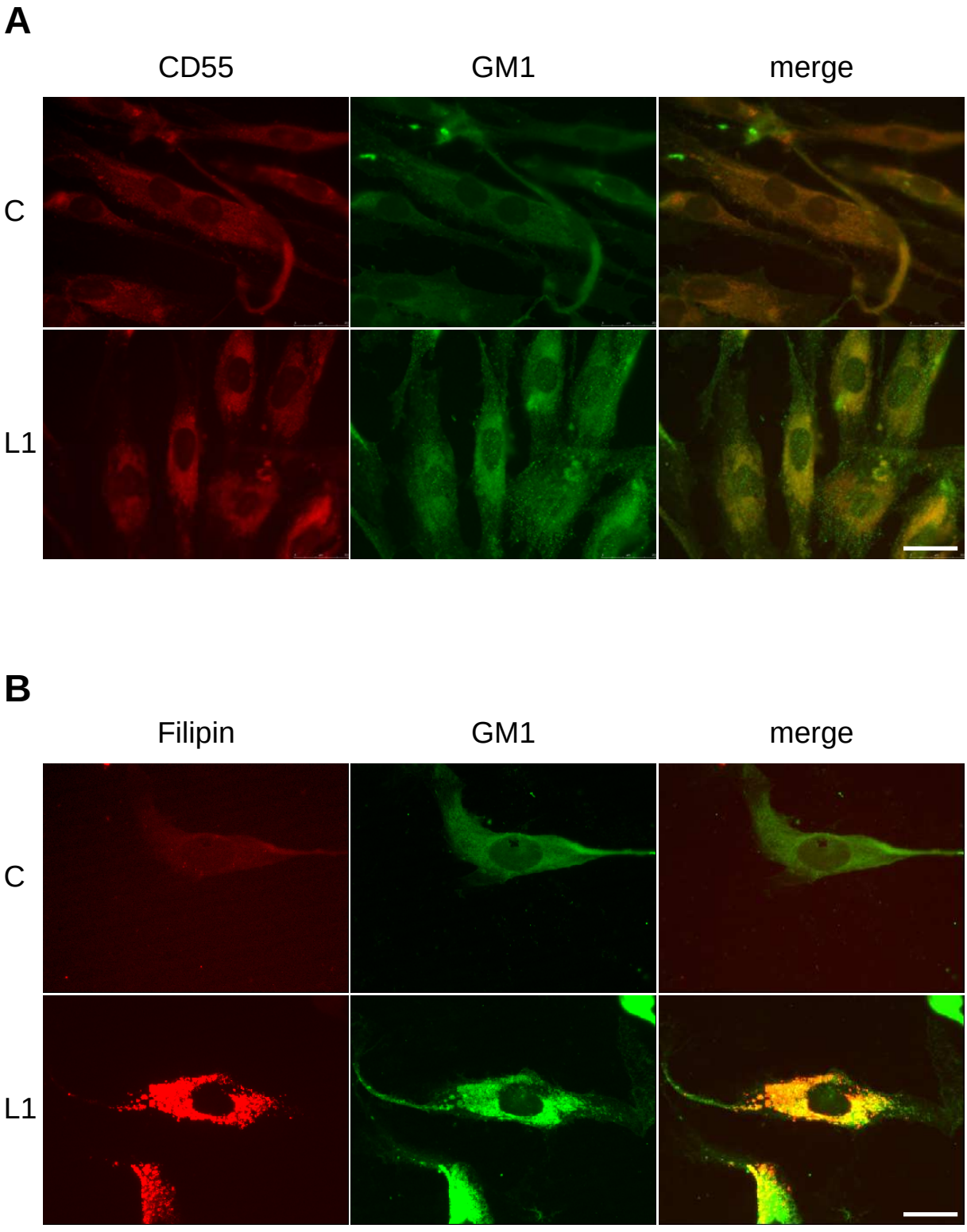

Figure 12. Distribution of lipid raft markers in NPC L1 (L1) and control fibroblasts (C). Cells were fixed and stained with anti-CD55 antibodies (visualized by Alexa Fluor 546) followed by the CTB-FITC conjugate (A) or with filipin followed by staining with the CTB-FITC conjugate (B). Images were analyzed by fluorescence microscopy. Merge images were created. Scale bar, 25 μm. (A) Published in Domon *et al*., BBRC, 2011

the perinuclear region of the cell, most likely representing the late endosome/lysosome compartment (Chevallier *et al*., 2008; Lusa *et al.*, 2001).

To verify the colocalization between lipid microdomains and cholesterol, a double staining of GM1 and cholesterol was performed (Fig. 12B). The merge images of these two markers showed abnormal accumulation of cholesterol and GM1 in the late endosome/ lysosome compartment of NPC L1 cells (Fig. 12B) suggesting that the cholesterol present in this compartment may be implicated in the formation of lipid microdomains.

The obtained results are in agreement with the study of (Lusa *et al*., 2001) that using radiolabeled cholesterol, reported the evidence that there is more cholesterol in membrane microdomains isolated from *NPC*$^{-/-}$ cells than from control cells.

4.1.3. Biochemical characterization of detergent resistant membranes (DRMs)

The extended accumulation of cholesterol in NPC cells could also result in a change in cellular membrane composition and influence the amount and content of lipid microdomains. Thus, to check if there are differences between lipid microdomains in NPC L1 and control fibroblast cells, lipid microdomains were isolated and their composition was analyzed.

Resistance of these microdomains to solubilization with mild detergents and subsequent extraction of detergent-resistant membranes constitute an experimental approach in defining membrane domains enriched in cholesterol (Lindner and Naim, 2009).

In order to isolate DRMs, the PNS from each cell line was treated with Triton X-100 and the different fractions obtained after ultracentrifugation on sucrose gradients were isolated and tested for the presence of CD55 and GM1. Both markers of DRMs were found in the fractions of the NPC L1 cells corresponding to 16–30% sucrose (Fig. 13). Similar distribution of CD55 and GM1 was observed in control cells (Fig. 13), which is in agreement with the findings of other researchers demonstrating that DRMs are usually localized in 5-35% of sucrose (Babiychuk and Draeger, 2006; Sengupta *et al*., 2008; Fiedler *et al.*, 1993; von Haller *et al.*, 2001).

There was much more CD55 detected in NPC L1 than in normal cells which confirmed the results of fluorescence visualization, suggesting differences in the DRMs content between the NPC L1 and control cells.

The analysis of total cholesterol content revealed, that in the case of both, NPC and control cell lines, 50 % of total cellular cholesterol was localized in the fractions containing

DRMs. This is in agreement with the studies performed on other cells, for example on the brains isolated form NPC mice (te Vruchte *et al*., 2004).

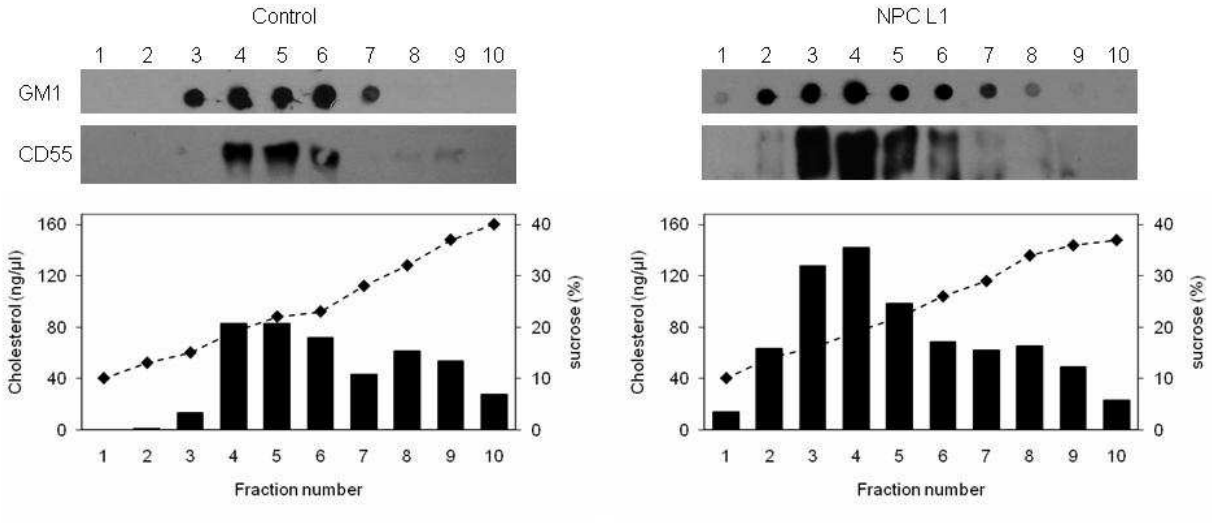

Figure 13. Biochemical identification of DRMs isolated from NPC L1 and control cells with 1% Triton X-100. Each fraction obtained after ultracentrifugation was tested for the presence of CD55 (Western blot), GM1 (dot blot) as well as for cholesterol (bars) and sucrose (dots) contents. One set of representative results of three independent experiments performed at the same conditions is shown. The experimental values varied by 5%. Published in Domon *et al*., BBRC, 2011

The comparison between NPC and control cells showed that the PNS from NPC fibroblasts contained twice as much cholesterol as the PNS from the control cells (Fig. 11). Also, cholesterol quantification of fractions from the sucrose gradient (Fig. 13) revealed that the NPC L1 cells contained twice as much cholesterol as the control cells. In the case of NPC L1 cells, a peak of cholesterol was observed in the fractions 3–5 which had the highest content of GM1 and CD55. In the case of control cells the peak of cholesterol was much smaller, but nevertheless it was observed in fractions 4–6, i.e., in the fractions where CD55 and GM1 were also detected.

4.1.4 Distribution of AnxA6 and cholesterol-enriched microdomains in NPC L1 and control fibroblasts

There are some lines of evidence suggesting that AnxA6 followed cholesterol distribution during the endocytic pathway and interacted with the endocytic machinery (Creutz and Snyder, 2005; Grewal *et al*., 2010; de Diego *et al*., 2002). Furthermore, U18666A-induced cholesterol accumulation in late endosomes of Chinese chamster ovary (CHO) and normal rat kidney (NRK) cells, led to the translocation of AnxA6 to this compartment (de Diego *et al*., 2002). Last but not least, the interaction of AnxA6 with NPC1

may favor the hypothesis that AnxA6 is implicated in late endosomal cholesterol transport (Cubells *et al*., 2007). Therefore, in the next part of this work we aimed to verify whether in NPC L1 and control fibroblasts AnxA6 is implicated in the formation and stabilization of lipid microdomains.

To visualize AnxA6 and lipid microdomains distribution in NPC L1 and control fibroblasts, fluorescence double staining of AnxA6 and GM1 was performed. In control cells, AnxA6 was uniformly distributed in the cell whereas in NPC cells it was more intensively localized in the perinuclear region of the cell which is in agreement with the previous results of Sztolsztener and co-workers (Sztolsztener *et al*., 2010) (Fig. 14). There was much more GM1 detected in the NPC L1 cells and the merge images suggest a possible colocalization of AnxA6 and GM1 in this cell line, therefore implying the presence of AnxA6 at rafts of the intracellular organelles.

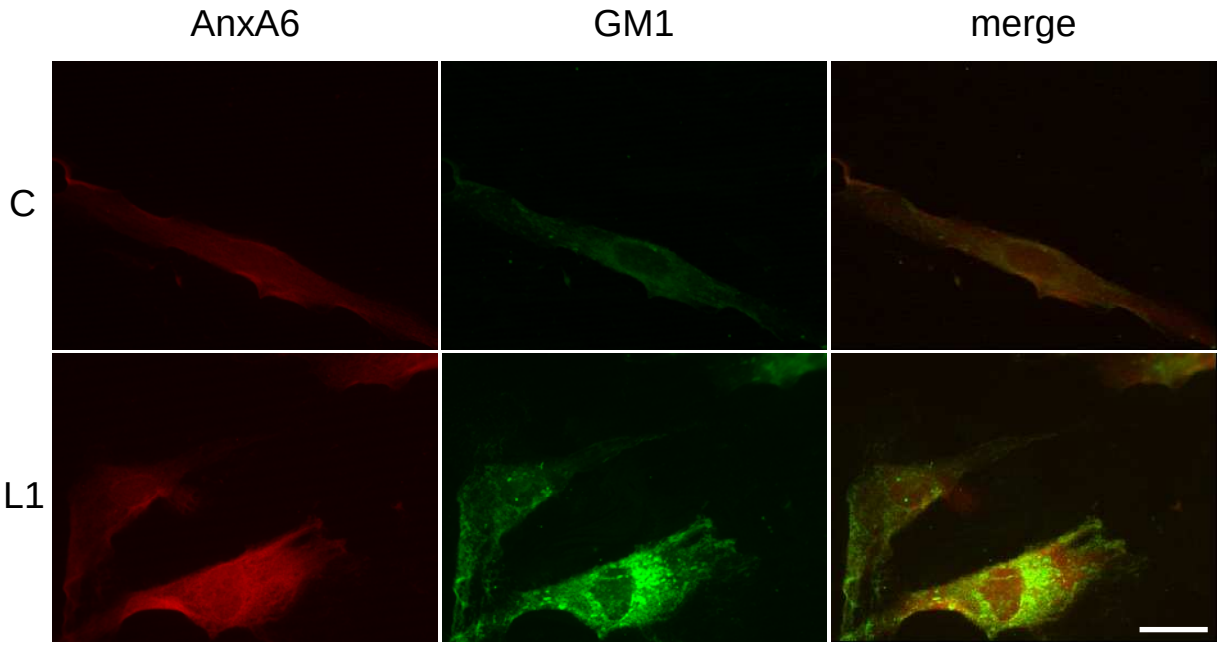

Figure 14. Distribution of AnxA6 and GM1 in NPC L1 (L1) and control fibroblasts (C). Cells were fixed and stained with anti-AnxA6 antibodies (visualized by Alexa Fluor 633) followed by the CTB-FITC conjugate. Images were analyzed by fluorescence microscopy. Merge images were created. Scale bar, 25 μm.

4.1.5. Analysis of AnxA6 interactions with DRMs in the absence and presence of Ca^{2+}

To verify if AnxA6 is associated with lipid microdomains of NPC L1 and control fibroblasts, AnxA6 content in DRMs was tested. First, DRMs were prepared from PNS fractions in the same conditions as described in the paragraph 4.1.3, i.e., in the absence of

Ca^{2+} (Fig. 15A). The fractions obtained after sucrose density gradient centrifugation were analyzed for the presence of AnxA6. In parallel, the fractions enriched in DRMs were identified by testing the presence of GM1 all along the sucrose gradient. DRMs isolated from PNS fractions in the absence of Ca^{2+} did not contain AnxA6 (Fig. 15). However, we observed that there was slightly more AnxA6 in the non-DRM fractions isolated from NPC cells than in those from the control cells (Fig. 15A) which is in agreement with the visualization by fluorescence microscopy. The comparison of AnxA6 distribution along the sucrose gradient (Fig. 15A) with the distribution of cholesterol (Fig. 13) revealed that, even though AnxA6 was not found in the DRM fractions, it was detected in fractions 8-10, which were enriched in cholesterol.

To avoid the eventual contamination by AnxA6 present in the cytosol, DRMs were also prepared in the same conditions from purified membranes (see Material and Methods, paragraph 3.2.2). Similarly to DRMs isolated from PNS, DRMs isolated from membrane fractions in the absence of Ca^{2+} did not contain AnxA6 (Fig. 15B). We observed that there was slightly more AnxA6 in the non-DRM fractions isolated from NPC cells than in those from control cells (Fig. 15B).

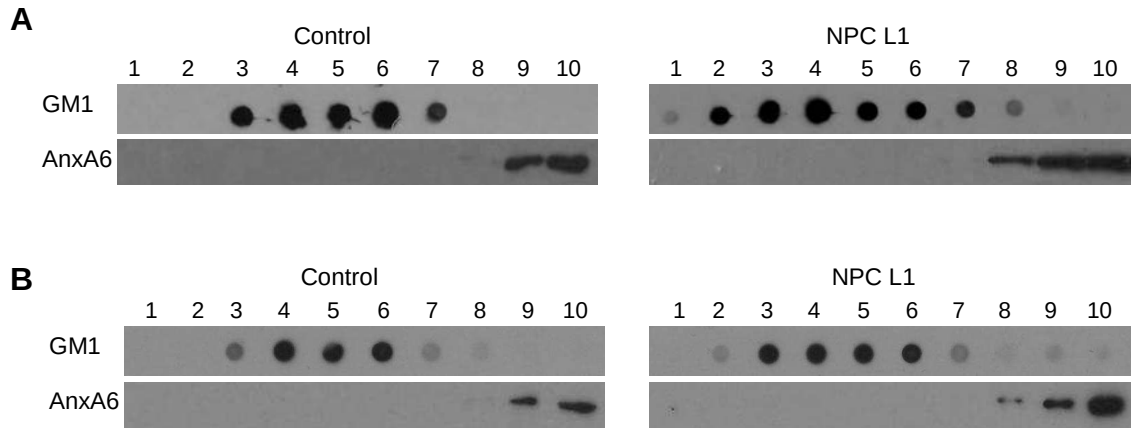

Figure 15. AnxA6 distribution between DRM and non-DRM fractions in NPC L1 and control cells. DRMs were prepared from PNS (A) and total membranes (B) in the absence of Ca^{2+}. Fractions of the sucrose gradient were tested for the presence of AnxA6 (Western blot) and GM1 (dot blot). (A) Published in Domon *et al.*, BBRC, 2011.

For most annexins the presence of Ca^{2+} seems to be a predominant factor enabling or enhancing their interactions with membrane microdomains. For example, Ca^{2+}-dependent association of annexin A6 with lipid rafts was observed in smooth muscle cells or in synaptic plasma membranes of rat brain (Babiychuk and Draeger, 2000; Orito *et al.*, 2001). Since AnxA6 interacts with membranes in a Ca^{2+}-dependent manner (Gerke and Moss, 2002), we

tested the effect of calcium on the possible association of AnxA6 with the cholesterol enriched microdomains.

The DRMs were prepared from PNS in the presence of Ca^{2+} and different fractions of the sucrose gradient were analyzed for the presence of both GM1 and AnxA6 (Fig. 16A). In control cells, AnxA6 was present in fractions which did not contain DRMs but, in the case of NPC L1 cells, the majority of AnxA6 was localized in fractions containing DRMs.

Similar results were obtained when DRMs were isolated from membrane fractions (Fig. 16B). The detection of GM1 and AnxA6 in the fractions revealed that in control cells AnxA6 was present in the membranes but it was localized outside DRMs. In the case of the NPC L1 cell line, the majority of AnxA6 was found in the DRM fractions.

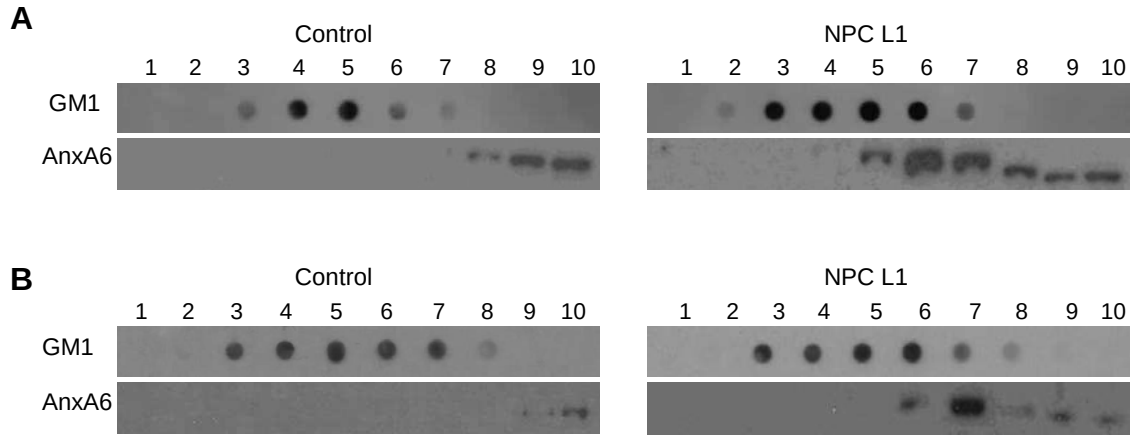

Figure 16. AnxA6 distribution between DRM and non-DRM fractions in NPC L1 and control cells. DRMs were prepared from PNS (A) and total membranes (B) in the presence of Ca^{2+}. Fractions of the sucrose gradient were tested for the presence of AnxA6 (Western blot) and GM1 (dot blot). (A) Published in Domon *et al*., BBRC, 2011.

Thus, at 40 μM Ca^{2+}, AnxA6 remained bound to cholesterol enriched microdomains in NPC cells, while it was not associated with microdomains in control cells. This suggests that both Ca^{2+} and cholesterol may play an important role in AnxA6 interactions with lipid microdomains in the cell.

4.1.6 Characterization of the lipid content of DRMs

Lipid microdomains contain all the major classes of lipids, including glycerophospholipids, sphingolipids and sterols. Cholesterol is known to interact with sphingomyelin to form a liquid-ordered phase (Quinn and Wolf, 2010; Björkbom *et al*., 2010; Matsumori *et al*., 2011). Domains formed by sphingomyelin and cholesterol, however,

represent a relatively small fraction of the lipids found in membrane rafts and the properties of other raft lipids are not well characterized (Quinn and Wolf, 2010).

It was previously found that in the mouse model, the NPC disease is associated with increased levels of glycosphingolipids, cholesterol and sphingosine in DRMs (teVruchte *et al*., 2004). Thus, we did experiments aiming to characterize the lipid composition of detergent resistant membranes isolated from NPC and control fibroblasts. Lipids were extracted and separated by thin layer chromatography as described in Materials and Methods, paragraph 3.2.5. Figure 17 summarizes the distribution of the main classes of phospholipids in the fractions obtained after sucrose gradient centrifugation. It is worth noticing that the thin layer chromatography is only a qualitative not a quantitative method, so the quantity of lipids may be treated as approximate only, but it may give some clues concerning the composition of DRMs.

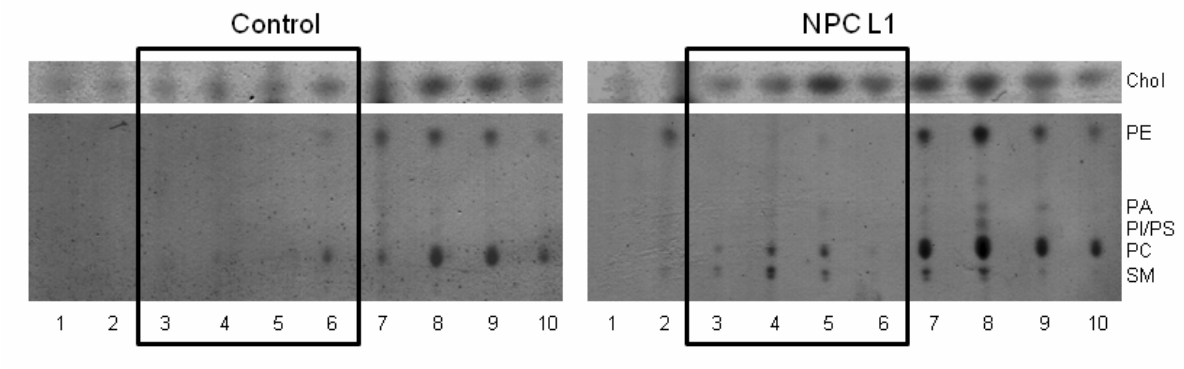

Figure 17. Chromatogram of lipids extracted from different DRM fractions obtained in the presence of Ca^{2+}. PNS fraction of control and NPC cells were extracted with 1% Triton X-100 followed by sucrose-density gradient ultracentrifugation. Lipids were separated using thin layer chromatography. Abbreviations used: Chol-cholesterol, PE–phosphatidylethanolamine, PA-phosphatidic acid, PI–phosphatidylinositol, PS-phosphatidylserine , PC-phosphatidylcholine, SM-sphingomyelin.

Cholesterol was detected in all fractions in both cell types. Phosphatidylcholine (PC) and phosphatidylethanolamine (PE) seemed to be the major phospholipids present in most of the fractions. However, in both cell lines, PE was present mostly in the fractions which did not contain lipid microdomains. The majority of PC was found in non-DRM fractions, however it was also present in DRMs. In contrast to DRMs isolated from control cells, DRMs isolated form NPC L1 cells were also enriched in sphingomyelin (SM). Other phospholipids, such as phosphatidic acid (PA), phosphatidylinositol (PI), phosphatidylserine (PS) were found in the fractions which did not contain DRMs.

4.1.7 Identification of lipid microdomains in the membranes of cellular organelles involved in endocytosis

Niemann-Pick type C disease is linked to abnormal cholesterol transport and accumulation of cholesterol mostly in the late endosome/lysosome compartment. In the following study, we wanted to isolate microdomains from cellular organelles implicated in endocytosis. Using the method previously described by Grewal *et al*., (2000) we isolated late endosomes/lysosomes (LE/LY), early endosomes (EE) and heavy membranes (HM). In order to isolate DRMs each fraction was treated with Triton X-100. Fractions enriched in DRMs were identified by testing the presence of GM1 all along the sucrose gradient (Fig. 18).

In the control cells before Triton X-100 extraction we observed the highest GM1 content in the HM fraction and some GM1 in LE/LY and EE. After incubation with Triton X-100 and sucrose gradient centrifugation we observed no GM1 in the LE/LY fractions. Sucrose fractions 3, 4, 5 (around 20 % sucrose) isolated form EE contained traces of GM1 which is consistent with the presence of DRMs in these fractions. In the case of HM we observed GM1 in almost all fractions, but most of it in 19 and 32-40 % sucrose. This suggests that in control cells DRMs are present in EE and HM (Fig.18).

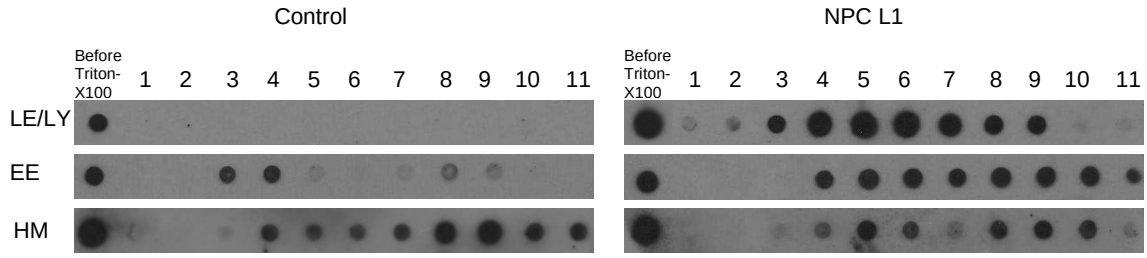

Figure 18. GM1 distribution in the fractions from different membrane compartments. Late endosomes/lysosomes, (LE/LY), early endosomes (EE) and heavy membranes (HM) were incubated with Triton X-100 followed by sucrose density gradient ultracentrifugation. GM1 content was analyzed using dot Blot, as described in the Materials and Methods section. The result of a typical experiment out of 3 is shown.

In the case of NPC cells we observed high GM1 content in the LE/LY and HM fractions and a lower one in the EE fractions. After sucrose gradient centrifugation of LE/LY, GM1 was mostly detected in fractions 3-7 which correspond to 16-30 % sucrose. Also the EE fractions contained more GM1 than control cells. The amount of GM1 in HM seemed to be comparable with that of the control cells.

These findings clearly demonstrate that NPC cells contain more DRMs in LE/LY and some more in the EE compartment. However, this disease seems not to influence the DRM content in the cell membrane.

4.2. Interaction of AnxA6 with cholesterol *in vitro*

In paragraph 4.1. of the thesis the experimental evidence has been provided suggesting that in the cell AnxA6 may specifically recognize and bind to membrane regions enriched in cholesterol identified as DRMs. The factors responsible for AnxA6 interaction with DRMs as well as the mechanism of the process remain to be elucidated.

The construction of a model imitating cellular membrane is one of the possible means to analyze the organization of the molecules and their interactions in cellular membrane. In our studies we chose lipid monolayers at the air/water interface as a membrane biomimetic system to monitor the changes induced by AnxA6-1 in the membranes. The main advantage of the use of monolayers is that we can test the interaction between a protein molecule and a lipid (such as cholesterol) which cannot form bilayers when it is pure. Furthermore, since the interactions between AnxA6-1 and the lipids present in the monolayers could affect the protein, we first studied the interfacial properties of AnxA6-1 alone using tensiometry and Polarization Modulation-InfraRed Reflection-Adsorption Spectroscopy (PM-IRRAS).

In the second part, we studied interactions of AnxA6 with different lipids and characterized the organization and insertion of AnxA6 into different lipid monolayers using Langmuir monolayers. Those interactions were also visualized using Brewster Angle Microscopy (BAM).

4.2.1 Interfacial properties of human recombinant annexin A6 isoform 1

Our cellular model revealed that Ca^{2+} plays a key role in AnxA6 interactions with DRMs. Also, other studies proved that AnxA6 interactions with phospholipids may depend on pH (Golczak *et al*., 2004) or on the presence of Ca^{2+} (Babiychuk and Draeger, 2000).

Before analyzing AnxA6 interactions with lipids, we tested the behavior of AnxA6-1 alone at the air/water interface. To elucidate the factors that may influence AnxA6-1 adsorption at the air/water interface, the experiments were performed using buffers at pH 5.0 and pH 7.4 in the presence or in the absence of Ca^{2+}. We chose a pH 5.0 buffer to mimic the pH in the late endosome/lysosome compartment and a pH 7.4 buffer corresponding to physiological pH.

First, we focused on the AnxA6-1 behavior at the air/water interface at pH 5.0. The kinetics of AnxA6-1 adsorption at the air/water interface was recorded using Langmuir monolayers by measuring the surface pressure at a constant area as a function of time. Figure 19 depicts the kinetics of the surface pressure after injection of 16 nM AnxA6-1 into the subphases containing 20 mM citrate buffer, pH 5.0, 100 mM NaCl, 0.1mM EGTA or

containing 20 mM citrate buffer, pH 5.0, 100 mM NaCl, 1 mM $CaCl_2$. After protein injection, the surface pressure was continuously recorded during 60 min (for further details see Materials and Methods, paragraph 3.3.3). In the absence of calcium, we observed a lag period of about 15 min before any detectable increase in the surface pressure. This lag period suggested that AnxA6 did not completely cover the interface. After that, we observed a fast increase in the surface pressure at a rate of 0.6 mN/m/min and 60 min after the protein injection, the surface pressure reached a plateau at about 12 mN/m (Fig. 19, dashed line). In the presence of Ca^{2+}, a similar adsorption profile was obtained (Fig. 19, full line).

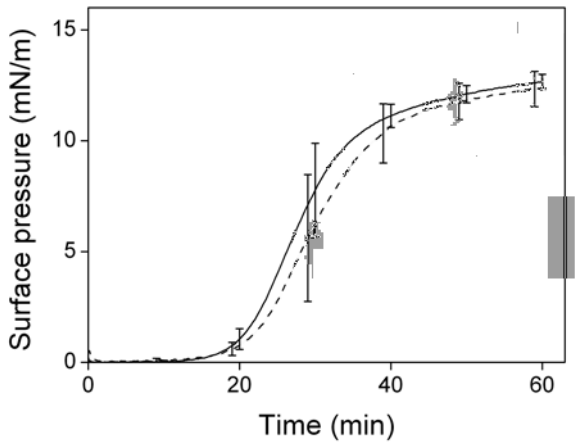

Figure 19. The effect of calcium on the partition of rec hAnxA6-1 to the air/water interface at pH 5.0. Protein was injected into the subphase at a final concentration of 16 nM and the surface pressure was continuously recorded. Time zero corresponds to the protein injection. Dashed line corresponds to the buffer containing 20 mM citrate buffer, pH 5.0, 100 mM NaCl, 0.1mM EGTA and full line to the buffer containing 20 mM citrate buffer, pH 5.0, 100 mM NaCl and 1 mM $CaCl_2$. Curves represent the average of three independent experiments with error bars. For the sake of graph clarity, the error bars are shown only to the experimental points only at 10 min intervals. Used in Domon *et al*., JCIS, 2010.

At pH 7.4, in the absence of calcium, a change in the surface pressure was observed 20 min after AnxA6-1 injection. The surface pressure increased at a rate of 0.2 mN/m/min and after 60 min a plateau at ~5 mN/m was observed (Fig. 20, dashed line). At the same pH in the presence of Ca^{2+}, the lag period was shorter (10 min), the pressure increased at the rate of 0.4 mN/m/min and the maximal surface pressure of the protein layer was reached at ~12 mN/m (Fig. 20, full line). Thus, the addition of Ca^{2+} to the buffer increased AnxA6 adsorption at the air/water interface.

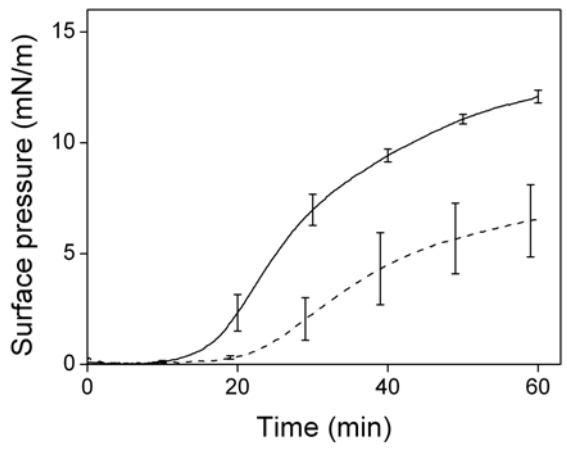

Figure 20. The effect of calcium on the partition of rec hAnxA6-1 to the air/water interface at pH 7.4.
Protein was injected into the subphase to a final concentration of 16 nM and the surface pressure was continuously recorded. Time zero corresponds to the protein injection. Dashed line corresponds to the buffer containing 20 mM Tris buffer, pH 7.4, 100 mM NaCl, 0.1mM EGTA and full line to the buffer containing 20 mM Tris buffer, pH 7.4, 100 mM NaCl and 1 mM $CaCl_2$. Curves represent the average of three independent experiments. For the sake of graph clarity, the error bars are shown only to the experimental points only at 10 min intervals. Used in Domon *et al*., JCIS, 2010.

The differences in the formation of an AnxA6 layer at the air/water interface, as indicated by the increase of surface pressure, may be explained by an increase in the hydrophobicity of AnxA6 molecules upon acidification (Golczak *et al*., 2004). We may also suspect that, at pH 7.4, the binding of Ca^{2+} ions to the protein could change the structure and/or the orientation of AnxA6.

Thus, the origin of the different behaviors observed at pH 7.4 in the absence or presence calcium was analyzed using PM-IRRAS, which is an IR spectroscopy method adapted to the air/water interface. The PMIRRAS spectra of AnxA6-1 at the air/water interface were recorded at pH 7.4 in the presence and in the absence of Ca^{2+} during monolayer compression (Fig. 21).

PMIRRAS spectra of AnxA6-1 at pH 7.4 displayed two characteristic regions. The amide-I band is the result of stretching vibration of carbonyl bonds and to a lesser extent of N-H bonds, while the amide-II band corresponds to stretching vibrations of N-C or N-H bonds. The amide-I and amide-II bands are centered at 1655-1650 cm^{-1} and 1544 cm^{-1}, respectively (Fig. 21).

In the absence of Ca^{2+}, the band located at 1650 cm^{-1} corresponds to an α-helical structure while the two bands at 1624 cm^{-1} and 1682 cm^{-1} suggest the presence of β-sheet structures, (Fig. 21, thick line). Furthermore, the compression of the AnxA6-1 monolayer did not affect the location of the amide-I and amide-II bands (data not shown), indicating that the secondary structure is not surface pressure-dependent.

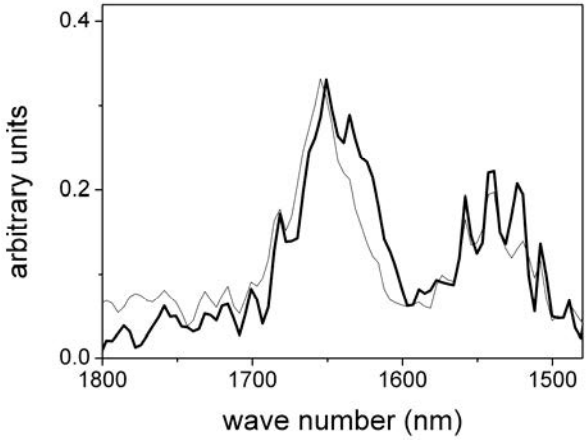

Figure 21. PM-IRRAS spectra of rec hAnxA6-1 in pH 7.4 buffer containing 20 mM Tris–HCl, pH 7.4, 0.1 mM EGTA, 100 mM NaCl (thick line) or 20 mM Tris–HCl buffer, pH 7.4, 100 mM NaCl, 1 mM $CaCl_2$ (thin line). Spectra were collected at a surface pressure of 20 mN/m.

In the presence of Ca^{2+}, analysis of the amide-I region, characterized by a strong positive signal at 1655 cm^{-1}, suggests that at pH 7.4 AnxA6-1 adopts mainly an α-helical structure (Fig. 21, thin line). This is consistent with the previous finding of (Kirilenko *et al*., 2002). Furthermore, there were no surface pressure-induced changes in the amide-I and

amide-II bands location, suggesting that the secondary structure is independent of the compression state of the monolayer (data not shown).

4.2.2. Analysis of the interactions of AnxA6 with lipid monolayers

The interactions of AnxA6 with cholesterol and other constituents of lipid microdomains were then studied. The effect of pH and Ca^{2+} on the interactions between AnxA6 and lipid monolayers at the air/water interface was analyzed by tensiometry and BAM.

In the first step, the influence of cholesterol on the interactions between the protein and lipid monolayers at pH 5.0 was tested. Lipid mixtures containing different amounts of DPPC and cholesterol were spread at the air/water interface to obtain a surface pressure of about 5 mN/m (Fig. 22). After pressure stabilization, the protein was injected into the subphase (as indicated by an arrow) and the surface pressure was continuously recorded. In all the cases, the injection of AnxA6-1 caused an increase in the surface pressure, however the rate of this increase depended on the lipid composition of the monolayers. The lowest rate was observed for DPPC alone (~0.4 mN/m/min), while the highest was obtained for cholesterol alone (~1.7 mN/m/min).

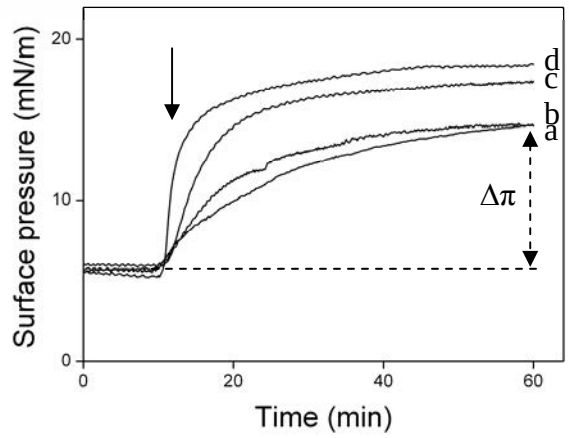

Figure 22. Kinetics of rec hAnxA6-1 adsorption to a lipid monolayer at pH 5.0. DPPC alone (a), DPPC:Chol at 70:30, molar ratio (b), DPPC:Chol at 50:50, molar ratio (c) or cholesterol alone (d) were spread at the air/water interface to obtain the desired initial pressure. After pressure stabilization, protein was injected into the subphase at a final concentration of 16 nM (as indicated by arrow) and pressure was continuously recorded. Published in Domon *et al*., JCIS, 2010.

Furthermore, the extent of surface pressure increase induced by AnxA6-1 ($\Delta\pi$) also depended on the lipid composition of the monolayer. The smallest $\Delta\pi$ (~9 mN/m) was observed for DPPC and DPPC:Chol (70:30, molar ratio). The highest $\Delta\pi$ (~13 mN/m) was observed for the monolayer containing only cholesterol (Fig. 22).

Similar experiments were performed for various monolayers at different initial surface pressures. For each lipid monolayer, the value of $\Delta\pi$, determined at different initial pressures

(π_i), were plotted as a function of the initial surface pressure. By extrapolating the regression of the plot to the x axis, we determined the exclusion surface pressure (pressure of the lipid monolayer up to which AnxA6 may be inserted into the monolayer) for each lipid monolayer (Fig. 23). The uncertainty in the exclusion surface pressures was calculated from the equation: $(\sigma(\Delta\pi) \times (1 - r^2)^{1/2})/(\sigma(\pi_i) \times (n - 2)^{1/2})$, where σ is the standard deviation, r is the correlation coefficient, and n is the number of points (Calvez *et al.*, 2009).

The exclusion pressure was 9 mN/m for the DPPC monolayer and it increased with the increase in cholesterol content, reaching ~30 mN/m for pure cholesterol monolayers (Fig. 23). It should be underlined that the exclusion pressure of AnxA6 interactions with DPPC and DPPC:Chol (70:30, molar ratio) monolayers is below the pressure of biological membranes (Silvius *et al*., 2003; Calvez *et al*., 2009).

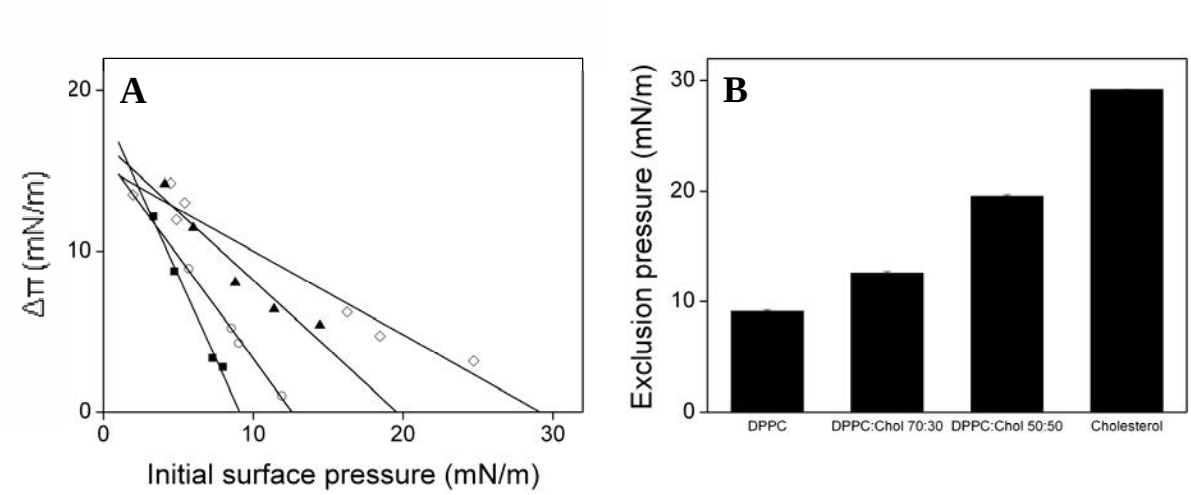

Figure 23. (A) Adsorption of rec hAnxA6-1 to different lipid monolayers. Maximal changes of the surface pressure ($\Delta\pi$) after protein injection were obtained from the kinetics of protein-induced changes in surface pressure of monolayers containing different amounts of cholesterol. The resulting $\Delta\pi$ were plotted as a function of the initial surface pressure for the DPPC alone (filled squares), DPPC:Chol at 70:30, molar ratio (open circles), at 50:50, molar ratio (filled triangles), or Chol alone (open diamonds). The subphase was 20 mM citrate buffer, pH 5.0 containing 0.1 mM EGTA, 100 mM NaCl. The final concentration of AnxA6 was 16 nM. (B) Histograms of the exclusion pressure of AnxA6 in the presence of lipid monolayers obtained form their respective regression curve from Fig. 23A. The error bars have been determined from the regression curves. All these data are statistically significant (Student's t test): $p<0.001$; Published in Domon *et al*., JCIS, 2010.

The effects of AnxA6-1 on biomimetic monolayers at the air/water interface was visualized by recording BAM images during the adsorption of AnxA6-1 to two different lipid monolayers at pH 5.0.

Figure 24 depicts the results obtained with a DPPC monolayer. The lipid was spread at the air/water interface to obtain a DPPC monolayer at 4 mN/m (Fig. 24, image 1). Next, AnxA6 was injected to the subphase and its adsorption to the monolayer was followed using tensiometry (Fig. 24). BAM images were taken during the AnxA6-1 adsorption until the

AnxA6-induced pressure reached a plateau (at 14 mN/m). The adsorption of the protein induced an increase in the gray level as compared to the DPPC monolayer before the injection of AnxA6-1 (Fig. 24, compare images 1 and 2). We also observed changes in the morphology of the DPPC monolayer. Large brighter zones appeared inside the uniformly organized background, while the small condensed domains of DPPC disappeared (Fig. 24, compare images 1 and 2). Furthermore, the organization of the AnxA6-1/DPPC monolayer at 14 mN/m was completely different from that of a pure DPPC monolayer at the same pressure (Fig. 24B, image A_R). The large brighter zones (Fig. 24, image 2) might correspond to AnxA6-enriched domains and suggest participation of the protein in membrane lateral organization.

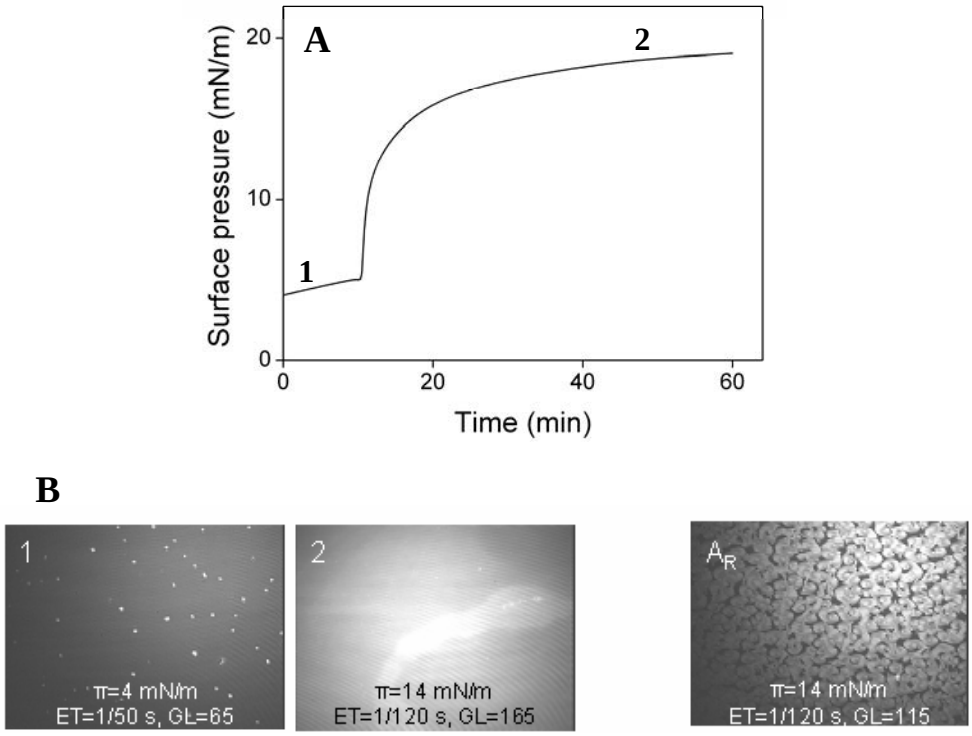

Figure 24. Visualization of the interactions between AnxA6 and a lipid monolayer composed of DPPC. (A) Kinetics of the AnxA6-1 adsorption to the lipid monolayer at pH 5.0. Numbers correspond to the pressures at which BAM images presented below were taken. (B) BAM images recorded before AnxA6 injection under a monolayer (1). BAM imaging of the interface after AnxA6 injection (final concentration of 16 nM) beneath the monolayer of DPPC when the surface pressure reached a plateau (2). The subphase was 20 mM citrate buffer at pH 5.0 with 0.1 mM EGTA and 100 mM NaCl. Reference images were taken during the compression of a monolayer constituted of DPPC (A_R). Reference gray level (GL) was 25 when exposure time (ET) was 1/50 s. The image size was 430 x 320 µm. Used in Domon *et al.*, JCIS, 2010.

Similar experiments were performed to analyze the interactions of AnxA6 with the monolayer composed of DPPC:Chol (70:30, molar ratio) at pH 5.0. The lipid was spread at the air/water interface to obtain a DPPC monolayer at 2.5 mN/m (Fig. 25, image 1). Next,

AnxA6 was injected to the subphase and the AnxA6 adsorption to the monolayer was followed using tensiometry (Fig. 25A). BAM images were taken during the AnxA6-1 adsorption until the AnxA6-induced pressure reached a plateau (at 16 mN/m). The adsorption of the protein induced an increase in the gray level as compared with the DPPC:Chol (70:30, molar ratio) monolayer before the injection of AnxA6-1 (Fig. 25B, compare images 1, 2 and 3). We also observed changes in the morphology of the DPPC:Chol (70:30, molar ratio) monolayer. Furthermore, the organization of the AnxA6-1/DPPC:Chol (70:30, molar ratio) monolayer at 12 and 16 mN/m was completely different from that of a DPPC:Chol (70:30, molar ratio) monolayer at the same pressure (Fig. 25B, image A_R).

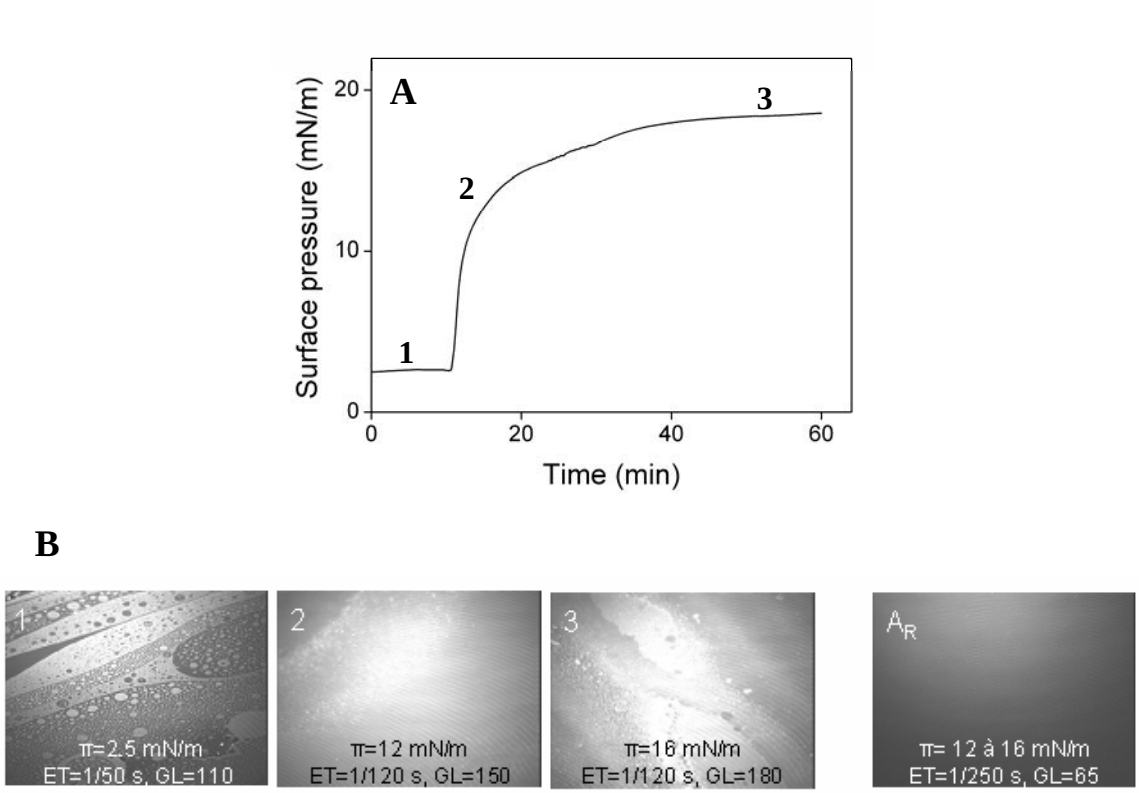

Figure 25. Visualization of the interactions between AnxA6 and lipid monolayer composed of DPPC:Chol (70:30, molar ratio). (A) Kinetics of the AnxA6-1 adsorption to the lipid monolayer at pH 5.0. Numbers correspond to the pressure at which BAM images presented below were taken. (B) BAM images recorded before AnxA6 injection under a monolayer (1). BAM imaging of the interface after AnxA6 injection (final concentration of 16 nM) beneath the monolayer of DPPC:Chol (70:30, molar ratio) when the surface pressure was 12 mN/m (2) and when the surface pressure reached a plateau (3). The subphase was 20mM citrate buffer at pH 5.0 with 0.1 mM EGTA and 100 mM NaCl. Reference images were taken during the compression of a monolayer constituted of DPPC:Chol (70:30, molar ratio) (A_R). Reference gray level (GL) was 25 when exposure time (ET) was 1/50 s. The image size was 430 x 320 µm. Used in Domon *et al.*, JCIS, 2010.

Furthermore the increase in the grey level seemed to be higher than that observed for monolayers made exclusively of DPPC. Under these conditions, the initial organization of the DPPC:Chol monolayer disappeared during AnxA6-1 adsorption and was replaced by a new

one, similar to the organization of DMPS/DMPE monolayers in the presence of AnxA6 (Golczak *et al*., 2004). The BAM investigation strongly suggests the role of AnxA6-1 molecules in stimulating the lateral organization of the membranes containing cholesterol. This assembly into microdomains may resemble lipid rafts. Our results are interesting because such a role of annexins was already postulated and shown for AnxA2 (Chasserot-Golaz *et al*., 2005).

In the next part of this work, the effect of cholesterol on AnxA6 interactions with lipid monolayers was tested at pH 7.4 in the absence of Ca^{2+}. The kinetics of AnxA6 interactions with lipid monolayers were recorded as previously described for pH 5.0. Fig. 26 shows the kinetics obtained with DPPC monolayers containing various amounts of cholesterol at π_i ~5 mN/m. We observed that AnxA6 did not induce any changes in the surface pressure of a DPPC monolayer, meaning that at pH 7.4 AnxA6 was not inserted into this monolayer. In the case of DPPC:Chol (70:30, molar ratio) monolayers, AnxA6 induced only small changes in the surface pressure ($\Delta\pi$) ~2.5 mN/m. The best insertion of AnxA6 was observed for a monolayer composed only of cholesterol.

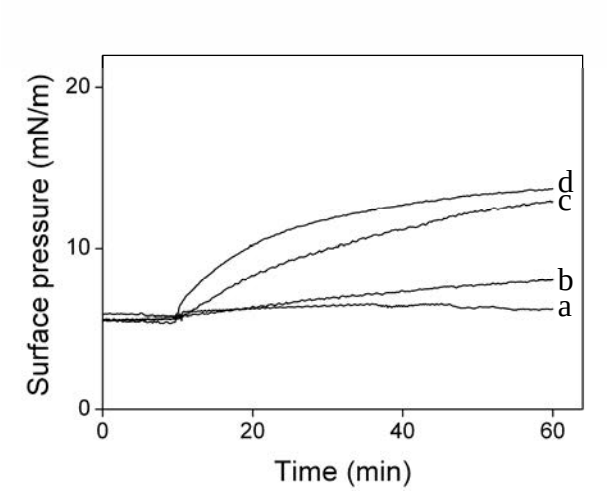

Figure 26. Kinetics of the rec hAnxA6-1 adsorption to lipid monolayers at pH 7.4. DPPC alone (a), DPPC:Chol at 70:30, molar ratio (b), DPPC:Chol at 50:50, molar ratio (c) or cholesterol alone (d) were spread at the air/water interface to obtain the desired initial pressure. After pressure stabilization, protein was injected into the subphase (20 mM Tris buffer, pH 7.4, 100 mM NaCl, 0.1 mM EGTA) at a final concentration of 16 nM and the surface pressure was continuously recorded. (a) Used in Domon *et al*., JCIS, 2010.

For each lipid monolayer, $\Delta\pi$ values, determined at different initial pressures of the monolayer (π_i), were plotted as a function of the initial surface pressure (Fig. 27). Whatever the π_i, AnxA6 did not insert into the DPPC monolayer. Thus we may conclude that at pH 7.4, in the absence of Ca^{2+}, AnxA6 does not interact with monolayers composed only of DPPC.

The same experiments were performed for monolayers containing cholesterol. The exclusion pressure obtained for DPPC:Chol (70:30, molar ratio) monolayers was ~12 mN/m and increased with the increase in cholesterol content of the monolayer. The value for DPPC:Chol (50:50, molar ratio) monolayers was ~20 mN/m and reached ~30 mN/m for pure cholesterol monolayers.

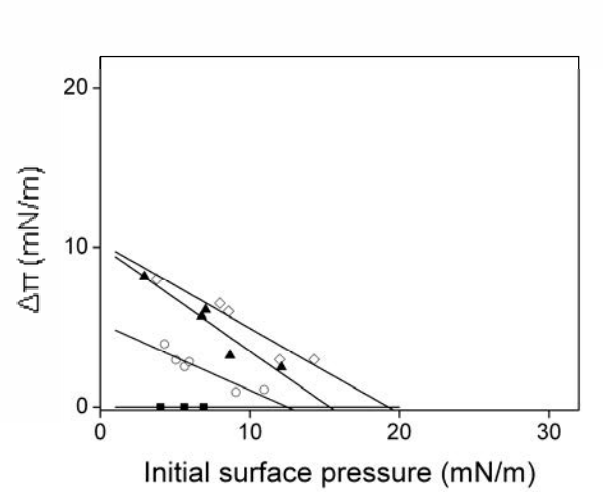

Figure 27. AnxA6-1 adsorption to different lipid monolayers. Maximal changes of the surface pressure ($\Delta\pi$) after protein injection were obtained from the kinetics of protein-induced changes in surface pressure of monolayers containing different amounts of cholesterol. The resulting $\Delta\pi$ values were plotted as a function of the initial surface pressure for the DPPC alone (filled squares), DPPC:Chol at 70:30 molar ratio (open circles), at 50:50 molar ratio (filled triangles), or Chol alone (open diamonds). The subphase was 20 mM citrate buffer, pH 5.0, containing 0.1 mM EGTA and 100 mM NaCl. The final concentration of AnxA6 was 16 nM. Published in Domon *et al*., JCIS, 2010.

The data obtained in this paragraph demonstrated that at pH 7.4 the interactions of AnxA6 with lipid monolayer were weaker than at pH 5.0. Similar results were observed for AnxA6 interactions with other lipids. For example, the increase of pH decreased AnxA6 interactions with asolectin liposomes (Golczak *et al*., 2004). This may be due to the increase in protein hydrophobicity at acidic pH as previously described in Golczak *et al*., (2001a).

Based on the results obtained for AnxA6 adsorption at the air/water interface and on the experiments performed with other lipids (Golczak *et al*., 2004) we may presume that the presence of Ca^{2+} will influence the interactions of AnxA6 with lipid monolayers. Thus, the experiments were performed in a pH 7.4 buffer containing 1 mM $CaCl_2$.

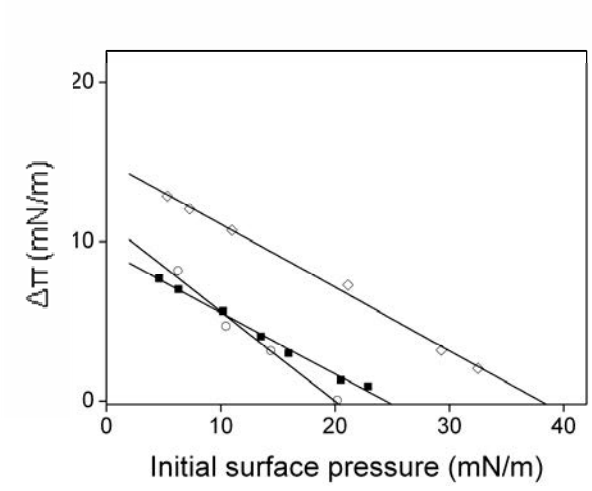

Figure 28. Ca^{2+}-dependent AnxA6-1 adsorption to different lipid monolayers. Maximal changes of the surface pressure ($\Delta\pi$) after protein injection were obtained from the kinetics of protein-induced changes in surface pressure of monolayers containing different lipids. The resulting $\Delta\pi$ values were plotted as a function of the initial surface pressure for DPPC alone (filled squares), DPPC:Chol at 70:30, molar ratio (open circles), or Chol alone (open diamonds) monolayers at different surface pressures. The subphase was 20 mM Tris-HCl, pH 7.4 containing 1 mM$CaCl_2$, 100 mM NaCl.

The kinetics of AnxA6 interactions with DPPC monolayers containing different amounts of cholesterol were recorded at different initial pressures and Fig. 28 shows the resulting $\Delta\pi/\pi_i$ curves. We found that the exclusion pressure for AnxA6 interactions with a

DPPC monolayer was ~20 mN/m, ~25 mN/m for DPPC:Chol (70:30, molar ratio) and ~40 mN/m for cholesterol monolayers (Fig. 28).

Figure 29 gives the comparison of the exclusion pressures at pH 7.4 in the presence and in the absence of Ca^{2+}. It is clearly visible that at pH 7.4 the presence of Ca^{2+} enabled insertion of AnxA6 into a pure DPPC monolayer. In the case of monolayers containing cholesterol, the presence of Ca^{2+} enhanced the interaction of AnxA6 with the monolayers.

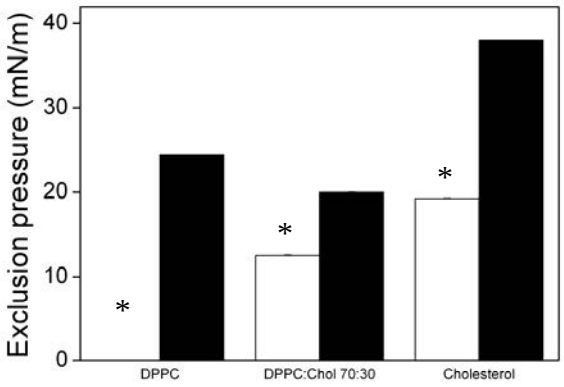

Figure 29. Histograms of the exclusion pressure of AnxA6 in the presence of lipid monolayers obtained from their respective regression curves from Fig.27 and Fig. 28. The subphase was 20 mM Tris-HCl, pH 7.4, containing 0.1 mM EGTA, 100 mM NaCl (white bars) or 20 mM Tris-HCl, pH 7.4 containing 1 mM$CaCl_2$, 100 mM NaCl (black bars). The final concentration of AnxA6 was 16 nM. The error bars have been determined from the regression curves. Significant differences between AnxA6 affinity to the monolayers in the absence or presence of Ca^{2+} are marked (Student's t test): * $p<0.05$

From the results shown above we may conclude that not only cholesterol but also Ca^{2+} ions are involved in AnxA6 interactions with lipid monolayers.

4.2.3. Interactions of AnxA6-1 with lipid monolayers mimicking membrane microdomains

We previously demonstrated that in the case of the NPC disease AnxA6 localized in the DRMs in a Ca^{2+}-dependent manner. The thin layer chromatography demonstrated that the DRMs isolated form NPC cells contained more cholesterol, phosphatidylcholine and sphingomyelin (Fig. 17). Thus we analyzed the interactions of AnxA6 with monolayers containing sphingomyelin. The interactions of AnxA6-1 with sphingomyelin (SM), SM:Chol (50:50, molar ratio) and DPPC:Chol:SM (30:30:30, molar ratio) monolayers were analyzed at pH 7.4 in the absence of calcium ions.

Figure 30 shows that in the absence of Ca^{2+}, AnxA6 did not interact with pure SM monolayers, but it interacted with monolayers composed of SM:Chol (50:50, molar ratio) and of DPPC:Chol:SM (30:30:30, molar ratio). Similar exclusion pressures (about 15 mN/m) were obtained for both monolayers. Thus, sphingomyelin does not seem to be the lipid target of AnxA6 in the microdomains.

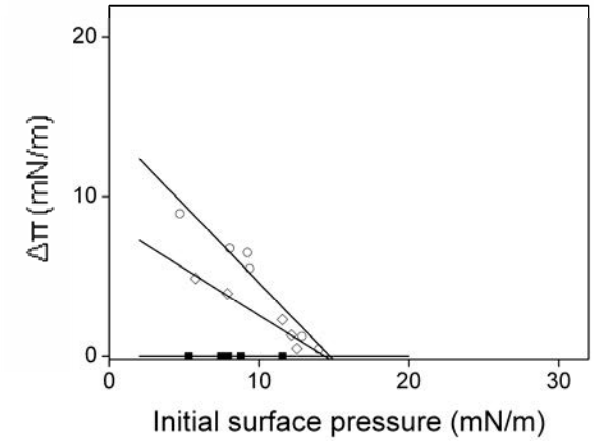

Figure 30. Adsorption of rec hAnxA6-1 to sphingomyelin-containing monolayers. Maximal changes of the surface pressure (Δπ) after protein injection were obtained from the kinetics of protein-induced changes in surface pressure of monolayers containing different lipids. The resulting Δπ values were plotted as a function of the initial surface pressure for SM alone (filled squares), SM:Chol at 50:50 molar ratio (open circles), or SM:Chol:DPPC at 30:30:30 molar ratio (open diamonds) at different surface pressures. The subphase was 20 mM Tris-HCl buffer, pH 7.4 containing 1 mM EGTA, 100 mM NaCl.

Since our results on the isolation of DRMs suggested that Ca^{2+} plays a role in the location of AnxA6-1 in the DRMs isolated from NPC cells, 1 mM $CaCl_2$ was aded to the subphase buffer at pH 7.4. The interactions of AnxA6 with monolayers composed of SM, SM:Chol (50:50, molar ratio) and DPPC:Chol:SM (30:30:30, molar ratio) were then analyzed.

Figure 31 presents the comparison of the exclusion pressures obtained for SM, SM:Chol (50:50, molar ratio) and DPPC:Chol:SM (30:30:30, molar ratio) in the presence and in the absence of Ca^{2+}.

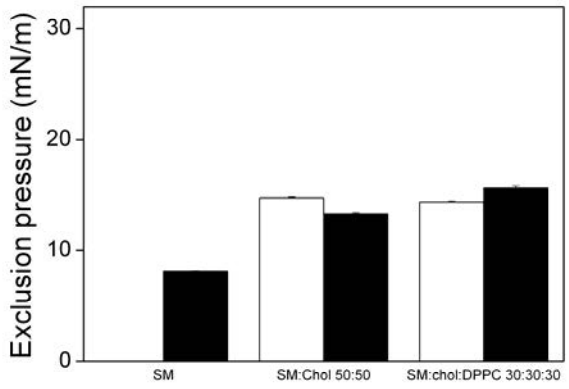

Figure 31. Histogram of Ca^{2+}-dependent interactions of rec hAnxA6-1 with the sphingomyelin-containing monolayers obtained from their regression curves. The subphase was 20 mM Tris-HCl, pH 7.4, containing 0.1 mM EGTA, 100 mM NaCl (white bars) or 20 mM Tris-HCl, pH 7.4 containing 1 mM$CaCl_2$, 100 mM NaCl (black bars). The final concentration of AnxA6-1 was 16 nM. The error bars have been determined from the regression curves.

The presence of Ca^{2+} in the buffer enabled the insertion of AnxA6-1 to the monolayers composed of SM, but it did not change the interactions between AnxA6-1 and the monolayers composed of SM:Chol (50:50, molar ratio) nor with the monolayers composed of DPPC:Chol:SM (30:30:30, molar ratio).

These findings suggest that even though sphingomyelin is an important component of the DRMs, it does not greatly affect AnxA6 interactions with the lipid monolayers and confirm the role played by cholesterol.

4.2.4. Factors affecting the interactions between AnxA6 and cholesterol *in vitro*

After having analyzed external factors implicated in AnxA6-cholesterol interactions, we focused on structural elements of cholesterol and AnxA6 that may be involved in these interactions.

4.2.4.1. Role of the hydroxyl group of cholesterol

In order to determine whether the –OH group of cholesterol plays a role in its interaction with AnxA6, we replaced cholesterol by cholesteryl acetate (Chol-Ac). The kinetic profiles of AnxA6-1 binding to pure Chol-Ac monolayers were determined at different initial surface pressures as described above (data not shown) and $\Delta\pi$ values were plotted as a function of the initial surface pressure. Regardless of the subphase pH (7.4 or 5.0), the injection of 16 nM AnxA6-1 beneath the Chol-Ac monolayer induced a surface pressure increase for initial pressures lower than 10 mN/m (Fig. 32).

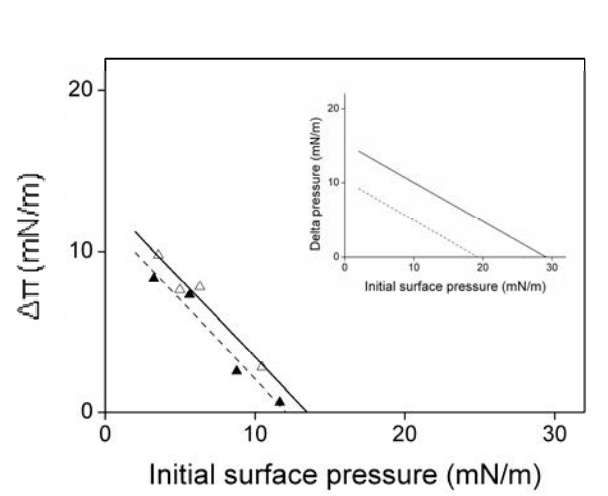

Figure 32. Influence of pH on the interactions between rec hAnxA6-1 and monolayers of cholesteryl acetate. $\Delta\pi$ values, obtained from the kinetic curves of protein-induced changes in the surface pressure, were plotted as a function of the initial surface pressure of the lipid film. The subphase was 20 mM citrate buffer, pH 5.0, 0.1 mM EGTA, 100 mM NaCl (full line) or 20 mM Tris-HCl, pH 7.4 containing 0.1 mM EGTA, 100 mM NaCl (dashed line). To facilitate the comparison the insert gives the results obtained with Chol monolayers at pH 5.0 (full line) and at pH 7.4 (dashed line). The final concentration of AnxA6 was 16 nM. Published in Domon *et al*., JCIS, 2010.

The exclusion surface pressures were 12 mN/m at pH 7.4 and 13.5 mN/m at pH 5.0. The difference between these two exclusion pressures is insignificant and indicates that pH did not play a key role in AnxA6-1 affinity for Chol-Ac. Furthermore, the exclusion pressures observed with Chol-Ac were lower than those obtained with pure Chol monolayers (Fig. 32, insert), suggesting that the presence of the CH_3COO- group in cholesteryl acetate instead of –OH group in cholesterol strongly diminishes the interaction of AnxA6-1 with the biomimetic membranes.

4.2.4.2. Importance of the VAAEIL sequence of AnxA6-1

Due to alternative mRNA splicing of the 21st exon, in mammalian cells, annexin A6 is expressed in two isoforms: AnxA6-1 and AnxA6-2, the latter lacking the 524-VAAEIL-529 sequence at the start of repeat 7 (Smith *et al*., 1994). It was previously shown that AnxA6-2 is characterized by a higher affinity for Ca^{2+}, lower hydrophobicity and lower negative surface charge, as compared to AnxA6-1 (Kaetzel *et al*., 1994). Based on these findings we decided to check whether the absence of this sequence will have any effect on the affinity to the air/water interface or on the interactions with cholesterol.

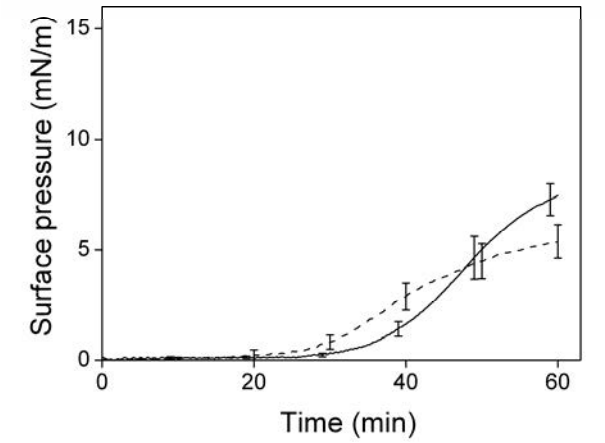

Figure 33. Influence of pH on the adsorption of AnxA6-2 isoform at the air/water interface. The subphase was pH 5.0 buffer (full line) or pH 7.4 buffer (dashed line) in the absence of Ca^{2+}. Protein was injected into the subphase to a final concentration of 16 nM and pressure was continuously recorded. Curves represent the average of three independent experiments. For the sake of graph clarity, the error bars are shown only for experimental points at 10 min intervals.

Experiments were performed at pH 7.4 and at pH 5.0 in the absence of Ca^{2+}. At pH 7.4 AnxA6-2 induced changes in the surface pressure with a plateau at ~5.5 mN/m (Fig. 33, dashed line). Decreasing the pH to 5.0 slightly affected the kinetics of AnxA6-2 adsorption and the plateau was reached at 7.5 mN/m (Fig. 33, full line).

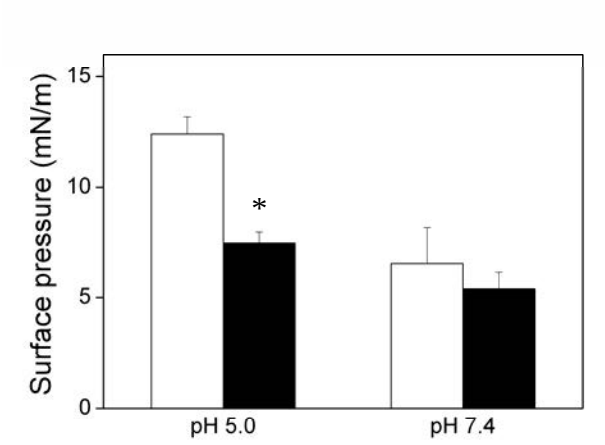

Figure 34. Histogram of pH-dependent adsorption of AnxA6-1 (white bars) and AnxA6-2 (black bars) at the air/water interface 60 min after protein injection. The subphase was 20 mM citrate buffer, pH 5.0, containing 0.1 mM EGTA, 100 mM NaCl or 20 mM Tris-HCl, pH 7.4 containing 0.1 mM EGTA, 100 mM NaCl (black bars). The final concentration of AnxA6 was 16 nM. Bars represent the average of three independent experiments. Significant differences between AnxA6-1 and AnxA6-2 isoforms are marked (Student's t test): * $p<0.05$.

The result obtained for the AnxA6-2 isoform at pH 7.4 did not differ much from the result obtained for the AnxA6-1 isoform, while at pH 5.0 the plateau observed for AnxA6-1 was about towfold higher (Fig. 34). This result may be explained by similar, low hydrophobicity of both isoforms at pH 7.4. At pH 5.0 the hydrophobicity of the AnxA6-1 isoform strongly increases, while for AnxA6-2 it remains unchanged (Strzelecka-Kiliszek *et al*., 2008).

Previous data concerning the AnxA6-2 isoform suggested that the VAAEIL sequence might be implicated in AnxA6-membrane interactions (Strzelecka-Kiliszek *et al*., 2004). To verify this hypothesis, the adsorption of AnxA6-2 to different sterol monolayers was studied at pH 5.0. The determination of the exclusion pressures of cholesterol and cholesteryl acetate monolayers upon AnxA6-2 addition are shown in Fig. 35.

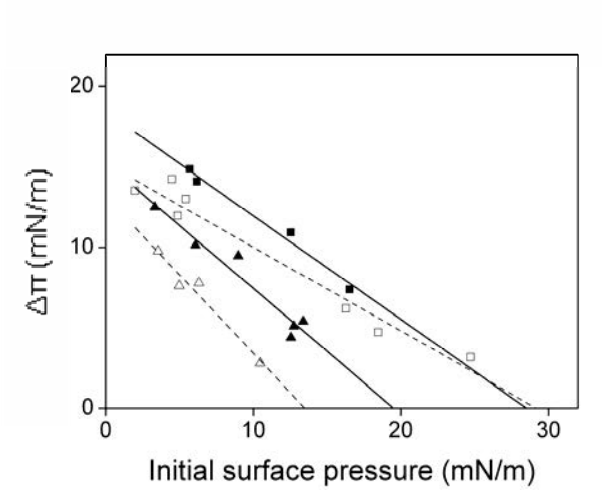

Figure 35. Interactions of AnxA6-2 isoform with monolayers composed of cholesterol or cholesteryl acetate. Δπ values, obtained from the kinetic curves of protein-induced changes in surface pressure, were plotted as a function of the initial pressure of the lipid film. Subphase was 20 mM citrate buffer, pH 5.0 containing 0.1 mM EGTA, 100 mM NaCl. Full squares and full triangles correspond to pure cholesterol or pure Chol-Ac monolayers, respectively. The results obtained at pH 5.0 with the wild type AnxA6-1 and pure Chol (open squares) or Chol-Ac (open triangles) monolayers were added for comparison.

The injection of AnxA6-2 beneath the pure cholesterol monolayer allowed us to estimate the exclusion pressure of 28.5 mN/m, while the exclusion pressure after AnxA6-2 injection beneath the cholesteryl acetate monolayer was estimated to be 19.5 mN/m. The comparison of these exclusion pressures of both isoforms showed that there was no difference between isoforms in the interactions with cholesterol, but AnxA6-2 interacted stronger than AnxA6-1 with cholesteryl acetate monolayers (Fig. 35, dashed lines).

4.2.4.3. Importance of the linker region of AnxA6-1

Previous studies demonstrated that the linker region of AnxA6 may be important for AnxA6 interactions with membranes (Avila-Sakar *et al*., 2000; Buzhynskyy *et al*., 2009). It was also demonstrated that the W343 residue present in the linker region of AnxA6-1 and implicated in GTP-binding and ion channel forming activity, may be important for AnxA6-membrane interactions (Kirilenko *et al*., 2006). Also, the phosphorylation-mimicking

mutation T356D in this region may induce changes of AnxA6 affinity to the membranes by increasing the flexibility of this region of the protein (Freye-Minks *et al*., 2003).

To investigate the role played by W343 in the AnxA6 surface properties, experiments were performed with AnxA6-1 W343F mutant in neutral and acidic pH conditions. At pH 7.4, in the absence of calcium, the W343F mutant induced changes in the surface pressure with a plateau at 5 mN/m (Fig. 36, full line). This result is similar to that obtained for wild type AnxA6 in the same conditions (Fig. 20, dashed line). In contrast, the adsorption of AnxA6 W343F was not affected by decreasing pH to 5.0 (Fig. 36, dotted line). At pH 5.0, wild type AnxA6 significantly increased the interface pressure and the maximal lateral pressure of the protein layer was reached at 12 mN/m (Fig. 19, dashed line). The pH-insensitive adsorption of AnxA6 W343F suggests that W343 affects the hydrophobicity of AnxA6 (Golczak *et al*., 2004; Kirilenko *et al*., 2006).

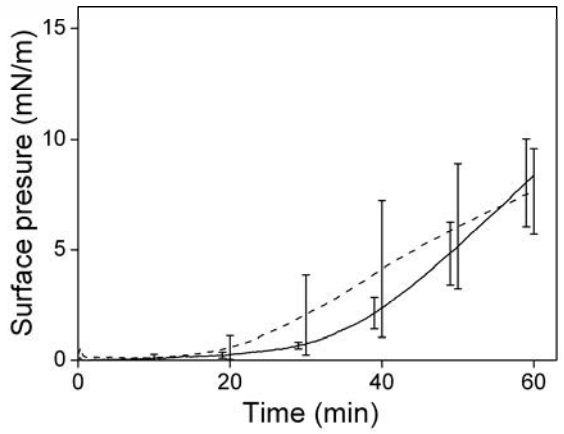

Figure 36. Influence of pH on the adsorption of the AnxA6-1 W343F mutant at the air/water interface. The subphase was pH 5.0 buffer (dotted line) or pH 7.4 buffer (full line). Protein was injected into the subphase to a final concentration of 16 nM and pressure was continuously recorded. Curves represent the average of three independent experiments. For the sake of graph clarity, the error bars are shown only for experimental points at 10 min intervals. Published in Domon *et al*., JCIS, 2010.

Considering that the W343 residue of AnxA6-1 (due to its aromatic ring) might be involved in the interaction with cholesterol, the adsorption of the AnxA6-1 W343F mutant to different sterol monolayers was studied at pH 5.0.

Figure 37 (full lines) gives the determination of the exclusion pressures of cholesterol and cholesteryl acetate monolayers after injection of the AnxA6-1 W343F mutant. The injection of the AnxA6-1 W343F mutant beneath pure cholesterol monolayer allowed us to estimate an exclusion pressure of 36 mN/m, while the exclusion pressure after AnxA6-1 W343F mutant injection beneath a pure cholesteryl acetate monolayer could be estimated at 15 mN/m. Comparison of these exclusion pressures obtained with the mutant protein with the corresponding data obtained with the wild-type protein (Fig. 37, dotted lines) showed that the

AnxA6-1 W343F mutant interacted more strongly with cholesterol than AnxA6-1, while both proteins exhibit similar affinity towards cholesteryl monolayers.

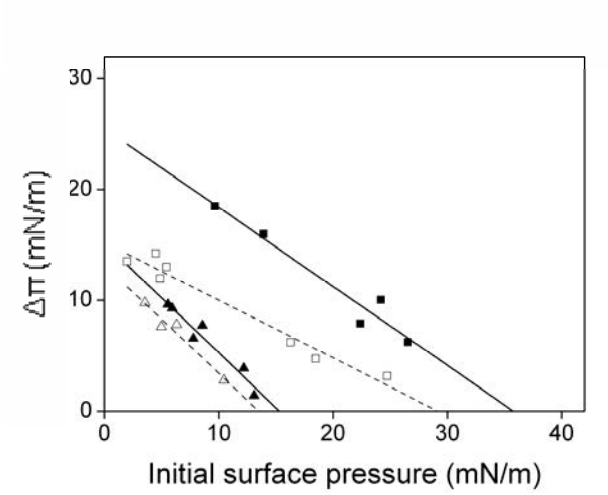

Figure 37. Interactions of AnxA6 W343F with monolayers of cholesterol or cholesteryl acetate. Δπ values, obtained from the kinetic curves of protein-induced changes in surface pressure, were plotted as a function of the initial pressure of the lipid film. Subphase was 20 mM citrate buffer, pH 5.0 containing 0.1 mM EGTA, 100 mM NaCl. Full squares and full triangles correspond to pure cholesterol or pure Chol-Ac monolayers, respectively. The results obtained at pH 5.0 with the wild type AnxA6-1 and pure Chol (open squares) or Chol-Ac (open triangles) monolayers were added for comparison. Published in Domon *et al.*, JCIS, 2010.

Summarizing, the results presented in this part of the thesis show the importance of the cholesterol content in the monolayers for the AnxA6-monolayer interactions. It was also demonstrated that pH 5.0 and the presence of Ca^{2+} enhanced AnxA6 interactions with cholesterol containing monolayers. These results confirmed also our hypothesis that the –OH group of cholesterol and the linker region of AnxA6 are implicated in AnxA6-monolayer interactions.

CHAPTER 5
DISCUSSION

The Niemann-Pick disease type C is a lysosomal lipid storage disorder characterized by altered vesicular transport and abnormal accumulation of cholesterol and other lipids in the late endosome/lysosome compartment. Even though it was demonstrated that the NPC disease is caused by mutations in either one of the two proteins i.e., NPC1 and NPC2, of the LE/LY compartment, the mechanism of cholesterol accumulation in NPC cells is still not well understood. In the present work we were, in particular, interested in the characterization of detergent-resistant membranes isolated from NPC fibroblasts. Secondly, we aimed to analyze the properties of a protein implicated in cholesterol transport i.e., AnxA6, and we focused on the putative mechanism of AnxA6-1 interaction with cholesterol-enriched membranes.

5.1 Comparisom between lipid microdomains of NPC and control fibroblasts

In the first part of the thesis, we tested the hypothesis that abnormal cholesterol storage in LE/LY compartment of NPC cells induces also changes in DRMs quantity and composition. We observed that NPC L1 fibroblasts contained a significantly higher amount of lipid rafts in comparison to control fibroblasts that is consistent with a defect in cholesterol turnover in these cells (Fig. 12, Fig. 13). The fluorescent visualization of cholesterol using filipin staining demonstrated characteristic punctuate accumulation of free cholesterol in perinuclear endocytic structures (Fig. 12B). The staining pattern of NPC L1 cells did not differ from that observed in the cells with deleted *NPC1* gene. For example NPC1-deficient mice hepatocytes (Vainio *et al.*, 2005) or CHO NPC1$^{-/-}$ cells (Kosicek *et al.*, 2010) exhibited the same characteristic NPC phenotype.

The visualization of GM1 and CD55, markers of lipid rafts, revealed that lipid domains were located mostly in the perinuclear region of NPC cells probably corresponding to the late endosome/lysosome compartment (Fig. 12A). The results of DRM isolation from the organelles implicated in endocytosis (LE/LY, EE compartment and HM) confirmed our hypothesis that in cells derived from NPC patients the DRMs were mostly accumulated in the late endosome/lysosome compartment (Fig. 18). There was no GM1 in LE/LY isolated from control cells, however there was a lot of GM1 in LE/LY from NPC cells. EE of control cells contained some GM1 and in NPC cells we detected a bit more GM1. There was no difference in the GM1 content in HM of both cell lines. These findings are in agreement with those of other researchers (Lusa *et al*., 2001) suggesting the accumulation of cholesterol in LE/LY fractions.

The differences in DRM content may originate from the different lipid organization in both cell types. In normal cells both the early and recycling endosomes as well as the trans-Golgi network are enriched in membrane lipids that are expected to form membrane microdomains (Mukherjee *et al*., 1998, Gagescu *et al.*, 2000). In contrast, late endosomes and lysosomes do not accumulate microdomains because of the activity of sphingolipid hydrolases. In NPC cells the situation is different because the glycosphingolipid and sphingosine content is very high (Simons and Gruenberg, 2000). Elevated levels of glycosphingolipids, sphingosine and cholesterol were observed in membrane microdomains isolated from mutant Npc1-null cells from liver, spleen or brain of a NPC patient as well as from U18666A and progesterone induced NPC cell culture models (te Vruchte *et al*., 2004). Thus, we propose that the accumulation of cholesterol and sphingolipids in the late endosome/lysosome compartment in NPC cells (Simons and Gruenberg, 2000) could induce the excessive formation of microdomains.

Another typical feature of NPC cells is that the storage material is highly complex and includes multiple classes of lipids (Lloyd-Evans *et al.*, 2008; te Vruchte *et al*., 2004; Lloyd-Evans and Platt 2010). The lipids that progressively accumulate in this disease include cholesterol, sphingomyelin (SM) (Butler *et al*., 1993), multiple glycosphingolipids (GSLs) and the sphingolipid catabolic product, sphingosine (Lloyd-Evans *et al*., 2008).

The analysis of lipid association with DRM revealed that in the case of NPC L1 cells, DRMs were enriched with cholesterol, sphingomyelin, but they also contained phosphatidylcholine (PC) (Fig. 17). Of these three, PC is a major component of detergent-soluble membranes, whereas cholesterol and SM associate strongly with DRMs. This is not surprising in view of the results of other researchers. The studies on the plasma membrane of $NPC1^{-/-}$ Balb/c mice hepatocytes using [^{14}C]cholesterol or [^{3}H]choline revealed that cholesterol, SM and PC exhibited an increased tendency to associate with DRMs. The most pronounced difference was seen in the DRM association of PC. This probably reflects changes in PC fatty acyl chain composition observed in NPC (the acyl chain saturation of major PLs, SM and PC in particular, was increased in the plasma membrane of NPC cells, and the fatty acyl chain lengths of these lipids were decreased), and indicates that both the raft- and non-raft-favoring lipids exhibit increased detergent resistance in NPC membranes (Vainio *et al*., 2005). The increased content of saturated free fatty acids was also observed in whole cell homogenates of fibroblasts and SPM-3T3 mice hepatocytes (Koike *et al*., 1998). Also PNS, and LE/LY isolated from the human NPC L1 fibroblast cell line contained more free saturated fatty acids than the corresponding fractions from control fibroblasts.

5.2 Annexin A6 – the protein implicated in endocytosis is also implicated in lipid raft formation in NPC disease

Membrane dynamics encompass multiple lipid-lipid, and lipid-protein interactions. The mechanism of lipid rafts formation and stabilization is still unknown but there are many proteins that may be implicated in this process. We focused on AnxA6, the largest member of annexins, and in the next part of the thesis we aimed to shed a new light on the mechanism of AnxA6 participation in the NPC-induced changes in the organization of DRMs.

Our results demonstrated that in NPC L1 fibroblasts AnxA6 translocated to the late endosome/lysosome compartment (Fig. 14), where we observed abnormal accumulation of unesterified cholesterol and markers of lipid rafts (Fig. 12). These observations could suggest AnxA6 implication in membrane related processes, such as endocytic trafficking, and its contribution to the etiology of NPC disease. Our findings are also supported by the findings of other researchers who, using other cellular models, showed colocalization of AnxA6 with cholesterol. For example, Grewal *et al*., 2000 demonstrated that after incubation of CHO cells with LDL particles, AnxA6 translocated to the late endosome/lysosome compartment. Also, U18666A-induced accumulation of cholesterol in the late endosomal compartment resulted in a significant accumulation of AnxA6 in these vesicles in CHO cells (de Diego *et al.,* 2002). Overexpression of AnxA6 in CHO cells resulted in accumulation of cholesterol in the perinuclear region. On the other hand, knock-down of the AnxA6 gene restored the cellular distribution of cholesterol (Cubells *et al*., 2007).

The sequestration of cholesterol in late endosomes is not only representative of an NPC-like phenotype, but is also associated with reduced cholesterol levels in other cellular compartments, in particular the Golgi and the plasma membrane. Furthermore, increased late endosomal cholesterol is accompanied by a rearrangement of AnxA6 intracellular distribution, leading to the translocation of a significant amount of AnxA6 to LE compartment (de Diego *et al*., 2002, Grewal *et al*., 2000). Reduced cholesterol levels in the Golgi and at the cell surface are probably responsible for the retention of caveolin-1 in the Golgi complex and the reduced number of caveolae observed at the cell surface. Given that AnxA6 expression correlates with the number of caveolae in various cell types (Cubells *et al.,* 2007), we hypothesize that AnxA6 expression levels could be a marker indicative of the potential abundance of caveolae in quite a lot of different cells and tissues.

Also, in the light of the findings described in the former paragraph (suggesting that the endocytic cholesterol is mostly located in microdomains) we supposed that AnxA6 is

implicated in the formation and/or stabilization of lipid microdomains. The isolation of DRM revealed that the differences in lipid compositions of NPC and control fibroblasts influenced also AnxA6 localization and insertion into lipid microdomains. In the absence of Ca^{2+}, AnxA6 was found outside DRMs. However, when the DRM preparation was done in the presence of 40 μM Ca^{2+}, AnxA6 was found to localize in DRM fractions enriched in GM1 (Fig. 15, Fig. 16). This Ca^{2+} concentration is not physiological, it nonetheless enabled the insertion of AnxA6 to the DRMs isolated from NPC L1 fibroblasts.

The translocation of AnxA6 to the DRM fractions of NPC L1 cells may be explained as follows. AnxA6 was described to bind phospholipids in a Ca^{2+}- dependent manner, here we showed that low Ca^{2+} concentration is sufficient to induce AnxA6 association with DRMs in cells that contain elevated cholesterol but not in control ones. This suggests that both cholesterol and Ca^{2+} influence AnxA6 interactions with membranes and points out that cholesterol is the main target of AnxA6 in the microdomains. Our data suggest that calcium concentration is an important factor when NPC disease, AnxA6 and cholesterol homeostasis are considered.

The Ca^{2+}-dependent translocation of AnxA6 to the DRMs of NPC is a very important finding while analyzing NPC disease. Abnormal calcium homeostasis is an emerging factor in the pathogenesis of the primary lysosomal sphingolipid storage disorders such as Gaucher disease, Sandhoff disease and GM1 gangliosidosis (Hughes and Pastores, 2010; Lloyd-Evans *et al*., 2008; Ginzburg *et al*., 2004; Jeyakumar *et al*., 2005). It was demonstrated that intracellular cholesterol transport depends on intracellular Ca^{2+} concentration (Luzio *et al*., 2007). Recently published data demonstrate that in lysosomes isolated from NPC fibroblasts Ca^{2+} concentration was 2,5 times lower (209 μM) than in those from control fibroblasts (550 μM), and it is worth mentioning that no difference in pH of this cellular compartment was detected (Lloyd-Evans *et al*., 2008). Because the exchange of contents between LE/LY is a calcium dependent process that requires ongoing tubulovesicular late endocytic trafficking (LE/LY fusion) (Luzio *et al*., 2005) the low Ca^{2+} concentration in NPC disease could induce impaired LE/LY fusion and vesicular transport (Lloyd-Evans *et al*., 2008; Ko *et al*., 2001; Mayran *et al*., 2003). Probably the low calcium concentration could also influence the behavior of proteins that interact with membranes in a Ca^{2+}-dependent manner and are implicated in cholesterol endocytosis e.g., AnxA6. Since, AnxA6 is proposed to be implicated in the formation and stabilization of lipid domains, the increased lipid raft content and the defect in calcium homeostasis could influence AnxA6 interactions with microdomains. AnxA2 and AnxA6 were shown to translocate to DRMs (membrane rafts) in a Ca^{2+}-

dependent manner, in smooth muscle plasmalemma (Babiychuk and Draeger., 2000) and synaptic plasma membrane of rat brain (Orito *et al.,* 2001). Similar results were obtained for AnxA6 in CHO cells (Enrich *et al*., 2011). At the steady-state, AnxA6 and AnxA2 seem to be components of membrane rafts (caveolae) as well as non-raft domains (clathrin-coated pits) and seem to be involved in endocytosis. In clathrin-coated pits both annexins are associated with the μ-subunits of the clathrin adaptor complex AP2 in a Ca^{2+}-dependent manner (Creutz and Snyder, 2005). In addition, AnxA2 and AnxA6 have been identified in isolated caveolae fractions from different cells and tissues (Calvo and Enrich, 2000; Pol *et al*., 1997; Sprenger *et al*., 2004; Foster *et al*., 2003; Aboulaich *et al*., 2004) and a complex of AnxA2 and caveolin appears to facilitate the transport of esterified cholesterol from the plasma membrane to internal membranes (Smart *et al.,* 2004; Uittenbogaard *et al*., 2002).

To summarize, our results suggest that AnxA6 could be implicated in the formation and stabilization of lipid microdomains and that its main target is cholesterol.

5.3 Interaction between AnxA6 and lipid microdomain-mimicking monolayers depends on the presence of cholesterol and Ca^{2+}

To validate our presumption that in the lipid microdomains cholesterol is the main target of AnxA6, we created artificial lipid monolayers with a lipid composition similar to our cellular model. Three main components found in DRMs isolated from NPC fibroblasts were analyzed: cholesterol, SM and PC. At pH 7.4 AnxA6 did not interact with microdomains composed only of SM or DPPC. The presence of cholesterol was the factor enabling the interactions of AnxA6 with the monolayer (Fig. 27, Fig. 30). The increasing content of cholesterol in the monolayer increased AnxA6 insertion into the monolayer. Thus, we could conclude that cholesterol is the main target of AnxA6 in the microdomains. This supports also our hypothesis that in the NPC disease the translocation of AnxA6 to the LE/LY compartment is linked to abnormal accumulation of cholesterol in the microdomains.

The only doubt is why the interactions of AnxA6 with the monolayers composed of DPPC:Chol:SM (30:30:30, molar ratio) or SM:Chol (50:50, molar ratio) are so weak?

This could be due to a particular organization of lipids in the lipid microdomains, which could differ from the organization of lipid monolayers. Those differences could be also due to the presence of many types of proteins and lipids and/or to the particular interactions between cholesterol and phospholipids.

Cholesterol is an alicyclic lipid molecule, consisting of four fused rings, a 3β-hydroxyl and a hydrophobic tail, all of which are important in interacting with phospholipids (Yeagle, 1985). It is a major constituent of plasma membranes of eukaryotic cells, contributing to 30–40 mol% of the lipid fraction (Brown and London, 1998). Sphingolipids, as represented by sphingomyelin (SM), are one of the major classes of membrane phospholipids in eukaryotic organisms (Barenholz and Thompson, 1999). SMs and phosphatidylcholines (PCs) constitute more than 50% of the membranes' phospholipids and are strongly enriched in the external leaflet of the plasma membrane (Barenholz and Thompson, 1999). Both phospholipid classes contain phosphoryl choline as the polar head group, but their backbones differ. SM has sphingosine as the hydrophobic backbone, together with an amide-linked acyl chain. PCs are glycerophospholipids with two acyl chains linked to the glycerol backbone with carbonyl ester linkages. Compared with natural glycerophospholipids, naturally occurring SMs are enriched in long saturated fatty-acyl chains, have a higher melting temperature, are more hydrophobic and can undergo tight packing in cell membranes due to the absence of the kinked structure of unsaturated acyl chains (Barenholz and Thompson, 1999). For example, sphingomyelin from chicken egg yolk contains primarily palmitic acid.

It was postulated that cholesterol affects the packing of sphingolipid molecules by occupying the space between the saturated hydrocarbon chains of the sphingolipids and causing condensation of the molecules. The association of cholesterol with sphingolipids is most likely strengthened by hydrogen bonding between the -OH group of the sterol and the amide group of the sphingolipid ceramide backbone (Simons and Ikonen, 2000; Brown and London, 2000). We suggest that cholesterol-sphingomyelin interactions might play a role in AnxA6 insertion to the monolayer.

However, in order to explain the phenomenon of AnxA6 association with membranes, it is essential to analyze the possible mode of interaction between AnxA6 and cholesterol and the factors implicated in this interaction.

5.4 AnnexinA6 interactions with lipid rafts are based on its interactions with cholesterol

Several lines of evidence suggesting that annexin A6 could interact with cholesterol exist in the literature, however, the precise mechanism of its interactions with cholesterol is still a matter of investigations. This is probably due to the fact that in the AnxA6 molecule, in contrast to other cholesterol binding proteins, no specific cholesterol-sensing domain was

found. Sterol-sensing domains (SSDs), motifs conserved in evolution, consist of approximately 180 amino acid residues organized into a cluster of five consecutive membrane-spanning domains. They are found in proteins which have key roles in different aspects of cholesterol homeostasis or cholesterol-linked signaling such as sterol-regulated movement or the trafficking of specific cargos. The SSDs are present in several membrane proteins, including NPC1, NPC2, HMG-CoA reductase, and the SREBP cleavage–activating protein (Zhang *et al*., 2011; Chang *et al*., 2006).

Taking into consideration the information given above, in the second part of the thesis we focused on the putative mechanism of AnxA6 interactions with cholesterol-enriched microdomains, and in particular on the mechanism of AnxA6 interaction with cholesterol. To explain this phenomenon we used a biomimetic system-Langmuir monolayers.

5.4.1 AnxA6 interactions with cholesterol depend on pH and the presence of Ca^{2+}

First, we focused on the external factors that may influence AnxA6-cholesterol interactions. Our studies demonstrated that at acidic pH the interactions of AnxA6 with cholesterol-containing monolayers are stronger than at pH 7.4. (Fig. 22-23, Fig, 26-27). We suppose that this may be due to changes in the structure of AnxA6 induced by acidic pH. As we showed, acidic pH induced changes in AnxA6 affinity at the air/water interface (Fig.19, Fig. 20). Also the studies of other researchers demonstrated that at acidic pH AnxA6 undergoes profound conformational changes (Golczak *et al*., 2001b). Studies on the porcine annexin A6 using fluorescence and far-UV circular dichroism (CD) measurements demonstrated a profound increase in protein hydrophobicity at acidic pH and the appearance of a conformational state that varied from the native AnxA6 structure at pH close to 7.0 (Golczak *et al*., 2001c).

We suggest that these conformational changes of AnxA6 could have influence on interactions with cholesterol. The pH affected also AnxA6 interactions with other lipids, for example with DPPC (Fig. 23 filled squares, Fig. 27, filled squares). Also the previous studies from our laboratory demonstrated that at acidic pH, porcine liver AnxA6 was able to bind to phospholipid bi- and monolayers in a Ca^{2+}-independent manner, at acidic pH (half-maximal binding to asolectin liposomes occurred at pH 5.3) (Golczak *et al.*, 2001b). AnxA6 interaction with phospholipids at low pH is probably due to a Ca^{2+}-independent increase in the area of the exposed hydrophobic surface of AnxA6 (Golczak *et al*., 2001c). In this respect, AnxA6 is similar to other members of the annexin family of proteins (AnxA5 and AnxA12) (Köhler *et al*., 1997; Isas *et al*., 2000; Cartailler *et al*., 2000). Changes in the hydrophobic surface of

AnxA6 accompanied a Ca^{2+}-independent transformation of AnxA6 from a soluble to an integral membrane protein able to affect membrane permeability to cations at acidic pH (Golczak *et al*., 2001b). Furthermore, a Ca^{2+}-independent conformational change resulting in a partial conversion of the α-helical structure to ß-sheet structures was observed in the AnxA6 molecule (Golczak *et al*., 2001c; Golczak *et al*., 2004). In addition, far-UV CD data showed that the number of α-helical segments in AnxA6 was smaller at acidic pH while the average length of the remaining α-helical segments did not change (Golczak *et al*., 2001c).

To understand the mechanism underlying the properties of AnxA6 at low pH, it is necessary to recall its cellular localization, the known links to disease and its potential involvement in functional pathways. AnxA6 associates specifically with membranes of low pH compartments (i.e. late endosomes and synaptosomes) in a number of cell types, which is indicative of its involvement at late stages of the endocytic pathway (Grewal *et al*., 2000; Pons., 2000; Kamal *et al*., 1998, Sztolsztener *et al*., 2010). There are some other unrelated proteins sharing similar properties. For example, it was also demonstrated that the membrane association of endosomal coat proteins (COPs), involved in membrane transport in the endocytic pathway, depends on acidic endosomal pH. It was found that membrane recruitment of endosomal COPs depends on a small cytosolic GTP-binding protein, ARF1. The membrane association of ARF1 is sensitive to endosomal pH, perhaps due to a binding to a transmembrane protein that changes its conformation on the cytosolic side of the endosome membrane upon acidification of the endosome lumen (Gu and Gruenberg, 2000). Therefore, ARF1 acts as a cytosolic component of the transmembrane pH-sensing mechanism (Gu and Gruenberg, 2000). It can be speculated that AnxA6 also reveals transmembrane pH-sensing properties that may explain its preferential binding to late endosomes characterized by an acidic interior. However, in contrast to ARF1, AnxA6 probably does not require any additional endosomal proteins for binding to endosome membrane, being itself a pH-dependent protein. If so, it is possible that under physiological conditions AnxA6 may sense lower pH values than those in the cytosol.

In the next part of the thesis we tested the importance of the presence of Ca^{2+} on AnxA6 interactions with cholesterol. As it was already mentioned in the first part of the Discussion, isolation of lipid microdomains suggested that at pH 7.4 the presence of Ca^{2+} is an important factor in AnxA6-DRMs interactions. Also our studies using lipid monolayers demonstrated that the presence of Ca^{2+} enhanced AnxA6 interaction with cholesterol containing monolayers (Fig. 29). At the same time AnxA6 alone was shown to undergo

conformational changes induced by the presence of Ca^{2+} and we observed the appearance of ß-sheet structures (Fig. 21). The presence of ß-sheet structures could enhance the hydrophobicity of AnxA6 and facilitate the interactions with membranes (Golczak *et al*., 2001c).

We suggest that under certain experimental conditions the presence of Ca^{2+} affects the conformational state of AnxA6, and change the mode of action between AnxA6 and cholesterol containing monolayers. The importance of Ca^{2+} in AnxA6 interactions with membranes was tested using other lipids that are present in membranes. For example, it has been previously demonstrated that AnxA6 interacted with negatively charged phospholipids in a Ca^{2+}-dependent manner and that the mode of interactions differed in the presence and absence of Ca^{2+} (Buzhynskyy *et al*., 2009). The influence of Ca^{2+} was already demonstrated for the AnxA6 interaction with PS containing membranes. It was found that AnxA6 presents two modes of membrane association depending on Ca^{2+}-concentration. At low Ca^{2+}-concentration (~60–150 μM), AnxA6 was able to bind PS-containing membranes but was not able to aggregate membranes. At high Ca^{2+}-concentration (~2 mM), AnxA6 was able to bind two membranes simultaneously (Buzhynskyy *et al.*, 2009). These results are in agreement with the observation made by other researchers that calcium concentration influenced annexin A6 binding to membranes (Zaks and Creutz, 1990; Avila-Sakar *et al*., 2000).

Our results clearly indicate the role of pH and Ca^{2+} in the interactions with cholesterol containing monolayers. However, apart from the external factors that may be responsible for AnxA6-cholesterol interactions we wanted to identify the structural elements of AnxA6 and cholesterol that could be responsible for these interactions.

5.4.3 The –OH group of cholesterol is implicated in the AnxA6-cholesterol interaction

Cholesterol is composed of a single 3ß-hydroxyl as the only polar component, a nearly planar assembly of four rings, and a short alkyl chain (van Meer, 2005). While the steroid and the hydrocarbon chain are embedded in the membrane, alongside the nonpolar fatty acid chains of the other lipids, the hydroxyl group of cholesterol was found to interact with the polar head groups of the membrane phospholipids and sphingolipids. We suggested that the AnxA6-cholesterol interaction is stimulated by the –OH group of cholesterol that is exposed to the surface of the monolayer facing the aqueous solution. Our data demonstrated that replacement of the –OH group of cholesterol by the CH_3COO- group in cholesteryl acetate

resulted in a less efficient AnxA6 insertion to the lipid monolayer (Fig. 32) thus pointing out the importance of the hydroxyl group of cholesterol in these interactions.

The results obtained by other researchers concerning the mechanism of interaction of other proteins with cholesterol suggest that the 3*ß*-hydroxyl group of cholesterol seems also to be implicated in its interactions with the C-reactive protein (CRP) (Taskinen *et al.*, 2005) or with proteins implicated in cholesterol homeostasis (Radakrishnan *et al*., 2007). Scap recognizes the tetracyclic steroid nucleus and the 3*ß* -hydroxyl group of cholesterol. It binds the sterol equally well even when it lacks a side chain. It was able to recognize cholesterol in its usual orientation in the membrane, i.e., when its 3*ß* -hydroxyl is exposed at the surface and its side chain is buried in the hydrophobic bilayer (Radakrishnan *et al*., 2007).

The precise mechanism of the interaction of AnxA6 with the –OH group is yet to be determined. This interaction needs further investigation which will help to determine if there is a direct or a water-mediated interaction. There is also a possibility that there may be a particular interaction between a specific AnxA6 amino acid residue (ex.W343) and the –OH group of cholesterol, like it is in the case of the *Osh*4 protein (a homolog of the oxysterol binding proteins) of *Saccharomyces cerevisiae*. In the case of this protein, direct or water-mediated interactions between the 3-hydroxyl (3-OH) group of cholesterol and W46, Q96, Y97, N165, and/or Q181 as well as dispersive interactions with F42, L24, L39, I167, and I203 were observed (Singh *et al*., 2009).

5.4.4 The linker region and the VAAEIL sequence of AnxA6 are implicated in the AnxA6-cholesterol interaction

Moreover, it has been suggested that the W343 residue of AnxA6 which is located in a flexible linker between two adjacent modules of the AnxA6 molecule may be implicated in AnxA6 interactions with membranes (Avila-Sakar *et al*., 1998; Kawasaki *et al*., 1996). Due to the presence of the flexible linker region AnxA6-1 may exhibit two modes of association with lipid membranes depending on calcium concentration. In the first case, the two modules of one AnxA6 molecule are coplanar and present the same, parallel orientation, both of them binding to one supported lipid bilayer (SLB) surface via their membrane-binding convex faces. In the second case, AnxA6 molecule has a conformation with the two modules tilted with respect to the membrane plane. The orientation of the AnxA6 molecule in this model was chosen so as to maximize the interaction of the two convex faces with the membrane surface, in a symmetrical manner (Buzhynskyy *et al*., 2009). Thus, the flexible region seems

to play a crucial role in reorienting the AnxA6 molecule and influencing its interaction with membranes and its behavior in solution.

In the next part of the thesis we compared the interfacial behavior of AnxA6 and its W343F mutant and their interactions with cholesterol and cholesteryl acetate containing monolayers. Our analyses of the interfacial properties of AnxA6-1 and its W343F mutant demonstrated that these two annexins differed in their pH-sensitivity for adsorption at the air/water interface. Besides, it had been previously shown that AnxA6 undergoes pH-induced changes in the protein folding (Golczak *et al*., 2001b, Golczak *et al*., 2001c). Thus, on the basis of our findings, it can be speculated that the flexible region may regulate pH-dependent changes in AnxA6 shape in solution as well as regulate behavior of the protein at the air/water interface. This could be of particular importance for the function of AnxA6 as a protein involved in regulation of membrane dynamics and membrane organization, including formation and stabilization of membrane microdomains.

Furthermore the W343 residue of AnxA6 seems to be involved in the interaction with the cholesterol –OH group since its replacement by phenylalanine significantly affects the interaction of AnxA6 with cholesterol (Fig. 37). Taking into account that there is still adsorption of AnxA6 (wild type and W343F) to Chol-Ac monolayers, it can be assumed that, besides the involvement of the cholesterol -OH group, there are other factors responsible for the interaction between annexins and cholesterol.

Searching for the mechanism of AnxA6-cholesterol interaction we decided to check the effect of the VAAEIL sequence of AnxA6. AnxA6-1 (the larger isoform) is predominantly expressed in normal cells and tissues, and AnxA6-2 appears to be more abundant in some transformed cell lines (Edwards and Moss, 1995). Up to date, only the inhibitory effect of the AnxA6-1 isoform mRNA, but not that of AnxA6-2, on EGF-dependent Ca^{2+} influx in A431 cells has been described (Fleet *et al*., 1999). AnxA6-2 has a higher affinity for Ca^{2+}, lower hydrophobicity and lower negative surface charge (Strzelecka-Kiliszek *et al*., 2008), but the relationship between expression levels of AnxA6 splice variants and cellular transformation is still unknown.

Our analyses of the interfacial properties of both AnxA6-1 and AnxA6-2 isoforms demonstrated that these two annexins did not exhibit similar pH-sensitivity for their adsorption at the air/water interface (Fig. 34). In contrast to AnxA6-1 isoform, AnxA6-2 exhibited lower adsorption at the air/water interface at pH 5.0 but similar insertion to cholesterol monolayer. But it inserted more to the cholesterol acetate monolayer than AnxA6-1 (Fig. 35).

These data demonstrate that the general changes in hydrophobicity due to the absence of the VAAEIL sequence do not influence the interactions with cholesterol. This suggests that the VAAEIL sequence is not implicated in interactions with cholesterol.

5.5 Concluding remarks

The results described in this thesis focus on several aspects of AnxA6 interactions with lipid microdomains in NPC disease cells as well as on the mechanism of these interactions.

- First, we isolated DRMs and demonstrated the increase in the content of lipid microdomains in NPC fibroblasts especially in the late endosome/lysosome compartment.
    - AnxA6, the protein implicated in cholesterol transport in the cell was found to localize in the late endosome/lysosome compartment in NPC fibroblasts, and the isolation of detergent-resistant membranes from these cells proved that AnxA6 translocates to the DRMs only in the presence of Ca^{2+}.
- Secondly, to test whether AnxA6 is an important partner of cholesterol, we employed a monolayer technique. *In vitro* analysis of AnxA6-lipid monolayers interactions gave new information on AnxA6 association with membranes.
    - We demonstrated that the main target of AnxA6 in the lipid raft mimicking membranes is cholesterol.
    - We also showed that pH 5.0 favors the interaction between AnxA6 and lipid monolayers. At pH 7.4, cholesterol was the main factor enabling insertion of AnxA6 to the monolayer. The interaction was also enhanced by the presence of Ca^{2+}.
    - In addition, experiments using cholesteryl acetate and the W343F mutant of AnxA6-1 demonstrated that the -OH group of cholesterol and the linker region of AnxA6 could be responsible for AnxA6-cholesterol interactions.
- To extend our knowledge about membrane lipid microdomains in NPC type C disease as well as to further characterize the lipid microdomains the use of additional lipidomics analysis of lipid microdomains from specific cellular compartments would be important. It would be also interesting to verify the AnxA6 content in lipid microdomains isolated from particular cellular compartments.

References

Abi-Mosleh L, Infante RE, Radhakrishnan A, Goldstein JL, Brown MS. (2009) Cyclodextrin overcomes deficient lysosome-to-endoplasmic reticulum transport of cholesterol in Niemann-Pick type C cells. Proc Natl Acad Sci U S A 106(46):19316-19321.

Abi-Rizk G, Besson F. (2008) Interactions of Triton X-100 with sphingomyelin and phosphatidylcholine monolayers: influence of the cholesterol content. Colloids Surf B Biointerfaces 66(2):163-167.

Aboulaich N, Vainonen JP, Strålfors P, Vener AV. (2004) Vectorial proteomics reveal targeting, phosphorylation and specific fragmentation of polymerase I and transcript release factor (PTRF) at the surface of caveolae in human adipocytes. Biochem J. 383(2):237-248.

Assaife-Lopes N, Sousa VC, Pereira DB, Ribeiro JA, Chao MV, Sebastião AM. (2010) Activation of adenosine A2A receptors induces TrkB translocation and increases BDNF-mediated phospho-TrkB localization in lipid rafts: implications for neuromodulation. J Neurosci. 30(25):8468-8480.

Astanina K, Delebinski CI, Delacour D, Jacob R. (2010) Annexin XIIIb guides raft-dependent and -independent apical traffic in MDCK cells. Eur J Cell Biol. 89(11):799-806.

Avila-Sakar AJ, Creutz CE, Kretsinger RH. (1998) Crystal structure of bovine annexin VI in a calcium-bound state. Biochim Biophys Acta 1387(1-2):103-116.

Avila-Sakar AJ, Kretsinger RH, Creutz CE. (2000) Membrane-bound 3D structures reveal the intrinsic flexibility of annexin VI. J. Struct. Biol. 130(1):54-62.

Ayala–Sanmartin J. (2001) Cholesterol enhances phospholipid binding and aggregation of annexins by their core domain. Biochem Biophys Res Commun. 283(1):72–79.

Ayala-Sanmartin J, Henry JP, Pradel LA. (2001) Cholesterol regulates membrane binding and aggregation by annexin 2 at submicromolar Ca(2+) concentration. Biochim Biophys Acta 1510(1-2):18-28.

Babiychuk EB, Draeger A. (2000) Annexins in cell membrane dynamics. Ca^{2+}–regulated association of lipid microdomains. J Cell Biol. 150(5):1113–1124.

Babiychuk EB, Draeger A. (2006) Biochemical characterization of detergent-resistant membranes: a systematic approach. Biochem J. 397(3):407-416.

Babiychuk EB, Palstra RJ, Schaller J, Kämpfer U, Draeger A. (1999) Annexin VI participates in the formation of a reversible, membrane-cytoskeleton complex in smooth muscle cells. J Biol Chem. 274(49):35191-35195.

Balch WE, Morimoto RI, Dillin A, Kelly JW. (2008) Adapting proteostasis for disease intervention. Science 319(5865):916-919.

Bandorowicz-Pikula J, Kirilenko A, van Deursen R, Golczak M, Kuhnel M, Lancelin JM, Pikula S, Buchet R. (2003) A putative consensus sequence for the nucleotide-binding site of annexin A6. Biochemistry 42(30):9137-9146.

Banerjee P, Buse JT, Dawson G. (1990) Asymmetric extraction of membrane lipids by CHAPS. Biochim. Biophys. Acta 1044(3):305-314.

Banerji S, Ngo M, Lane CF, Robinson CA, Minogue S, Ridgway ND. (2010) Oxysterol binding protein-dependent activation of sphingomyelin synthesis in the golgi apparatus requires phosphatidylinositol 4-kinase IIα. Mol Biol Cell. 21(23):4141-50.

Barenholz Y, Thompson TE. (1999) Sphingomyelin: Biophysical aspects. Chem. Phys. Lipids 102(1-2):29–34.

Baron S, Vangheluwe P, Sepúlveda MR, Wuytack F, Raeymaekers L, Vanoevelen J (2010) The secretory pathway Ca^{2+}-ATPase 1 is associated with cholesterol-rich microdomains of human colon adenocarcinoma cells. Biochim Biophys Acta 1798(8):1512-1521.

Batetta B, Sanna F. (2006) Cholesterol metabolism during cell growth: Which role for the plasma membrane? European Journal of Lipid Science and Technology 108(8):687-699.

Björkbom A, Róg T, Kaszuba K, Kurita M, Yamaguchi S, Lönnfors M, Nyholm TK, Vattulainen I, Katsumura S, Slotte JP. (2010) Effect of sphingomyelin headgroup size on molecular properties and interactions with cholesterol. Biophys J. 99(10):3300-3308.

Blaudez D, Buffeteau T, Cornut JC, Desbat B, Escafre N, Pezolet M. (1994) Polarization modulation FTIR spectroscopy at the air-water interface. Thin Solid Films 242(1-2):146-150.

Blom TS, Linder MD, Snow K, Pihko H, Hess MW, Jokitalo E, Veckman V, Syvänen AC, Ikonen E. (2003) Defective endocytic trafficking of NPC1 and NPC2 underlying infantile Niemann–Pick type C disease. Hum Mol Genet. 12(3):257–272.

Boini KM, Zhang C, Xia M, Han WQ, Brimson C, Poklis JL, Li PL. (2010) Visfatin-induced lipid raft redox signaling platforms and dysfunction in glomerular endothelial cells. Biochim Biophys Acta 1801(12):1294-1304.

Bonnin S, El Kirat K, Becchi M, Dubois M, Grangeasse C, Giraud C, Prigent A-F, Lagarde M, Roux B, Besson F. (2003) Protein and lipid analysis of detergent-resistant membranes isolated from bovine kidney. Biochimie 85(12):1237-1244.

Bonnon C, Wendeler MW, Paccaud JP, Hauri HP. (2010) Selective export of human GPI-anchored proteins from the endoplasmic reticulum. J Cell Sci. 123(10):1705-1715.

Bradford MM. (1976) A rapid and sensitive method for the quantitation of microgram quantities of protein utilizing the principle of protein-dye binding. Anal. Biochem. 72:248-254.

Bretscher MS, Munro S. (1993) Cholesterol and the Golgi apparatus. Science 261(5126):1280-1281.

Brown DA, London E. (1998) Structure and origin of ordered lipid domains in biological membranes. J Membr Biol. 164(2):103-114.

Brown DA, London E. (2000) Structure and function of sphingolipid- and cholesterol-rich membrane rafts. J Biol Chem. 275(23):17221-17224.

Brown AJ, Sun L, Feramisco JD, Brown MS, Goldstein JL. (2002) Cholesterol addition to ER membranes alters conformation of SCAP, the SREBP escort protein that regulates cholesterol metabolism. Mol Cell. 10(2):237-245.

Burger A, Berendes R, Voges D, Huber R, Demange P. (1993) A rapid and efficient purification method for recombinant annexin V for biophysical studies. FEBS Lett. 329(1-2):25-28.

Butler JD, Vanier MT, Pentchev PG. (1993) Niemann-Pick C disease: cystine and lipids accumulate in the murine model of this lysosomal cholesterol lipidosis. Biochem. Biophys. Res. Commun. 196(1):154–159.

Buzhynskyy N, Golczak M, Lai-Kee-Him J, Lambert O, Tessier B, Gounou C, Bérat R, Simon A, Granier T, Chevalier JM, Mazères S, Bandorowicz-Pikula J, Pikula S, Brisson AR. (2009) Annexin-A6 presents two modes of association with phospholipid membranes. A combined QCM-D, AFM and cryo-TEM study. J Struct Biol. 168(1):107-116.

Calvez P, Bussières S, Eric Demers, Salesse C. (2009) Parameters modulating the maximum insertion pressure of proteins and peptides in lipid monolayers. Biochimie. 91(6):718-733.

Calvo M, Enrich C. (2000) Biochemical analysis of a caveolae-enriched plasma membrane fraction from rat liver. Electrophoresis 21(16):3386–3395.

Carrasco MP, Jiménez-López JM, Ríos-Marco P, Segovia JL, Marco C (2010) Disruption of cellular cholesterol transport and homeostasis as a novel mechanism of action of membrane-targeted alkylphospholipid analogues. Br J Pharmacol 160(2):355-366.

Carstea ED, Polymeropoulos MH, Parker CC, Detera-Wadleigh SD, O'Neill RR, Patterson MC, Goldin E, Xiao H, Straub RE, Vanier MT, et al. (1993) Linkage of Niemann-Pick disease type C to human chromosome 18. Proc Natl Acad Sci U S A 90(5):2002-2004.

Carstea ED, Morris JA, Coleman KG, Loftus SK, Zhang D, Cummings C, Gu J, Rosenfeld MA, Pavan WJ, Krizman DB, Nagle J, Polymeropoulos MH, et al. (1997) Niemann-Pick C1 disease gene: homology to mediators of cholesterol homeostasis. Science 277(5323):228-231.

Cartailler JP, Haigler HT, Luecke H. (2000) Annexin XII E105K crystal structure: identification of a pH-dependent switch for mutant hexamerization. Biochemistry 39(10):2475-2483.

Chang TY, Chang CC, Ohgami N, Yamauchi Y. (2006) Cholesterol sensing, trafficking, and esterification. Annu Rev Cell Dev Biol. 22:129-157.

Chang TY, Reid PC, Sugii S, Ohgami N, Cruz JC, Chang CC. (2005) Niemann–Pick type C disease and intracellular cholesterol trafficking. J Biol Chem. 280(22):20917–20920.

Chasserot-Golaz S, Vitale N, Umbrecht-Jenck E, Knight D, Gerke V, Bader MF. (2005) Annexin 2 promotes the formation of lipid microdomains required for calcium-regulated exocytosis of dense-core vesicles. Mol Biol Cell. 16(3):1108-1119.

Chevallier J, Chamoun Z, Jiang G, Prestwich G, Sakai N, Matile S, Parton RG, Gruenberg J. (2008) Lysobisphosphatidic acid controls endosomal cholesterol levels. J Biol Chem. 283(41):27871-27880.

Chichili GR, Westmuckett AD, Rodgers W. (2010) T cell signal regulation by the actin cytoskeleton. J Biol Chem. 285(19):14737-1446.

Cornut I, Desbat B, Turlet JM, Dufourcq J. (1996) In situ study by polarization modulated Fourier transform infrared spectroscopy of the structure and orientation of lipids and amphipathic peptides at the air-water interface. Biophys. J. 70(1), 305-312.

Coskun U, Simons K. (2010) Membrane rafting: from apical sorting to phase segregation. FEBS Lett. 584(9):1685-1693.

Creutz CE, Snyder SL. (2005) Interactions of the annexins with the mu subunits of the clathrin assembly proteins. Biochemistry 44:13795–13806.

Cubells L, Vilà de Muga S, Tebar F, Bonventre JV, Balsinde J, Pol A, Grewal T, Enrich C. (2008) Annexin A6–induced inhibition of cytoplasmic phospholipase A2 is linked to caveolin–1 export from the Golgi. J Biol Chem. 283(15):10174–10183.

Cubells L, Vilà de Muga S, Tebar F, Wood P, Evans R, Ingelmo–Torres M, Calvo M, Gaus K, Pol A, Grewal T, Enrich C. (2007) Annexin A6–induced alterations in cholesterol transport and caveolin export from the Golgi complex. Traffic 8(11):1568–1589.

Das M, Das DK. (2009) Lipid raft in cardiac health and disease. Curr Cardiol Rev. 5(2):105-111.

Davidson CD, Ali NF, Micsenyi MC, Stephney G, Renault S, Dobrenis K, Ory DS, Vanier MT, Walkley SU. (2009) Chronic cyclodextrin treatment of murine Niemann-Pick C disease ameliorates neuronal cholesterol and glycosphingolipid storage and disease progression. PLoS One. 4(9):e6951.

Davignon J, Dubuc G, Seidah NG. (2010) The influence of PCSK9 polymorphisms on serum low-density lipoprotein cholesterol and risk of atherosclerosis. Curr Atheroscler Rep. 12(5):308-315.

de Diego I, Schwartz F, Siegfried H, Dauterstedt P, Heeren J, Beisiegel U, Enrich C, Thomas Grewal T. (2002) Cholesterol modulates the membrane binding and intracellular distribution of annexin 6. J Biol Chem. 277(35):32187–32194.

Devlin C, Pipalia NH, Liao X, Schuchman EH, Maxfield FR, Tabas I. (2010) Improvement in lipid and protein trafficking in Niemann-Pick C1 cells by correction of a secondary enzyme defect. Traffic 11(5), 601–615.

Diaz O, Berquand A, Dubois M, Di Agostino S, Sette C, Bourgoin S, Lagarde M, Nemoz G and Prigent AF. (2002) The mechanism of docosahexaenoic acid-induced phospholipase D activation in human lymphocytes involves exclusion of the enzyme from lipid rafts. J. Biol. Chem. 277(42):39368-39378.

Draeger A, Monastyrskaya K, Babiychuk EB. (2011) Plasma membrane repair and cellular damage control: the annexin survival kit. Biochem Pharmcol. 81(6):703-712.

Dressler LG, Seamer LC, Owens MA, Clark GM, McGuire WL. (1988) DNA flow cytometry and prognostic factors in 1331 frozen breast cancer specimens. Cancer 61(3):420-427.

Edwards HC, Moss SE. (1995) Functional and genetic analysis of annexin VI. Mol Cell Biochem. 149-150:293-299.

El Kirat K, Chauvet JP, Roux B, Besson F. (2004) Streptomyces chromofuscus phospholipase D interaction with lipidic activators at the air-water interface. Biochim Biophys Acta 1661(2):144-153.

Enrich C, Rentero C, de Muga SV, Reverter M, Mulay V, Wood P, Koese M, Grewal T. (2011) Annexin A6-Linking Ca^{2+} signaling with cholesterol transport. Biochim Biophys Acta 1813(5):935-947.

Faiss S, Kastl K, Janshoff A, Steinem C. (2008) Formation of irreversibly bound annexin A1 protein domains on POPC/POPS solid supported membranes. Biochem Biophys Acta 1778(7-8):1601-1610.

Fatimathas L, Moss SE. (2010) Annexins as disease modifiers. Histol Histopathol. 25(4):527-532.

Feuk-Lagerstedt E, Movitz C, Pellmé S, Dahlgren C, Karlsson A. (2007) Lipid raft proteome of the human neutrophil azurophil granule. Proteomics 7(2):194-205.

Fiedler K, Kobayashi T, Kurzchalia TV, Simons K. (1993) Glycosphingolipid-enriched, detergent-insoluble complexes in protein sorting in epithelial cells. Biochemistry 32(25):6365-6373.

Fleet A, Ashworth R, Kubista H, Edwards H, Bolsover S, Mobbs P, Moss SE. (1999) Inhibition of EGF-dependent calcium influx by annexin VI is splice form-specific. Biochem Biophys Res Commun. 260(2):540-546.

Folch J, Lees M, Stanley GHS. (1957) A simple method for the isolation and purification of total lipids from animal tissues. Journal of Biological Chemistry 226(1):497–509.

Foster LJ, De Hoog CL, Mann M. (2003) Unbiased quantitative proteomics of lipid rafts reveals high specificity for signaling factors. Proc natl Acad Sci USA 100(10):5813-5818.

Freye-Minks C, Kretsinger RH, Creutz CE. (2003) Structural and dynamic changes in human annexin VI induced by a phosphorylation-mimicking mutation, T356D. Biochemistry. 42(3):620-630.

Futter CE, White IJ. (2007) Annexins and endocytosis. Traffic 8(8):951–958.

Gagescu R, Demaurex N, Parton RG, Hunziker W, Huber LA, Gruenberg J. (2000) The recycling endosome of Madin–Darby canine kidney cells is a mildly acidic compartment rich in raft components. Mol. Biol. Cell. 11(8):2775–2791.

Gelsthorpe ME, Baumann N, Millard E, Gale SE, Langmade SJ, Schaffer JE, Ory DS. (2008) Niemann-Pick type C1 I1061T mutant encodes a functional protein that is selected for endoplasmic reticulum-associated degradation due to protein misfolding. J Biol Chem. 283(13):8229-8236.

Gerke V, Creutz CE, Moss SE. (2005) Annexins: linking Ca^{2+} signalling to membrane dynamics. Nat Rev Mol Cell Biol. 6(6):449–461.

Gerke V, Moss SE. (2002) Annexins: from structure to function. Physiol Rev 82(2):331–371.

Gerlier D, Alais S, Chazal N. (2004) Les radeaux membranaires : des plates-formes de choix pour l'entrée, l'assemblage ou le bourgeonnement de virus. Virologie. 8(3):199-214

Ginzburg L, Kacher Y, Futerman AH. (2004) The pathogenesis of glycosphingolipid storage disorders. Semin.CellDev.Biol. 15(4):417–431.

Giocondi MC, Besson F, Dosset P, Milhiet PE, Le Grimellec C. (2007) Remodeling of ordered membrane domains by GPI-anchored intestinal alkaline phosphatase. Langmuir 23(18):9358-9364.

Godoy V, Riquelme G. (2008) Distinct lipid rafts in subdomains from human placental apical syncytiotrophoblast membranes. J Membr Biol. 224 (1-3):21-31.

Golczak M, Kicinska A, Bandorowicz-Pikula J, Buchet R, Szewczyk A, Pikula S. (2001b) Acidic pH-induced folding of annexin VI is a prerequisite for its insertion into lipid bilayers and formation of ion channels by the protein molecules. FASEB J. 15(6):1083-1085.

Golczak M, Kirilenko A, Bandorowicz–Pikula J, Desbat B, Pikula S. (2004) Structure of human annexin A6 at the air–water interface and in a membrane–bound state. Biophys J. 87(2):1215–1226.

Golczak M, Kirilenko A, Bandorowicz-Pikula J, Pikula S. (2001a) N- and C-terminal halves of human annexin VI differ in ability to form low pH-induced ion channels. Biochem Biophys Res Commun. 284(3):785-791.

Golczak M, Kirilenko A, Bandorowicz-Pikula J, Pikula S. (2001c) Conformational states of annexin VI in solution induced by acidic pH. FEBS Lett. 496(1):49-54.

Goldschmidt-Arzi M, Shimoni E, Sabanay H, Futerman AH, Addadi L. (2011) Intracellular localization of organized lipid domains of C16-ceramide/cholesterol. J Struct Biol. 175(1):21-30.

Goldstein JL, DeBose-Boyd RA, Brown MS. (2006) Protein sensors for membrane sterols. Cell 124(1):35-46.

Grewal T, Enrich C. (2006) Molecular mechanisms involved in Ras inactivation: the annexin A6-p120^{GAP} complex. BioEssays 28(12):1211-1220.

Grewal T, Enrich C. (2009) Annexins - modulators of EGF receptor signalling and trafficking. Cell Signal 21(6):847-858.

Grewal T, Heeren J, Mewawala D, Schnitgerhans T, Wendt D, Salomon G, Enrich C, Beisiegel U, Jäckle S. (2000) Annexin VI stimulates endocytosis and is involved in the trafficking of low density lipoprotein to the prelysosomal compartment. J Biol Chem. 275(43):33806-33813.

Grewal T, Koese M, Rentero C, Enrich C. (2010) Annexin A6-regulator of the EGFR/Ras signalling pathway and cholesterol homeostasis. Int J Biochem Cell Biol. 42(5):580-584.

Gu F, Gruenberg J. (2000) ARF1 regulates pH-dependent COP functions in the early endocytic pathway. J Biol Chem. 275(11):8154-8160.

Hao M, Lin SX, Karylowski OJ, Wüstner D, McGraw TE, Maxfield FR. (2002) Vesicular and non-vesicular sterol transport in living cells. The endocytic recycling compartment is a major sterol storage organelle. J Biol Chem. 277(1):609-617.

Hao M, Mukherjee S, Maxfield FR. (2001) Cholesterol depletion induces large scale domain segregation in living cell membranes. Proc Natl Acad Sci U S A. 98(23):13072-13077.

Harder T, Kellner R, Parton RG, Gruenberg J. (1997) Specific release of membrane-bound annexin II and cortical cytoskeletal elements by sequestration of membrane cholesterol. Mol Biol Cell. 8(3):533-545

Harder T, Simons K. (1997) Caveolae, DIGs, and the dynamics of sphingolipid-cholesterol microdomains. Curr Opin Cell Biol. 9(4):534-542.

Hayashi T, Su TP. (2010) Cholesterol at the endoplasmic reticulum: roles of the sigma-1 receptor chaperone and implications thereof in human diseases. Subcell Biochem. 51:381-398.

Hayes MJ, Longbottom RE, Evans MA, Moss SE. (2007) Annexinopathies. Subcell Biochem. 45:1-28.

Hayes MJ, Rescher U, Gerke V, Moss SE. (2004) Annexin–actin interactions. Traffic 5(8):571–576.

Hevonoja T, Pentikäinen MO, Hyvönen MT, Kovanen PT, Ala-Korpela M. (2000) Structure of low density lipoprotein (LDL) particles: basis for understanding molecular changes in modified LDL. Biochim Biophys Acta. 1488(3):189-210.

Heyraud S, Jaquinod M, Durmort C, Dambroise E, Concord E, Schaal JP, Huber P, Gulino-Debrac D. (2008) Contribution of annexin 2 to the architecture of mature endothelial adherens junctions. Mol Cell Biol. 28(5):1657-1668.

Hofman EG, Ruonala MO, Bader AN, van den Heuvel D, Voortman J, Roovers RC, Verkleij AJ, Gerritsen HC, van Bergen En Henegouwen PM. (2008) EGF induces coalescence of different lipid rafts. J Cell Sci. 121(15):2519-2528.

Horton JD, Goldstein JL, Brown MS. (2002) SREBPs: activators of the complete program of cholesterol and fatty acid synthesis in the liver. J Clin Invest. 109(9):1125-1131.

Hughes DA, Pastores GM. (2010) The pathophysiology of GD - current understanding and rationale for existing and emerging therapeutic approaches. Wien Med Wochenschr. 160(23-24):594-599.

Ikonen E, Jansen M. (2008) Cellular sterol trafficking and metabolism: spotlight on structure. Curr Opin Cell Biol. 20(4):371-377.

Infante RE, Wang ML, Radhakrishnan A, Kwon HJ, Brown MS, Goldstein JL (2008) NPC2 facilitates bidirectional transfer of cholesterol between NPC1 and lipid bilayers, a step in cholesterol egress from lysosomes. Proc Natl Acad Sci USA 105(40):15287–15292.

Ioannou YA. (2000) The structure and function of the Niemann-Pick C1 protein. Mol Genet Metab. 71(1-2):175-181.

Ioannou YA. (2001) Multidrug permeases and subcellular cholesterol transport. Nat Rev Mol Cell Biol. 2(9):657-668.

Isas JM, Cartailler JP, Sokolov Y, Patel DR, Langen R, Luecke H, Hall JE, Haigler HT. (2000) Annexins V and XII insert into bilayers at mildly acidic pH and form ion channels. Biochemistry 39(11):3015-3022.

Jäckle S, Beisiegel U, Rinninger F, Buck F, Grigoleit A, Block A, Gröger I, Greten H, Windler E. (1994) Annexin VI, a marker protein of hepatocytic endosomes. J Biol Chem. 269(2):1026-1032.

Jeon JY, Hwang SY, Cho SH, Choo J, Lee EK. (2010) Effect of cholesterol content on affinity and stability of factor VIII and annexin V binding to a liposomal bilayer membrane. Chem Phys Lipids 163(4-5):335-340.

Jeyakumar M, Dwek RA, Butters TD, Platt FM. (2005) Storage solutions:treating lysosomal disorders of the brain. Nat Rev Neurosci. 6(9):713–725.

Johnson SA, Stinson BM, Go MS, Carmona LM, Reminick JI, Fang X, Baumgart T. (2010) Temperature-dependent phase behavior and protein partitioning in giant plasma membrane vesicles. Biochim Biophys Acta 1798(7):1427-1435.

Kaetzel MA, Pula G, Campos B, Uhrin P, Horseman N, Dedman JR. (1994) Annexin VI isoforms are differentially expressed in mammalian tissues. Biochim Biophys Acta 1223(3):368–374.

Kamal A, Ying Y, Anderson RG. (1998) Annexin VI-mediated loss of spectrin during coated pit budding is coupled to delivery of LDL to lysosomes. J Cell Biol. 142(4):937-947.

Kastl K, Ross M, Gerke V, Steinem C. (2002) Kinetics and thermodynamics of annexin A1 binding to solid-supported membranes: a QCM study. Biochemistry 41(31):10087-10094.

Katzmann DJ, Odorizzi G, Emr SD. (2002) Receptor downregulation and multivesicular-body sorting. Nat Rev Mol Cell Biol. 3(12):893-905.

Kawasaki H, Avila-Sakar A, Creutz CE, Kretsinger RH. (1996) The crystal structure of annexin VI indicates relative rotation of the two lobes upon membrane binding. Biochim Biophys Acta 1313(3):277-282.

Kilsdonk EP, Yancey PG, Stoudt GW, Bangerter FW, Johnson WJ, Phillips MC, Rothblat GH. (1995) Cellular cholesterol efflux mediated by cyclodextrins. J Biol Chem. 270(29):17250-17256.

Kirilenko A, Golczak M, Pikula S, Buchet R, Bandorowicz-Pikula J. (2002) GTP-induced membrane binding and ion channel activity of annexin VI: is annexin VI a GTP biosensor? Biophys J. 82(5):2737-2745.

Kirilenko A, Pikula S, Bandorowicz-Pikula J. (2006) Effects of mutagenesis of W343 in human annexin A6 isoform 1 on its interaction with GTP: nucleotide-induced oligomer formation and ion channel activity. Biochemistry 45(15):4965-4973.
Klose C, Ejsing CS, García-Sáez AJ, Kaiser HJ, Sampaio JL, Surma MA, Shevchenko A, Schwille P, Simons K. (2010) Yeast lipids can phase-separate into micrometer-scale membrane domains. J Biol Chem. 285(39):30224-30232.

Ko DC, Binkley J, Sidow A, Scott MP. (2003) The integrity of a cholesterol–binding pocket in Niemann–Pick C2 protein is necessary to control lysosome cholesterol levels. Proc Natl Acad Sci USA 100(5):2518–2525.

Ko DC, Gordon MD, Jin JY, Scott MP. (2001) Dynamic movements of organelles containing Niemann-Pick C1 protein: NPC1 involvement in late endocytic events. Mol Biol Cell 12:601–614.

Köhler G, Hering U, Zschörnig O, Arnold K. (1997) Annexin V interaction with phosphatidylserine-containing vesicles at low and neutral pH. Biochemistry 36(26):8189-8194.

Koike T, Ishida G, Taniguchi M, Higaki K, Ayaki Y, Saito M, Sakakihara Y, Iwamori M, Ohno K. (1998) Decreased membrane fluidity and unsaturated fatty acids in Niemann-Pick disease type C fibroblasts. Biochim Biophys Acta 1406(3):327-35.

Kosicek M, Malnar M, Goate A, Hecimovic S. (2010) Cholesterol accumulation in Niemann Pick type C (NPC) model cells causes a shift in APP localization to lipid rafts. Biochemical and Biophysical Research Communications 393(3):404–409.

Laemmli UK. (1970) Cleavage of structural proteins during the assembly of the head of bacteriophage T4. Nature 227(5259):680-685.

Lafont F, Lecat S, Verkade P, Simons K. (1998) Annexin XIIIb associates with lipid microdomains to function in apical delivery. J Cell Biol. 142(6):1413-1427.

Lajoie P, Nabi IR. (2010) Lipid rafts, caveolae, and their endocytosis. Int Rev Cell Mol Biol. 282:135-163.

Lambert O, Cavusoglu N, Gallay J, Vincent M, Rigaud JL, Henry JP, Ayala–Sanmartin J. (2004) Novel organization and properties of annexin 2–membrane complexes. J Biol Chem. 279(12):10872–10882.

Lange Y, Ye J, Rigney M, Steck TL. (1999) Regulation of endoplasmic reticulum cholesterol by plasma membrane cholesterol. J Lipid Res. 40(12):2264-2270.

Legembre P, Daburon S, Moreau P, Moreau JF, Taupin JL. (2006) Modulation of Fas-mediated apoptosis by lipid rafts in T lymphocytes. J Immunol. 176(2):716-720.

Levental I, Grzybek M, Simons K. (2010) Greasing their way: lipid modifications determine protein association with membrane rafts. Biochemistry 49(30):6305-6316.

Lim LH, Pervaiz S. (2007) Annexin 1: the new face of an old molecule. FASEB J. 21(4):968-975.

Lindner R, Naim HY. (2009) Exp Cell Res. Domains in biological membranes. 315(17):2871-2878.

Liscum L. (2000) Niemann-Pick type C mutations cause lipid traffic jam. Traffic. 1(3):218-225.

Liscum L, Klansek JJ. (1998) Niemann-Pick disease type C. Curr Opin Lipidol. 9(2):131-135.

Liscum L, Munn NJ. (1999) Intracellular cholesterol transport. Biochim. Biophys. Acta. 1438(1):19–37.

Liscum L, Sturley SL. (2004) Intracellular trafficking of Niemann-Pick C proteins 1 and 2: obligate components of subcellular lipid transport. Biochim Biophys Acta 1685(1-3):22-27.

Liu B, Ramirez CM, Miller AM, Repa JJ, Turley SD, Dietschy JM. (2010b) Cyclodextrin overcomes the transport defect in nearly every organ of NPC1 mice leading to excretion of sequestered cholesterol as bile acid. J Lipid Res. 51(5):933-944.

Liu B, Turley SD, Burns DK, Miller AM, Repa JJ, Dietschy JM.(2009) Reversal of defective lysosomal transport in NPC disease ameliorates liver dysfunction and neurodegeneration in the npc1-/- mouse. Proc Natl Acad Sci USA 106(7):2377-2382.

Liu JP, Tang Y, Zhou S, Toh BH, McLean C, Li H. (2010a) Cholesterol involvement in the pathogenesis of neurodegenerative diseases. Mol Cell Neurosci. 43(1):33-42.

Lloyd-Evans E, Morgan AJ, He X, Smith DA, Elliot-Smith E, Sillence DJ, Churchill GC, Schuchman EH, Galione A, Platt FM. (2008) Niemann-Pick disease type C1 is a sphingosine storage disease that causes deregulation of lysosomal calcium. Nat Med. 14(11):1247-1255.

Lloyd-Evans E, Platt FM. (2010) Lipids on trial: the search for the offending metabolite in Niemann-Pick type C disease. Traffic 11(4):419–428.

Lusa S, Blom TS, Eskelinen EL, Kuismanen E, Månsson JE, Simons K, Ikonen E. (2001) Depletion of rafts in late endocytic membranes is controlled by NPC1-dependent recycling of cholesterol to the plasma membrane. J. Cell Sci. 114(10):1893-1900.

Luzio JP, Bright NA, Pryor PR. (2007) The role of calcium and other ions in sorting and delivery in the late endocytic pathway. Biochem Soc Trans. 35(5):1088-91.

Luzio JP, Pryor PR, Gray SR, Gratian MJ, Piper RC, Bright NA. (2005) Membrane traffic to and from lysosomes. Biochem Soc Symp. (72):77-86.

Martinez-Seara H, Róg T, Karttunen M, Vattulainen I, Reigada R. (2010) Cholesterol induces specific spatial and orientational order in cholesterol/phospholipid membranes. PLoS One 5(6):e11162.

Matsumori N, Tanada N, Nozu K, Okazaki H, Oishi T, Murata M. (2011) Design and synthesis of sphingomyelin-cholesterol conjugates and their formation of ordered membranes. Chemistry 17(31):8568-8575.

Maxfield FR, Tabas I. (2005) Role of cholesterol and lipid organization in disease. Nature 438(7068):612-621.

Maxfield FR, Wüstner D. (2002) Intracellular cholesterol transport. J Clin Invest. 110(7):891-898.

Mayer G, Poirier S, Seidah NG. (2008) Annexin A2 is a C-terminal PCSK9-binding protein that regulates endogenous low density lipoprotein receptor levels. J Biol Chem. 283(46):31791-31801.

Mayran N, Parton RG, Gruenberg J. (2003) Annexin II regulates multivesicular endosome biogenesis in the degradation pathway of animal cells. EMBO J. 22(13):3242–3253.

McGovern MM, Aron A, Brodie SE, Desnick RJ, Wasserstein MP. (2006) Natural history of Type A Niemann-Pick disease: possible endpoints for therapeutic trials. Neurology 66(2):228-232.

McGovern MM, Wasserstein MP, Aron A, Desnick RJ, Schuchman EH, Brodie SE. (2004) Ocular manifestations of Niemann-Pick disease type B. Ophthalmology 111(7):1424-1427.

Meikle PJ, Hopwood JJ, Clague AE, Carey WF. (1999) Prevalence of lysosomal storage disorders. JAMA. 281(3):249-54.

Mesmin B, Maxfield FR. (2009) Intracellular sterol dynamics. Biochim Biophys Acta 1791(7):636-645.

Monastyrskaya K, Babiychuk EB, Hostettler A, Wood P, Grewal T, Draeger A. (2009) Plasma membrane-associated annexin A6 reduces Ca^{2+} entry by stabilizing the cortical actin cytoskeleton. J Biol Chem. 284(25):17227-17242.

Mukherjee S, Ghosh RN, Maxfield FR. (1997) Endocytosis. Physiol. Rev. 77(3):759–803.

Mukherjee S, Maxfield FR. (2004a) Membrane domains. Annu Rev Cell Dev Biol. 20:839-66.

Mukherjee S, Maxfield FR. (2004b) Lipid and cholesterol trafficking in NPC. Biochim Biophys Acta. 1685(1-3):28-37.

Mukherjee S, Zha X, Tabas I, Maxfield FR. (1998) Cholesterol distribution in living cells: fluorescence imaging using dehydroergosterol as a fluorescent cholesterol analog, Biophys. J. 75(4):1915–1925.

Murai T, Maruyama Y, Mio K, Nishiyama H, Suga M, Sato C. (2011) Low cholesterol triggers membrane microdomain-dependent CD44 shedding and suppresses tumor cell migration. J Biol Chem. 286(3):1999-2007.

Nasir MN, Thawani A, Kouzayha A, Besson F. (2010) Interactions of the natural antimicrobial mycosubtilin with phospholipid membrane models. Colloids Surf B Biointerfaces. 78(1):17-23.

Naureckiene S, Sleat DE, Lackland H, Fensom A, Vanier MT, Wattiaux R, Jadot M, Lobel P. (2000) Identification of HE1 as the second gene of Niemann-Pick C disease. Science 290(5500):2298-2301.

Neumann AK, Itano MS, Jacobson K. (2010) Understanding lipid rafts and other related membrane domains. Biol Rep. 2:31.

Oliferenko S, Paiha K, Harder T, Gerke V, Schwärzler C, Schwarz H, Beug H, Günthert U, Huber LA. (1999) Analysis of CD44-containing lipid rafts: Recruitment of annexin II and stabilization by the actin cytoskeleton. J. Cell Biol. 146(4):843-854.

Ono A. (2010) Relationships between plasma membrane microdomains and HIV-1 assembly. Biol Cell. 102(6):335-350.

Orito A, Kumanogoh H, Yasaka K, Sokawa J, Hidaka H, Sokawa Y, Maekawa S. (2001) Calcium-dependent association of annexin VI, protein kinase Ca, and neurocalcin a on the raft fraction derived from the synaptic plasma membrane of rat brain. J. Neurosci. Res. 64(3):235–241.

Ory DS. (2000) Niemann-Pick type C: a disorder of cellular cholesterol trafficking. Biochim Biophys Acta 1529(1-3):331-339.

Park EK, Lee EJ, Lee SH, Koo KH, Sung JY, Hwang EH, Park JH, Kim CW, Jeong KC, Park BK, Kim YN. (2010) Induction of apoptosis by the ginsenoside Rh2 by internalization of lipid rafts and caveolae and inactivation of Akt. Br J Pharmacol. 160(5):1212-1223.

Patterson MC, Platt F. (2004) Therapy of Niemann-Pick disease, type C. Biochim Biophys Acta 1685(1-3):77-82.

Patterson MC, Vecchio D, Prady H, Abel L, Wraith JE. (2007) Miglustat for treatment of Niemann-Pick C disease: a randomized controlled study. Lancet Neurol. 6(9):765–772.

Patterson MC, Vanier MT, Suzuki K, Morris JA, Carstea E, Neufeld EB, Blanchette-Mackie JE, Pentchev PG. (2001) Niemann-Pick disease type c: a lipid trafficking disorder. In: Scriver CR, Beaudet AL, Sly WS, Valle D, Vogelstein B (eds) The Metabolic and Molecular Bases of Inherited Disease, 8th ed. New York, McGraw-Hill, p.3611-3643.

Pentchev PG, Vanier MT, Suzuki K, Patterson MC. (1995) Niemann-Pick disease type C: a cellular cholesterol lipidosis. In Scriver CR, Beaudet AL, Sly WS, Valle D, Stanbury JB, Wyngaarden JB, Fredrickson DS (eds). The Metabolic and Molecular Bases of Inherited Disease. Vol. II, 7th ed. New York:McGraw-Hill, p.2625–2639.

Pike LJ. (2009) The challenge of lipid rafts. J Lipid Res. 50:S323-8.

Pineda M, Wraith JE, Mengel E, Sedel F, Hwu WL, Rohrbach M, Bembi B, Walterfang M, Korenke GC, Marquardt T, Luzy C, Giorgino R, Patterson MC. (2009) Miglustat in patients with Niemann-Pick disease Type C (NP-C): a multicenter observational retrospective cohort study. Mol Genet Metab. 98(3):243-249.

Podszywalow-Bartnicka P, Strzelecka-Kiliszek A, Bandorowicz-Pikula J, Pikula S. (2007) Calcium- and proton-dependent relocation of annexin A6 in Jurkat T cells stimulated for interleukin-2 secretion. Acta Biochim. Pol. 54(2):261–271.

Pol A, Ortega D, Enrich C. (1997) Identification of cytoskeleton-associated proteins in isolated rat liver endosomes. Biochem J. 327(3):741-746.

Pommier AJ, Alves G, Viennois E, Bernard S, Communal Y, Sion B, Marceau G, Damon C, Mouzat K, Caira F, Baron S, Lobaccaro JM. (2010) Liver X Receptor activation downregulates AKT survival signaling in lipid rafts and induces apoptosis of prostate cancer cells. Oncogene 29(18):2712-2723.

Ponce J, Brea D, Carrascal M, Guirao V, Degregorio-Rocasolano N, Sobrino T, Castillo J, Dávalos A, Gasull T. (2010) The effect of simvastatin on the proteome of detergent-resistant membrane domains: decreases of specific proteins previously related to cytoskeleton regulation, calcium homeostasis and cell fate. Proteomics 10(10):1954-1965.

Pons M, Grewal T, Rius E, Schnitgerhans T, Jäckle S, Enrich C. (2001) Evidence for the involvement of annexin 6 in the trafficking between the endocytic compartment and lysosomes. Exp Cell Res. 269(1):13–22.

Pons M, Ihrke G, Koch S, Biermer M, Pol A, Grewal T, Jäckle S, Enrich C. (2000) Late endocytic compartments are major sites of annexin VI localization in NRK fibroblasts and polarized WIF–B hepatoma cells. Exp Cell Res 257(1):33–47.

Poulos A, Ranieri E, Shankaran P, Callahan JW. (1984) Studies on the activation of the enzymatic hydrolysis of sphingomyelin liposomes. Biochim Biophys Acta 793(2):141-148.

Pralle A, Keller P, Florin EL, Simons K, Hörber JK. (2000) Sphingolipid-cholesterol rafts diffuse as small entities in the plasma membrane of mammalian cells. J Cell Biol. 148(5):997-1008.

Quinn PJ, Wolf C. (2010) An X-ray diffraction study of model membrane raft structures. FEBS J. 277(22):4685-4698.

Radhakrishnan A, Ikeda Y, Kwon HJ, Brown MS, Goldstein JL. (2007) Sterol-regulated transport of SREBPs from endoplasmic reticulum to Golgi: oxysterols block transport by binding to Insig. Proc Natl Acad Sci U S A 104(16):6511-6518.

Ramjiawan B, Czubryt MP, Gilchrist JS, Pierce GN. (1996) Nuclear membrane cholesterol can modulate nuclear nucleoside triphosphatase activity. J Cell Biochem. 63(4):442-452.

Reineri S, Bertoni A, Sanna E, Baldassarri S, Sarasso C, Zanfa M, Canobbio I, Torti M, Sinigaglia F. (2007) Membrane lipid rafts coordinate estrogen-dependent signaling in human platelets. Biochim Biophys Acta 1773(2):273-8.

Ribeiro I, Marcão A, Amaral O, Sá Miranda MC, Vanier MT, Millat G. (2001) Niemann-Pick type C disease: NPC1 mutations associated with severe and mild cellular cholesterol trafficking alterations. Hum Genet. 109(1):24-32.

Rodriguez-Agudo D, Ren S, Wong E, Marques D, Redford K, Gil G, Hylemon P, Pandak WM. (2008) Intracellular cholesterol transporter StarD4 binds free cholesterol and increases cholesteryl ester formation. J Lipid Res. 49(7):1409-1419.

Rosenbaum AI, Maxfield FR. (2011) Niemann-Pick type C disease: molecular mechanisms and potential therapeutic approaches. J Neurochem. 116(5):789-795.

Rosenbaum AI, Rujoi M, Huang AY, Du H, Grabowski GA, Maxfield FR. (2009) Chemical screen to reduce sterol accumulation in Niemann-Pick C disease cells identifies novel lysosomal acid lipase inhibitors. Biochim Biophys Acta 1791(12):1155-1165.

Rosenbaum AI, Zhang G, Warren JD, Maxfield FR. (2010) Endocytosis of beta-cyclodextrins is responsible for cholesterol reduction in Niemann-Pick type C mutant cells. Proc Natl Acad Sci USA 107(12):5477-5482.

Ross M, Gerke V, Steinem C. (2003) Membrane composition affects the reversibility of annexin A2t binding to solid supported membranes: a QCM study. Biochemistry 42(10):3131-3141.

Sandvig K, van Deurs B. (2002) Transport of protein toxins into cells: pathways used by ricin, cholera toxin and Shiga toxin. FEBS Lett. 529(1):49-53.

Scheiffele P, Roth MG, Simons K. (1997) Interaction of influenza virus haemagglutinin with sphingolipid-cholesterol membrane domains via its transmembrane domain. EMBO J. 16(18):5501-5508.

Schengrund CL. (2010) Lipid rafts: keys to neurodegeneration. Brain Res Bull 82(1-2):7-17.

Schiffmann R. (2010) Therapeutic approaches for neuronopathic lysosomal storage disorders. J Inherit Metab Dis. 33(4):373-379.

Schwarzer S, Nobles M, Tinker A (2010) Do caveolae have a role in the fidelity and dynamics of receptor activation of G-protein-gated inwardly rectifying potassium channels? J Biol Chem. 285(36):27817-2726.

Scott C, Ioannou YA. (2004) The NPC1 protein: structure implies function. Biochim Biophys Acta 1685(1-3):8-13.

Sengupta P, Hammond A, Holowka D, Baird B. (2008) Structural determinants for partitioning of lipids and proteins between coexisting fluid phases in giant plasma membrane vesicles. Biochim Biophys Acta 1778(1):20-32.

Sever N, Yang T, Brown MS, Goldstein JL, DeBose-Boyd RA. (2003) Accelerated degradation of HMG CoA reductase mediated by binding of insig-1 to its sterol-sensing domain. Mol Cell. 11(1):25-33.

Shevchenko A, Wilm M, Vorm O, Mann M. (1996) Mass Spectrometric Sequencing of Proteins from Silver-Stained Polyacrylamide Gels. Anal. Chem. 68(5):850-858.

Silvius JR. (2003) Role of cholesterol in lipid raft formation: lessons from lipid model systems. Biochim Biophys Acta. 1610(2):174-183.

Simons K, Gruenberg J. (2000) Jamming the endosomal system: lipid rafts and lysosomal storage diseases. Trends Cell Biol. 10(11):459-462.

Simons K, Ikonen E. (1997) Functional rafts in cell membranes. Nature 387(6633):569–572.

Simons K, Ikonen E. (2000) How cells handle cholesterol. Science 290(5497):1721-1726.

Singh RP, Brooks BR, Klauda JB. (2009) Binding and release of cholesterol in the Osh4 protein of yeast. Proteins 75(2):468-477.

Smart EJ, De Rose RA, Farber SA. (2004) Annexin 2-caveolin 1 complex is a target of ezetimibe and regulates intestinal cholesterol transport. Proc Natl Acad Sci U S A 101(10):3450-3455.

Smith PD, Davies A, Crumpton MJ, Moss SE. (1994) Structure of the human annexin VI gene. Proc Natl Acad Sci U S A 91(7):2713-2717.

Soccio RE, Breslow JL. (2004) Intracellular cholesterol transport. Arterioscler Thromb Vasc Biol. 24(7):1150-1160.

Sprenger RR, Speijer D, Back JW, De Koster CG, Pannekoek H, Horrevoets AJ. (2004) Comparative proteomics of human endothelial cell caveolae and rafts using two-dimensional gel electrophoresis and mass spectrometry. Electrophoresis 25(1):156-172.

Staubach S, Razawi H, Hanisch FG. (2009) Proteomics of MUC1-containing lipid rafts from plasma membranes and exosomes of human breast carcinoma cells MCF-7. Proteomics 9(10):2820-2835.

Stögbauer F, Weigert J, Neumeier M, Wanninger J, Sporrer D, Weber M, Schefler A, Enrich C, Wood P, Grewal T, Aslanidis C, Buechler C. (2009) Annexin A6 is highly abundant in monocytes of obese and type 2 diabetic individuals and is downregulated by adiponectin in vitro. Exp Mol Med. 41(7):501-507.

Strzelecka-Kiliszek A, Buszewska ME, Podszywalow-Bartnicka P, Pikula S, Otulak K, Buchet R, Bandorowicz-Pikula J. (2008) Calcium- and pH-dependent localization of annexin A6 isoforms in Balb/3T3 fibroblasts reflecting their potential participation in vesicular transport. J Cell Biochem. 104(2):418-434.

Strzelecka-Kiliszek A, Tylki-Szymanska A, Bandorowicz-Pikula J. (2004) Annexins in Niemann-Pick type C disease. Annexins 1(3):206-216.

Sugii S, Reid PC, Ohgami N, Du H, Chang TY. (2003) Distinct endosomal compartments in early trafficking of low density lipoprotein-derived cholesterol. J Biol Chem. 278(29):27180-27189.

Sztolsztener ME, Strzelecka-Kiliszek A, Pikula S, Tylki-Szymanska A, Bandorowicz-Pikula J. (2010) Cholesterol as a factor regulating intracellular localization of annexin A6 in Niemann-Pick type C human skin fibroblasts. Arch Biochem Biophys. 493(2):221-233.

Taskinen S, Hyvönen M, Kovanen PT, Meri S, Pentikäinen MO. (2005) C-reactive protein binds to the 3beta-OH group of cholesterol in LDL particles. Biochem Biophys Res Commun. 329(4):1208-1216.

te Vruchte D, Lloyd–Evans E, Veldman RJ, Neville DC, Dwek RA, Platt FM, van Blitterswijk WJ, Sillence DJ. (2004) Accumulation of glycosphingolipids in Niemann–Pick C disease disrupts endosomal transport. J Biol Chem 279(25):26167–26175.

Tobe T. (2010) Cytoskeleton-modulating effectors of enteropathogenic and enterohemorrhagic Escherichia coli: role of EspL2 in adherence and an alternative pathway for modulating cytoskeleton through annexin A2 function. FEBS J. 277(11):2403-2408.

Troup GM, Wrenn SP. (2004) Temperature and cholesterol composition-dependent behavior of 1-myristoyl-2-[12-[(5-dimethylamino-1-naphthalenesulfonyl)amino]dodecanoyl]-sn-glycero-3-phosphocholine in 1,2-dimyristoyl-sn-glycero-3-phosphocholine membranes. Chem. Phys. Lipids. 131(2):167-182.

Uittenbogaard A, Everson WV, Matveev SV, Smart EJ. (2002) Cholesteryl ester is transported from caveolae to internal membranes as part of a caveolin-annexin II lipid-protein complex. J Biol Chem. 277(7):4925-4931.

Vainio S, Bykov I, Hermansson M, Jokitalo E, Somerharju P, Ikonen E. (2005) Defective insulin receptor activation and altered lipid rafts in Niemann-Pick type C disease hepatocytes. Biochem J. 391(3):465-472.

Valasek MA, Weng J, Shaul PW, Anderson RG, Repa JJ. (2005) Caveolin-1 is not required for murine intestinal cholesterol transport. J Biol Chem. 280(30):28103-28109.

van Meer G.(2005) Cellular lipidomics. EMBO J. 24(18):3159-3165.

Vance JE. (2006) Lipid imbalance in the neurological disorder, Niemann-Pick C disease. FEBS Lett. 580(23):5518-5524.

Vanier MT. (1999) Lipid changes in Niemann-Pick disease type C brain: personal experience and review of the literature. Neurochem Res. 24(4):481-489.

Vanier MT. (2010) Niemann-Pick disease type C. Orphanet J Rare Dis. 5:16.

Vanier MT, Millat G. (2003) Niemann-Pick disease type C. Clin Genet. 64(4):269-281.

Vetrivel KS, Thinakaran G. (2010) Membrane rafts in Alzheimer's disease beta-amyloid production. Biochim Biophys Acta 1801(8):860-867.

von Haller PD, Donohoe S, Goodlett DR, Aebersold R, Watts JD. (2001) Mass spectrometric characterization of proteins extracted from Jurkat T cell detergent-resistant membrane domains. Proteomics 1(8):1010-1021.

Wraith JE, Vecchio D, Jacklin E, Abel L, Chadha-Boreham H, Luzy C, Giorgino R, Patterson MC. (2010) Miglustat in adult and juvenile patients with Niemann-Pick disease type C: long-term data from a clinical trial. Mol. Genet. Metab. 99(4): 351–357.

Yang T, Espenshade PJ, Wright ME, Yabe D, Gong Y, Aebersold R, Goldstein JL, Brown MS. (2002) Crucial step in cholesterol homeostasis: sterols promote binding of SCAP to INSIG-1, a membrane protein that facilitates retention of SREBPs in ER. Cell 110(4):489-500.

Yang W, Di Vizio D, Kirchner M, Steen H, Freeman MR. (2010) Proteome scale characterization of human S-acylated proteins in lipid raft-enriched and non-raft membranes. Mol Cell Proteomics 9(1):54-70.

Yeagle PL. (1985) Cholesterol and the cell membrane. Biochim Biophys Acta. 822(3-4):267-287.

Zaks WJ, Creutz CE. (1990) Evaluation of the annexins as potential mediators of membrane fusion in exocytosis. J Bioenerg Biomembr. 22(2):97-120.

Zeuschner D, Stoorvogel W, Gerke V. (2001) Association of annexin 2 with recycling endosomes requires either calcium- or cholesterol-stabilized membrane domains. Eur J Cell Biol. 80(8):499-507.

Zhang C, Li PL. (2010) Membrane raft redox signalosomes in endothelial cells. Free Radic Res. 44(8):831-842.

Zhang JH, Ge L, Qi W, Zhang L, Miao HH, Li BL, Yang M, Song BL. (2011) The N-terminal domain of NPC1L1 protein binds cholesterol and plays essential roles in cholesterol uptake. J Biol Chem. 286(28):25088-25097.

Zhang T, Zhang X, Sun Z. (2010) Global network analysis of lipid-raft-related proteins reveals their centrality in the network and their roles in multiple biological processes. J Mol Biol 402(4):761-773.

Zidovetzki R, Levitan I. (2007) Use of cyclodextrins to manipulate plasma membrane cholesterol content: evidence, misconceptions and control strategies. Biochim Biophys Acta 1768(6):1311-1324.

TITRE en français.
Rôle de l'annexine A6 dans l'organisation des microdomaines membranaires enrichis en cholestérol. Mise en évidence sur des cellules atteintes de la maladie de Niemann-Pick et des monocouches lipidiques biomimétiques.

RESUME en français.
La maladie de Niemann-Pick de type C (NPC) est une lipidose lysosomale complexe due à une mutation d'un des gènes *NPC1* ou *NPC2*, qui codent pour ces protéines localisées dans les compartiments endo-lysosomaux (LE/LY). Leur absence altère le trafic intracellulaire et induit l'accumulation du cholestérol (Chol) dans les LE/LY. De plus, l'AnxA6 semble participer au transport vésiculaire du Chol en interagissant avec les microdomaines membranaires enrichis en Chol, ou avec le Chol lui-même. Dans ce travail, nous avons isolé des microdomaines membranaires résistant au Triton X-100 (également appelés DRMs pour detergent resistant membranes) à partir de lignée cellulaire NPC L1 ou de cellules saines. Les fibroblastes NPC contiennent plus de DRMs que les fibroblastes sains. Ceci semble être corrélé aux problèmes de transport du Chol dans les cellules NPC. Nous avons aussi montré qu'en présence de calcium, une partie de l'AnxA6 est associé aux DRMs, suggérant que l'AnxA6 participe à l'organisation de la membrane et par ce bias à l'étiologie de la maladie de NPC. Nous avons alors analysé les interactions de l'AnxA6-1 avec les microdomaines riches en Chol ainsi que l'implication de sa région flexible et de la séquence VAAEIL dans ces interactions. Leurs interactions avec des monocouches de Langmuir constituées de phosphatidylcholine, Chol et/ou d'acétate de cholestéryle. Nos résultats montrent que l'AnxA6 a la plus grande affinité pour les monocouches contenant du Chol ainsi que l'implication du groupement hydroxyle du Chol lors de ces interactions.

TITRE en anglais.
Annexin A6 involvement in the organization of cholesterol-rich membrane microdomains. Evidence from cells of the Niemann-Pick type C disease patients and biomimetic lipid monolayers.

RESUME en anglais.
The Niemann-Pick type C (NPC) disease is a lysosomal lipid storage disorder caused by mutations in one of the two genes *NPC1* or *NPC2* encoding proteins of the late endosome/lysosome compartment (LE/LY). Defect in these proteins alters vesicular transport and leads to abnormal accumulation of cholesterol (Chol) in LE/LY. There are some lines of evidence suggesting that annexin A6 (AnxA6) participates in vesicular transport of Chol and may interact with membrane domains enriched in Chol and bind Chol. In this work we characterized the membrane microdomains resistant to Triton X-100, i.e., detergent-resistant membranes (DRMs) isolated from NPC patient-derived fibroblasts and from control cells. NPC cells contain a significantly higher amount of DRMs than the control cells that is consistent with the defect in Chol turnover in NPC cells. We also studied the mechanism of AnxA6 involvement in the NPC-induced changes in the membrane organization and showed that in the presence of calcium some AnxA6 molecules associate with the DRMs. This suggests that AnxA6 may play a role in the membrane lateral organization, contributing thus to the etiology of NPC disease. We then focused on the interaction of AnxA6-1 with Chol-rich membranes and on the involvement of its flexible region and VAAEIL sequence in these interactions. For this purpose, kinetics of the interfacial adsorption of human recombinant AnxA6 to Langmuir monolayers containing phosphatidylcholine, Chol and/or cholesteryl acetate were measured. Our data suggest that AnxA6 exhibits the highest affinity to Chol-containing monolayers and that the hydroxyl group of Chol plays a pivotal role in the AnxA6-lipid interactions *in vitro*.

DISCIPLINE Biochimie

MOTS-CLES : Maladie NPC, cholestérol, annexine A6, micodomaines résistants aux détergents (DRMs).
Keys words: NPC disease, cholesterol, annexin A6, detergent-resistant membranes (DRMs)

INTITULE ET ADRESSE DE L'U.F.R. OU DU LABORATOIRE :

Université Claude Bernard Lyon 1,
UMR CNRS UCBL 5246 – ICBMS
43 bd du 11 Novembre 1918,
69622 Villeurbanne, France

Nencki Instytute of Experimental Biology
Polish Academy of Sciences
3 Pasteur Street
02-093 Warsaw, Poland

Annexin A6 involvement in the organization of cholesterol-rich membrane microdomains. Evidence from cells of the Niemann-Pick type C disease patients and biomimetic lipid monolayers.

The Niemann-Pick type C (NPC) disease is a lysosomal lipid storage disorder caused by mutations in one of the two genes, *NPC1* or *NPC2*, encoding proteins of the late endosome/lysosome (LE/LY) compartment. Defect in these proteins alter vesicular transport and lead to abnormal accumulation of cholesterol and other lipids in the LE/LY compartment. There are some lines of evidence suggesting that AnxA6 participates in vesicular transport of cholesterol, may interact with membrane domains enriched in cholesterol and bind cholesterol.

In this work we characterized the membrane microdomains resistant to solubilization by Triton X-100, i.e., detergent-resistant membranes (DRMs) isolated from NPC fibroblasts cell line L1 derived from an NPC patient and from a healthy individual. We observed that NPC fibroblasts contain a significantly higher amount of DRMs in comparison to control fibroblasts that is consistent with the defect in cholesterol turnover in these cells. We also studied the mechanism of AnxA6 involvement in the NPC-induced changes in the organization of membrane structure and showed that in the presence of calcium a certain pool of AnxA6 molecules associate with the DRMs. This suggests that AnxA6 may play a role in membrane lateral organization, and in this way contribute to the etiology of NPC disease.

We then focused on the putative mechanism of the interaction of AnxA6-1 with cholesterol-enriched membranes, as well as on the involvement of the AnxA6-1 flexible region and the VAAEIL sequence in this interaction. For this purpose, human recombinant AnxA6 was used together with Langmuir monolayers containing various lipids (phosphatidylcholine, cholesterol and/or cholesteryl acetate) and kinetics of the interfacial adsorption were measured. The obtained results suggest that at acidic pH and in the presence of Ca^{2+} at basic pH, AnxA6 exhibits the highest affinity for lipid monolayers enriched in cholesterol. Experiments with cholesteryl acetate proved that the hydroxyl group of cholesterol plays a pivotal role in the AnxA6-lipid interactions *in vitro*.

Keywords: NPC disease, cholesterol, annexin A6, detergent-resistant membranes (DRMs)

Udział aneksyny A6 w organizacji mikrodomen błonowych bogatych w cholesterol. Wyniki oparte na komórkach pacjentów z chorobą Niemann-Picka typu C oraz biomimetycznych monowarstw lipidowych.

Choroba Niemanna-Picka typu C (NPC) należy do lizosomalnych chorób spichrzeniowych wywołanych mutacją w jednym z dwóch genów *NPC1* lub *NPC2* kodujących białka przedziału późnych endosomów/lizosomów (LE/LY). Uszkodzenie jednego z tych białek upośledza transport pęcherzykowy i powoduje nadmierne gromadzenie cholesterolu i innych lipidów w przedziale LE/LY. Istnieją przesłanki sugerujące, że AnxA6 uczestniczy w transporcie pęcherzykowym cholesterolu oraz, że oddziałuje z domenami błonowymi wzbogaconymi w cholesterol, a nawet, że może wiązać cholesterol.

Celem pracy doktorskiej była charakteryzacja mikrodomen błonowych odpornych na działanie detergentu TritonX-100, ang. detergent-resistant membranes (DRMs) wyizolowanych z linii komórkowej NPC L1 pochodzącej od pacjenta ze zdiagnozowaną chorobą NPC oraz z komórek kontrolnych. Zaobserwowano, że fibroblasty NPC L1 zawierają znacznie więcej mikrodomen odpornych na działanie detergentu niż fibroblasty kontrolne, co najprawdopodobniej wynika z zaburzeń transportu cholesterolu w tych komórkach. Badano również mechanizm oddziaływania AnxA6 z błonami komórkowymi NPC. Otrzymane wyniki wykazują, że w obecności jonów wapnia, pula AnxA6 wiąże się z DRMs, co sugeruje udział AnxA6 w organizacji błon komórkach NPC, a tym samym udział w etiologii choroby NPC.

Kolejnym celem zrealizowanym w ramach doktoratu było znalezienie mechanizmu oddziaływania AnxA6-1 z mikrodomenami błonowymi wzbogaconymi w cholesterol, a także stwierdzenie, czy rejon łącznika AnxA6-1 oraz sekwencja VAAEIL, mogą uczestniczyć w tych oddziaływaniach. W tym celu przy użyciu monowarstw Langmuira przeanalizowaliśmy kinetykę oddziaływań rekombinowanej AnxA6 człowieka z różnymi lipidami (fosfatydylocholiną, cholesterolem i/lub octanem cholesterolu). Otrzymane wyniki sugerują, że w pH 5.0 i w obecności jonów Ca^{2+}, AnxA6 najsilniej oddziałuje z monowarstwami wzbogaconymi w cholesterol. Ponadto, doświadczenia z octanem cholesterolu dowiodły, że grupa hydroksylowa cholesterolu ma szczególne znaczenie w oddziaływaniach AnxA6 z lipidami *in vitro.*

Słowa kluczowe: choroba NPC, cholesterol, aneksyna A6, mikrodomeny odporne na działanie detergentu (DRMs)

Magdalena Małgorzata Domoń

List of publications

Experimental papers

Bojkowska K, Hamczyk MM, Tsai HW, Riggan A, Rissman EF. (2008) Neuropeptide Y influences acute food intake and energy status affects NPY immunoreactivity in the female musk shrew (Suncus murinus). Horm Behav.53(2):342-50.

Domon MM, Matar G, Strzelecka-Kiliszek A, Bandorowicz-Pikula J, Pikula S, Besson F (2010) Interaction of annexin A6 with cholesterol rich membranes is pH-dependent and mediated by the sterol OH, J Colloid Interface Sci 346, 436-41.*

Domon MM, Besson F, Bandorowicz-Pikula J, Pikula S (2011) Annexin A6 is recruited into lipid rafts of Niemann-Pick type C disease fibroblasts in a Ca^{2+}-dependent manner." Biochem Biophys Res Commun 405, 192-196.*

Reviews

Domon MM, Nasir MN, Matar G, Pikula S, Besson F, Bandorowicz-Pikula J (2010) Annexins as potential organizers of cholesterol-enriched membrane microdomains in Niemann-Pick type C disease and other lipidoses. Cell Mol Life Sci, in revision. *

* papers reported in this PhD thesis

Abstracts

Hamczyk MM, Pikula S, Besson F (2009) Isolation and reconstitution of lipid rafts to study interaction between annexin A6 and cholesterol. 14^{e} Journee Scientifique de l'Ecole Doctorale Interdisciplinaire Sciences-Sante, Villeurbanne (France), March 11.

Domon MM, Matar G, Pikula S, Besson F (2009) Analysis of the interaction between annexin A6 and interfacial monolayers. Influence of the subphase pH and the sterol content, 16eme Congres du Groupe Francais des Peptides et des Proteines, Albeville (France), 10-15 May.

Domon MM, Matar G, Pikula S, Besson F (2009) Analysis of the pH-dependent interactions between annexin A6 and interfacial lipid monolayers", 34th FEBS Congress on Life's Molecular Interactions, Prague (Czech Republic), July 4-9.

Domon MM, Pikula S, Besson F (2010) Role of interactions between annexin A6 and cholesterol in Niemann-Pick type C disease. Isolation and reconstitution of membrane microdomains", 10ème Journée Scientifique de l'Institut Multidisciplinaire de Biochimie des Lipides, Villeurbanne (France), June 21.

Domon MM, Bandorowicz-Pikula J, Pikula S, Besson F (2011) Calcium-dependent interactions of annexin A6 with lipid microdomains: evidence from lipid monolayers and Niemann-Pick type C disease fibroblasts, EMBO Young Scientists Forum, Warsaw (Poland), June 30 – July 1.

Pikula S**,** Domon MM**,** Besson F, Bandorowicz-Pikula J (2011) Annexins, cholesterol-interacting proteins, particiate in the organization of membrane microdomains enriched in cholesterol. Evidence from Niemann-Pick type C disease, 6th International Conference on Annexins, Barcelone (Spain), August 28-31.

Oral presentation

Domon MM. (2009) AnnexinA6–the protein interacting with cholesterol and participating in the organization of lipid microdomains. Seminar of Department of Biochemistry, Nencki Institute of Experimental Biology, October 26, Warsaw, Poland.